UNIVERSITE DU QUÉBEC À MONTRÉAL

RECONSTITUTIONS DES TEMPÉRATURES DE SURFACE AU CANADA : DES TEMPÉRATURES BASALES DU GLACIER LAURENTIDIEN AUX CHANGEMENTS RÉCENTS DU CLIMAT ARCTIQUE

THÈSE
PRÉSENTÉE
COMME EXIGENCE PARTIELLE
DU DOCTORAT EN SCIENCES DE L'ENVIRONNEMENT

PAR
CHRISTIAN CHOUINARD

MARS 2008

REMERCIEMENTS

Je me dois premièrement de remercier mon directeur de thèse, Jean-Claude Mareschal, qui a su me faire confiance lors de mon retour aux études et me guider dans ce difficile parcours qu'est une thèse de doctorat. Sa grande rigueur scientifique ainsi que la générosité avec laquelle il partage son savoir sont autant de qualités que je m'efforcerais d'appliquer dans mon propre cheminement professionnel.

Merci également à mon co-directeur, Hugo Beltrami, pour son soutien ainsi que pour les nombreuses discussions stimulantes ayant contribuées à améliorer cette thèse.

Des remerciements sincères aux membres de mon jury, Alessandro Forte, Claude Hillaire-Marcel ainsi que Claude Jaupart, pour avoir accepté d'évaluer cette thèse. Une mention particulière se doit d'aller à Claude Jaupart avec qui j'ai eu l'immense plaisir de travailler sur le terrain au cours de ma thèse. Les échanges autant scientifiques que personnels que nous avons partagés au fil des années resteront à jamais gravés dans ma mémoire. Outre sa grande notoriété scientifique, ce sont sa générosité, son humanisme, son humour ainsi que son sens profond de la famille qui en font à mes yeux un grand exemple de réussite professionnelle ainsi que personnelle.

Je tiens à remercier tout spécialement ma conjointe Izabel pour son soutien indéfectible ainsi que pour tous les sacrifices qu'elle a du faire pour me permettre de réaliser mon objectif. Sans elle, rien de tout ceci n'aurait été possible.

Un gros merci à tous les membres de ma famille qui par leurs encouragements incessants et leur conviction profonde en mes capacités à mener à terme un si gros projet ont été de tout temps dans mes pensées au cours des quatre dernières années.

Et enfin merci à tous mes amis du GEOTOP qui m'ont accompagné au cours de ce périple ! Chantal, Christelle, Sandrine, Ben, Super Haricot Vert, Greg, André, Roman, Jean-François et tous les autres. Votre présence a grandement contribué à mon épanouissement autant académique que personnel.

TABLE DES MATIÈRES

LISTE DES FIGURES

LISTE DES TABLEAUX

RÉSUMÉ

La méthode de reconstitution de l'histoire de la température à la surface du sol (HTSS) à partir de profils de température mesurés dans des forages est présentée et mise en application afin d'apporter quelques éléments de réponse à des questions portant sur les changements climatiques passés. La thèse est divisée en trois chapitres dont le premier porte principalement sur des aspects méthodologiques et les deux autres sur des problèmes de détermination des changements de températures de surface auxquels la méthode fournit des solutions.

Le premier chapitre porte sur la sélection de profils de température lors de reconstitutions régionales de l'HTSS. Différents procédés de reconstitutions d'HTSS régionales à partir d'ensembles de profils de température sont comparés afin de déterminer quels avantages peut présenter une sélection de profils de température non contaminés par des perturbations non climatiques par rapport à une analyse globale de tous les profils mesurés. Les résultats montrent que la résolution ainsi que la stabilité des résultats sont grandement améliorées par une sélection minutieuse des profils de température. Non seulement l'inversion simultanée de profils très bruités n'améliore pas la résolution de la solution, mais l'inclusion de ces profils cause de fortes instabilités et peut fausser les résultats. Même si le nombre de profils non contaminés est généralement faible (par exemple, seuls 13 des 73 forages mesurés au Manitoba et en Saskatchewan sont considérés non contaminés), il est toujours préférable de sélectionner les profils afin d'obtenir une HTSS stable, fiable et ayant une bonne résolution. Si les profils contaminés par des perturbations non climatiques ne peuvent être éliminés, le meilleur moyen d'obtenir une HTSS stable est de faire la moyenne des inversions individuelles de chacun des profils, cependant la résolution de la solution sera très faible.

Le deuxième chapitre présente une HTSS des 400 dernières années au site minier Raglan, situé dans le nord de la péninsule d'Ungava, déterminée à l'aide de profils de température mesurés dans des forages creusés dans le pergélisol. Des écarts très prononcées par rapport à l'état stationnaire sont observés dans les 200 premiers mètres des profils de température mesurés et sont interprétés comme ayant été causés par les variations récentes de la température à la surface du sol. Seul un des profils de température n'est pas affecté par des perturbations non climatiques et est donc analysé en détail à l'aide de trois méthodes indépendantes, soit deux méthodes d'inversion et une méthode directe. Les résultats montrent un réchauffement de 1.4 K entre le milieu du 18^{e} siècle et 1940. Ce réchauffement est suivi d'une période de refroidissement caractérisée par une chute des températures de surface d'environ 0.4 K dura entre 40 et 50 ans. Depuis les 15 dernières années, les températures de surface ont bondi de plus de 1.7 K dans la région.

Le troisième chapitre présente des HTSS de plus de 30000 ans déterminés par l'inversion de profils de température très profonds (2000 mètres) situés à divers endroits au Canada. Ces HTSS permettent entre autre de déterminer les températures à la base du glacier Laurentidien (températures basales) au dernier maximum glaciaire. Pour ce faire, quatre nouveaux profils très profonds mesurés à Sudbury et Manitouwadge sont analysés et interprétés conjointement avec quatre profils profonds déjà publiés

(Flin Flon, Thompson, Balmertown et Sept-Îles). Une ré-analyse complète de tous les profils déjà publiés est effectuée afin de permettre une comparaison objective de tous les résultats. Les résultats montrent que sous la portion sud du glacier Laurentidien, les températures basales avaient des valeurs entre 0 et -2 °C au dernier maximum glaciaire. Ces résultats sont en accord avec les prédictions des modèles isostatiques et des observations de surface qui suggèrent que les températures basales devaient être près du point de fusion de la glace afin de permettre un écoulement rapide de la glace basale. Les reconstitutions de l'HTSS permettent également d'étudier l'amplitude et la chronologie de l'optimum climatique de l'Holocène pour chacun des sites étudiés. Les valeurs obtenues sont en accord avec les résultats de multiples études utilisant différents proxies.

Mots clés : Paléoclimatologie, géophysique, inversions, reconstitutions climatiques, tempŕatures de surface, forages, anomalies de température, flux de chaleur.

ABSTRACT

The method of inferring ground surface temperature histories (GSTH) from borehole temperature depth profiles is presented and applied to different problems related to past climate change. The thesis is divided in three chapters, the first of which deals mainly with methodological aspects and the remaining two deal with different issues regarding the reconstruction of past surface temperature to which the method brings solutions.

The first chapter deals with the selection of temperature depth profiles for regional GSTH reconstructions. Different regional GSTH reconstruction procedures are compared in order to determine if, in opposition to using an entire regional dataset, there is an advantage gained by selecting profiles which are not affected by non climatic perturbations. Results show that when performing simultaneous inversions of multiple profiles, the resolution and the stability of the solution are much improved by a careful selection of profiles not affected by non climatic perturbations. Not only does the inclusion of noisy profiles not improve the resolution of the solution, but it even causes strong instabilities in the inversion which distort the solution. Even if usually few profiles within a given region meet the selection criteria (e.g. only 13 of the 73 profiles measured in the Manitoba and Saskatchewan region can be considered unaffected by non climatic perturbations), it is always preferable to select profiles in order to infer a GSTH that is stable, accurate and has a good resolution. If the profiles affected by non climatic perturbations can not be eliminated, averaging of the individual inversions yields the most stable result, but with very poor resolution.

The second chapter presents a 400 years GSTH at the Raglan mine site, located at the northern tip of the Ungava peninsula, inferred using temperature depth profiles recorded in permafrost. Marked deviations from steady-state in the upper 200 meters of the profiles are assumed to be caused by recent variations in ground surface temperatures. One profile which is least affected by non climatic perturbations is analyzed with great detail using two independent inverse methods and a direct method. The results show a 1.4 K warming between the mid-18^{th} century and 1940. Between the 1940s and the 1990s, a cooling episode in this region was characterized by a 0.4 K drop in surface temperatures. In the past 15 years, surface temperatures have warmed by a sharp 1.7 K.

The third chapter presents 30000 years GSTHs inferred from very deep temperature depth profiles (2000 meters) located at different sites across Canada. These GSTHs, among other things, allow the determination of temperatures at the base of the Laurentide ice sheet (basal temperatures) at the last glacial maximum. Four new very deep temperature depth profiles measured in Sudbury and Manitouwadge are analyzed and discussed jointly with four previously published profiles (Flin Flon, Thompson, Balmertown and Sept-Îles). A complete reanalysis of the previously published profiles is performed in order to allow an objective comparison of all results. The new results show that under the southern portion of the Laurentide ice sheet, values of basal temperatures were between 0 and -2°C at last glacial maximum. These results are in agreement with predictions from both isostatic models and surface observations which suggest that in order to allow fast basal flows, temperatures

had to be near the pressure melting point of ice. The inferred GSTH are also used to study the chronology and amplitude of the Holocene climate optimum at each site. The results are in agreement with those from numerous studies using multiple proxies.

Keywords : Paleoclimatology, geophysics, inversions, climate reconstructions, surface temperatures, boreholes, temperature anomalies, heat flow.

CHAPITRE 1

INTRODUCTION

Les changements climatiques et en particulier le réchauffement global occupent une place de premier ordre dans les sphères scientifiques, politiques et médiatiques depuis déjà plusieurs années. Les observations globales du climat montrent que ce réchauffement a présentement lieu et les modèles de circulation globale prédisent qu'il va se poursuivre (IPCC, 2007). Ces modèles de circulation globale sont constamment raffinés et améliorés afin de mieux circonscrire les paramètres touchant le climat global. Le moyen de calibration le plus élémentaire est de tenter de reproduire les climats passés à l'aide de ces modèles. En outre, afin de pouvoir prédire comment le climat évoluera dans le futur, il est essentiel de comprendre comment il a évolué dans le passé. Dans cette optique, les méthodes de reconstitutions paléoclimatiques fournissent des données essentielles permettant la calibration des modèles de circulation globale. De plus, l'accroissement des connaissances apportée par les reconstitutions paléoclimatiques par rapport aux enregistrements météorologiques existants est nécessaire puisqu'elle permet de placer les changements climatiques actuels en perspective face à la variablité naturelle du climat à long terme.

Le dernier événement climatique global majeur à s'être déroulé sur Terre remonte à la dernière glaciation, qui fut caractérisée par la présence de calottes glaciaires sur une partie importante de l'hémisphère nord. Un modèle qui réussirait à correctement reproduire le climat terrestre depuis le dernier maximum glaciaire (il y a 20000 ans) jusqu'à aujourd'hui pourrait être considéré comme étant très robuste dans ses prédictions du climat futur (Mix *et al.*, 2001). Le climat de la dernière glaciation était intimement lié aux calottes glaciaires par le biais de multiples mécanismes de rétroaction (Manabe et Broccoli, 1985; Imbrie *et al.*, 1992). Afin de comprendre ces interactions, il est donc essentiel de comprendre la dynamique de ces calottes glaciaires (Clark *et al.*, 1999). Un des paramètres qui influence l'évolution d'un glacier est la distribution des températures basales, soit les températures à la base du glacier. Ces températures déterminent la possibilité que la glace à la base du glacier se soit écoulé sous forme de rivières de

glace ainsi que la vitesse d'écoulement de cette glace, une variable qui régit l'épaisseur qu'un glacier peut atteindre à cet endroit. Des modèles numériques ainsi que des observations géologiques démontrent que les vitesses d'écoulement devaient être relativement élevées sous la portion sud du glacier (Hicock et Dreimanis, 1992; Dyke *et al.*, 2003; Peltier, 2004). La seule méthode basée sur des données réelles permettant de déterminer quelles étaient les températures à la base du glacier est l'inversion de profils de températures mesurés dans des forages très profonds (plus de 2000 mètres).

Les mesures de température dans des forages peuvent également servir à valider les prédictions à court terme des modèles de circulation globale. En effet, lorsque des scénarios d'augmentation des gaz à effets de serre sont testés par les modèles de circulation globale, ceux-ci prédisent que, du à des phénomènes de rétroaction qui mettent en cause entre autres l'albédo et la glace de mer, une augmentation plus rapide des températures de surface devrait être observée dans les hautes latitudes de l'hémisphère nord (Houghton *et al.*, 1996; Flato *et al.*, 2000; Serreze *et al.*, 2000; Moritz *et al.*, 2002; Serreze et Francis, 2006). Des études ont déjà montré que ce réchauffement important s'opère depuis la fin du petit âge glaciaire, il y a de ça environ 150 ans (Overpeck *et al.*, 1997). Cependant, les données existantes des températures de l'air à la surface du sol montrent que le réchauffement de l'Arctique n'a pas été constant au cours du dernier siècle (Jones et Kelly, 1983; Przybylak, 2000; Serreze *et al.*, 2000; Moritz *et al.*, 2002). Certaines régions se sont réchauffées très rapidement alors que d'autres ont subi des périodes de refroidissement. Ces divergences sont tout à fait normales pour cette région de la planète et la seule anomalie climatique commune à toutes les régions de l'Arctique depuis la dernière déglaciation est le réchauffement des 150 dernières années (Kerwin *et al.*, 2004). Cependant, il existe présentement un manque important de données permettant de décrire l'évolution récente du climat dans plusieurs régions de l'Arctique. Les données météorologiques sont insuffisantes et la plupart des méthodes de reconstitution du climat présentent des lacunes lorsque vient le temps de reconstruire le climat récent (400 dernières années).

1.1 Les reconstitutions de l'histoire des températures à la surface du sol à partir de profils de température mesurés dans des forages profonds

Les variations de la température à la surface de la Terre sont enregistrées sous la forme de perturbations au régime de température à l'état stationnaire dans les premiers kilomètres de la

croûte terrestre (Lane, 1923). Ces perturbations transitoires de la température de surface sont atténuées exponentiellement à mesure qu'elles se propagent en profondeur. Cette atténuation se produit sur une échelle de longueur δ qui décrit la profondeur de pénétration des oscillations de températures de surface. La profondeur de pénétration dépend à la fois de la fréquence ω des variations de températures de surface ainsi que de la diffusivité thermique κ et peut être décrite sous la forme : $\delta = \sqrt{\kappa/2\omega}$. Les roches ayant une faible diffusivité thermique ($\approx 10^{-6} m^2 s^{-1}$), les oscillations de température de surface de courte période telles les variations diurnes ou annuelles ne pénètrent que de quelques centimètres à quelques mètres dans le sous-sol. Ainsi, les varations de la température de surface des 500 dernières années sont-elles enregistrées jusqu'à des profondeurs d'environ 400 mètres et les variations des derniers 20000 ans causent des perturbations mesurables jusqu'à des profondeurs dépassant les 2500 mètres.

Il est possible de mesurer la température de la partie supérieure de la croûte terrestre en effectuant des mesures de la température de l'eau reposant dans les forages d'exploration minière. Si l'on s'assure de laisser assez de temps afin que la perturbation de température engendrée par le processus de forage se dissipe complètement, l'eau dans le forage se trouvera alors à la même température que le millieu rocheux ambiant. En utilisant un dispositif très simple constitué d'une thermistance montée au bout d'un cable conducteur, on peut mesurer la température de l'eau dans les forages et ainsi construire un profil de température en fonction de la profondeur. La température au long du profil est contrôlée par le flux de chaleur provenant de la croûte et du manteau terrestre et les perturbations climatiques ou non-climatiques provenant de la surface. Les autres paramètres pouvant affecter le profil sont les variations de la conductivité thermique dues aux changements de types de roches en profondeur ainsi que la production de chaleur en profondeur due à la décroissance des éléments radioactifs présents naturellement dans les roches. Ces paramètres sont déterminés à l'aide de mesures effectuées sur des échantillons sélectionnés sur le terrain.

L'interprétation d'un profil de température afin d'en déduire l'histoire de la température à la surface du sol (HTSS) représente un problème géophysique inverse. Un problème inverse se présente lorsque les paramètres d'un modèle doivent être obtenus à partir de données mesurées. Dans le cas de l'HTSS, les paramètres à obtenir sont les variations des températures de surface et ceux-ci sont déterminés à partir des perturbations que ces variations ont causé dans la croûte terrestre. Le modèle quant à lui est basé sur l'équation de la chaleur à une dimension qui

suppose que les variations de températures sont appliquées sur une surface plane et que les propriétés physiques ne dépendent que de la profondeur (Carslaw et Jaeger, 1959). La première formulation du problème inverse de détermination de l'HTSS fut faite par Hotchkiss et Ingersoll (1934). Bien que quelques interprétations de l'HTSS à partir de profils de température aient été publiées avant 1983 (Beck et Judge, 1969; Cermak, 1971; Beck, 1982), la première application de techniques d'inversions pour déduire une HTSS d'un profil de température mesuré dans un forage fut l'étude publiée par Vasseur *et al.* (1983). Depuis, de nombreux chercheurs ont publié des études qui utilisent des techniques d'inversion afin de fournir l'HTSS un peu partout autour du globe (Lachenbruch et Marshall, 1986; Nielsen et Beck, 1989; Beltrami *et al.*, 1992; Wang *et al.*, 1992; Pollack *et al.*, 1996; Bodri et Cermak, 1997). Ces études confirment toutes un accroissement récent des températures à la surface du sol.

L'avantage principal de la méthode de reconstitution de l'HTSS utilisant des profils de température face aux différents proxies utilisés pour reconstruire des paléoclimats (pollen, microfossiles, anneaux d'arbres, etc.), est qu'elle représente la seule qui utilise des températures afin de déduire des températures. Donc, les paramètres qui affectent les autres proxies simultanément avec la température, comme par exemple les précipitations ou la salinité, ne représentent pas un problème lorsque l'on utilise des profils de température pour reconstruire l'HTSS. Cependant, le défaut majeur de la méthode de reconstitution de l'HTSS à partir de profils de température est l'importante perte de résolution temporelle lorsque l'on tente de reconstruire des variations de températures de surface de plusieurs milliers d'années (Mareschal *et al.*, 1999). Cette perte de résolution fait en sorte qu'à long terme seules les grandes tendances demeurent et que tous les événements climatiques ponctuels, aussi sévères soient-ils (par exemple le Younger-Dryas), se trouvent complètement effacés du signal.

1.2 Applications de la méthode de reconstitution des températures de surface à partir de profils de température à différents problèmes de nature environnementale

Les résultats de cette thèse sont présentés en trois chapitres distincts prenant la forme de trois articles scientifiques en langue anglaise. Le choix de la langue anglaise a été fait afin de permettre la publication des articles dans des périodiques scientifiques internationaux. Le premier article est déjà publié, le deuxième est accepté et présentement sous presse et le troisième est en

préparation. Les grandes questions auxquelles les différents chapitres tentent de répondre sont décrites dans les trois sections suivantes.

1.2.1 La sélection de profils de température non-perturbés par des phénomènes non-climatiques pour les reconstitutions régionales des températures de surface

Le premier chapitre porte essentiellement sur la méthode de reconstitution d'une HTSS régionale à partir de profils de température mesurés dans des forages. Un des problèmes fondamentaux de cette méthode est celui des perturbations des températures en profondeur engendrées par des phénomènes non-climatiques. Ces phénomènes sont nombreux et chacun peut créer de sérieux ennuis lorsque vient le temps d'analyser un profil de température.

Une topographie trop accidentée a pour effet d'annuler la condition à la limite supérieure de notre modèle (qui suppose une température uniforme appliquée sur une surface plane). Un lac ou une grande rivière agit comme un immense réservoir de chaleur et modifie complètement le régime thermique du sous-sol à plusieurs centaines de mètres autour de celui-ci. Les feux de forêts, la déforestation et l'urbanisation ont tous pour effet de modifier les conditions à la surface du sol, de sorte que le bilan énergétique à la surface est modifié indépendamment du climat. La circulation d'eau dans un forage fait en sorte qu'il ne repose plus à l'état stationnaire et que les températures mesurées ne représentent plus le régime thermique du sous-sol à cet endroit. Un gisement minéralisé ayant des valeurs de conductivité thermique beaucoup plus élevées que celles du substratum environnant peut engendrer un phénomène de réfraction qui modifiera le régime thermique de la région environnante, de sorte que tout forage situé près du gisement risque d'être affecté par ce phénomène.

Tous ces phénomènes doivent être clairement documentés lorsque possible puisqu'ils ont le potentiel de complètement fausser une analyse de l'HTSS. Par exemple, si un profil de température mesuré dans un forage est donné à un spécialiste de la méthode afin d'en déduire une HTSS mais qu'aucune information sur les conditions à la surface ne lui est communiquées, il lui sera impossible d'interpréter les résultats avec certitude. Les perturbations non-climatiques ont non-seulement le potentiel de complètement éclipser un signal climatique, mais dans certains cas peuvent aller jusqu'à parfaitement ressembler à un tel signal.

De plus, les profils de température mesurés dans une même régions sont souvent faiblement corrélés (Gosselin et Mareschal, 2003). Par conséquent, deux profils de température mesurés dans des forages situés non loin l'un de l'autre peuvent éventuellement produire deux HTSS différentes. Ceci est généralement du aux différences de conditions de surface entre les deux sites (marécages, forêts, clairières, etc.).

Afin d'éliminer les problèmes reliés aux phénomènes non-climatiques et à la faible corrélation des HTSS, plusieurs chercheurs ont tenté de déduire des HTSS régionales en inversant simultanément des profils de températures ayant été mesurés dans des forages d'une même région (Beltrami *et al.*, 1992; Clauser et Mareschal, 1995; Pollack *et al.*, 1996). De telles inversions supposent que les variations de la température de l'air, et par conséquent de la température du sol, sont corrélées sur des distances d'environ 500 km (Hansen et Lebedeff, 1987; Jones *et al.*, 1999). En théorie, une inversion simultanée permettrait de tirer le signal commun à tous les profils de température utilisés lors de l'inversion et ainsi d'améliorer la résolution du signal puisque les perturbations dues aux climat devraient être corrélées, ce qui n'est pas le cas des perturbations non-climatiques. En pratique, Beltrami *et al.* (1997) ont démontré que le gain de résolution des inversions simultanées n'était pas très important.

Cependant, un détail est demeuré source de débat entre les chercheurs qui utilisent cette méthode : lorsque l'on déduit une HTSS régionale à partir d'une inversion simultanée de profils de températures, faut-il utiliser tous les profils mesurés dans la région afin d'avoir le plus de sources de signal possible ou au contraire, faut-il éliminer ceux que l'on sait perturbés par des phénomènes non-climatiques ? Les méthodes d'inversions simultanées n'ont été initialement testées que sur des séries de données synthétiques puisque jusqu'à maintenant il n'existait aucune région sur Terre contenant une densité de forages profonds assez importante pour permettre de tester la méthode avec des données réelles.

La première partie de la thèse consiste en une analyse de tous les profils de températures mesurés au cours des 20 dernières années par l'équipe formée de chercheurs du GEOTOP-UQAM-McGill et de l'Institut de Physique du Globe de Paris (IPGP) sous la direction de Jean-Claude Mareschal (GEOTOP) et de Claude Jaupart (IPGP). Plus de 300 forages ont été mesurés pendant cette période. De ces forages, 299 ont pu être divisés en trois grandes régions afin de permettre une analyse de la méthode d'inversion simultanée. Les forages de chacune des régions

ont tous été inversés individuellement ainsi que simultanément. Les inversions individuelles ont été moyennées afin de permettre une comparaison avec les inversions simultanées. Afin de tester l'effet des perturbations non-climatiques sur une inversion simultanée, des centaines d'inversions simultanées ont été faites en éliminant systématiquement un seul profil de l'ensemble. Pour toutes les régions, les résultats des analyses simultanées et moyennées sont comparées et discutées. Enfin, des recommandations sont émises afin de guider tous ceux qui entreprendront d'utiliser la méthode de reconstitution de l'HTSS à partir de profils de température mesurés dans des forages.

1.2.2 Reconstitution de l'histoire des températures de surface des 400 dernières années dans le grand nord québécois

Le deuxième chaptre porte sur la reconstitution des températures de surface des 400 dernières années à la propriété minière Raglan, située au nord de la péninsule d'Ungava, dans le grand nord québécois. Cette étude apporte des informations climatologiques essentielles puisque le manque de données météorologiques de plus de 80 ans dans cette région du monde rend l'étude de l'amplitude des changements climatiques de l'Arctique très difficile.

Des études portant sur l'évolution du climat du nord du Québec ont déjà été effectuées en utilisant différentes méthodes, (paléolimnologie, croissance de coins de pergélisols, dégradation du pergélisol, etc.), mais chacune de ces méthodes présente un problème lorsque vient le temps de décrire le climat des 400 dernières années. Les méthodes paléolimnologiques et palynologiques permettent des reconstitutions à long terme, mais la réponse des écosystèmes lacustres et de la végétation aux changement climatiques à ces latitudes est très lente et ne permet pas de reconstitution récente (Kerwin *et al.*, 2004; Fallu *et al.*, 2005).

Les études du pergélisol permettent quant à elles de définir des périodes plus chaudes ou plus froides au cours du passé récent, mais pas les températures absolues (Laberge et Payette, 1995; Kasper et Allard, 2001; Payette *et al.*, 2004). Des études d'évolution du pergélisol décrivent ainsi une période de refroidissement entre les années 1940 et les années 1990 (Wang et Allard, 1995; Allard *et al.*, 1995). Cette période de refroidissement, également décrite par des climatologues (Jones et Kelly, 1983; Przybylak, 2000), a eu lieu dans plusieurs endroits de l'Arctique à des échelles différentes. Il est essentiel de bien identifier la distribution spatiale ainsi que l'amplitude

des changements brusques du climat afin de pouvoir comprendre quels mécanismes de forçage sont en cause lors de tels événements climatiques (Rind et Overpeck, 1993).

La deuxième partie de la thèse consiste en une analyse de quatre profils de température mesurés dans trois forages situés dans le grand nord québécois. Trois méthodes de reconstitution de l'HTSS sont utilisées (une méthode directe et deux méthodes d'inversion) afin de déterminer avec la meilleure résolution possible l'amplitude des variations des températures à la surface du sol au cours des 400 dernières années. Les résultats sont comparés aux données météorologiques des 60 dernières années à Iqaluit et Kuujjuaq. L'échelle temporelle de la reconstitution permet de comparer les amplitudes des signaux de refroidissement dus au petit âge glaciaire et au refroidissement du 20^e siècle ainsi que le signal de réchauffement drastique des 15 dernières années.

1.2.3 Reconstitution de l'histoire des températures de surface à la base du glacier Laurentidien lors du dernier maximum glaciaire ainsi que pendant l'optimum climatique de l'Holocène

Le troisième chapitre porte sur la reconstitution des températures de surface des 50000 dernières années sur le bouclier canadien à partir de profils de température mesurés dans des forages très profonds. Ces mesures représentent les seules données réelles permettant d'évaluer l'évolution de la température sous le glacier Laurentidien.

Deux études portant sur les reconstitutions des températures à la base du glacier Laurentidien à partir de profils de température ont déjà été publiées (Rolandone *et al.*, 2003; Mareschal *et al.*, 1999). Mais la résolution spatiale des résultats de ces études est très limitée puisque l'une de ces études est basée sur trois mesures dans le centre du Canada, et l'autre sur une seule mesure située sur la côte est canadienne. De plus, la profondeur de certains forages utilisés est à la limite de la détection d'un signal de température au dernier maximum glaciaire (moins de 1800 mètres). Les résultats de ces études montrent des températures variables sous le glacier Laurentidien, avec des valeurs allant de températures près du point de fusion de la glace au centre du Canada à des températures beaucoup plus froides sur la côte est canadienne, soit en bordure du glacier.

La troisième partie de la thèse consiste ainsi en une analyse de tous les profils de température

très profonds mesurés au Canada. Deux nouveaux sites ontariens contenant des forages de plus de 2000 mètres, un à Sudbury et l'autre à Manitouwadge, ont été récemment mesurés et sont présentés. Deux méthodes d'inversions, la méthode de décomposition des valeurs singulières et la méthode de Monte-Carlo, sont utilisées pour reconstituer l'HTSS des 50000 dernières années. Afin de permettre une comparaison objective des résultats de l'analyse des nouveaux profils de température avec ceux de Rolandone *et al.* (2003) et Mareschal *et al.* (1999), une ré-analyse complète de tous les profils de température préalablement étudiés en utilisant les deux méthodes d'inversion est également présentée. Ces reconstitutions permettent de déterminer en quelques points les températures basales du glacier Laurentidien au dernier maximum glaciaire ainsi que l'évolution subséquente des températures lors du réchauffement post-glaciaire et de l'Holocène. Pour toutes les régions étudiées, une comparaison de l'amplitude ainsi que de la chronologie de l'optimum climatique de l'Holocène avec différents proxies est également présentée.

1.3 Originalité et contribution

Les trois articles formant cette thèse reposent tous sur des travaux originaux n'ayant jamais été effectués par d'autres chercheurs. Ma contribution aux articles est primordiale puisque j'ai réalisé le traitement de toutes les données, les analyses, les interprétations ainsi que la rédaction des trois manuscrits. Les trois articles sont cosignés par mon directeur de thèse, le Dr. Jean-Claude Mareschal, qui a participé à plusieurs échanges d'idées sur les différents sujets de la thèse ainsi qu'aux révisions des trois manuscrits. Le deuxième article est également cosigné par le Dr. Richard Fortier du centre d'études nordiques de l'Université Laval. Le Dr. Fortier nous a permis d'avoir accès à un site de forage situé sur le site minier Raglan et a participé aux prises de mesures ainsi qu'à la révision du manuscrit.

CHAPITRE 2

SELECTION OF BOREHOLE TEMPERATURE DEPTH PROFILES FOR REGIONAL CLIMATE RECONSTRUCTIONS

Publié dans *Climate of the Past* (2007), vol.3, pages 297-313.

2.1 Résumé

Les profils de température mesurés dans les forages sont communément utilisés afin de déterminer les variations temporelles à l'échelle centenaire des températures à la surface du sol. Dans cette étude nous comparons différents procédés de reconstruction régionale de l'histoire de la température à la surface du sol (HTSS) à partir d'ensembles de profils de température. En particulier, nous nous penchons sur la question de la sélection de profils non contaminés par des perturbations non climatiques et comparons les résultats d'inversions simultanées de profils avec des moyennes d'inversions individuelles de ces mêmes profils. De tous les profils de température mesurés au Canada, très peu rencontrent les critères de sélection (par exemple, 13 des 73 profils dans la région du Manitoba et de la Saskatchewan rencontrent les critères). Nos résultats montrent que la résolution ainsi que la stabilité des inversions utilisant des profils sélectionnés sont de beaucoup supérieurs aux résultats des inversions utilisant tous les profils disponibles. Lorsque l'on utilise seulement des profils sélectionnés, les moyennes des HTSS obtenues d'inversions individuelles sont pratiquement identiques aux HTSS obtenues d'inversions simultanées. Ceci n'est pas le cas lorsque tous les profils disponibles sont utilisés pour l'inversion : la moyenne des inversions individuelles est différente de l'inversion simultanée. Nous démontrons également que l'inversion simultanée de profils très bruités n'apporte non seulement aucune amélioration à la résolution de la solution, mais au contraire tend à induire de fortes instabilités dans l'inversion. Lorsqu'il est impossible d'éliminer les profils bruités d'une étude régionale de l'HTSS, la moyenne d'inversions individuelles produit le résultat le plus stable, mais avec une très faible résolution.

2.2 Abstract

Borehole temperature depth profiles are commonly used to infer time variations in the ground surface temperature on centennial time scales. We compare different procedures to obtain a regional ground surface temperature history (GSTH) from an ensemble of borehole temperature depth profiles. We address in particular the question of selecting profiles that are not contaminated by non climatic surface perturbations and we compare the joint inversion of all the profiles with the average of individual inversions. Very few profiles of the Canadian data set meet the selection criteria (e.g. only 13 out of 73 profiles in Manitoba and Saskatchewan were retained). We show that the resolution and the stability of the inversion of selected profiles are much improved over those for a complete data set. When profiles have been selected, the average GSTH of individual inversions and the GSTH of the joint inversion are almost identical. This is not observed when the entire data set is inverted : the average of individual inversions is different from the joint inversion. We also show that the joint inversion of very noisy data sets does not improve the resolution but, on the contrary, causes strong instabilities in the inversion. When the profiles that are affected by noise can not be eliminated, averaging of the individual inversions yields the most stable result, but with very poor resolution.

2.3 Introduction

In recent years, borehole temperature data have been used to provide additional evidence for recent climatic changes in several parts of the world (e.g. Cermak, 1971; Vasseur *et al.*, 1983; Lachenbruch et Marshall, 1986; Nielsen et Beck, 1989; Beltrami *et al.*, 1992; Wang, 1992; Bodri et Cermak, 1997; Pollack *et al.*, 1996). Indeed, transient surface temperature perturbations propagate downward and, although attenuated, are recorded in the Earth's subsurface as perturbations of a steady state temperature regime.

Because surface temperature oscillations are damped over a length scale δ (skin depth) which depends on their frequency ω and on thermal diffusivity κ ($\delta = \sqrt{\kappa/2\omega}$), the earth acts as a filter and the record of the ground surface temperature history (GSTH) is blurred. Because of the low thermal diffusivity of rocks ($\approx 10^{-6}\mathrm{m}^2\mathrm{s}^{-1}$), the short period oscillations, such as the diurnal or annual cycles, have skin depth ranging from a few centimetres to a couple of meters. Variations of ground surface temperature of the last 200-300 years are recorded in the first 200

meters, whereas the effect of the post-glacial warming is observed down to 2500 meters. The interpretation of temperature profiles in terms of the GSTH presents all the characteristics of ill-posed geophysical inversion problems : their solution is not unique and it is unstable (e.g. Jackson, 1972; Tikhonov et Arsenin, 1977; Menke, 1989; Parker, 1994).

The first application of inversion techniques to infer the GSTH from borehole temperature profile was the study by Vasseur *et al.* (1983). In the last fifteen years, several papers have addressed the problem of inversion of borehole temperature data and different methods have been proposed to invert the GSTH from one or several temperature profiles. Many other papers deal « empirically » with practical considerations.

The interpretation of borehole temperature profiles is based on the one dimensional heat equation ; it assumes that a uniform boundary condition is applied on a plane surface and that physical properties only depend on depth. Although corrections can be applied to correct heat flow for the effect of topography (Blackwell *et al.*, 1980), this is rarely done in climate studies because the amplitude of the climatic signals is often smaller than the uncertainty on these corrections. Other variations in surface boundary condition can affect the temperature measured at depth and need to be accounted for : proximity to lakes or large rivers, recent forest fires, changes in vegetation cover, deforestation. Other perturbations include refraction by lateral changes in thermal conductivity, water circulation in the borehole, etc.. These effects need to be well documented since they produce distortions of the temperature profiles similar to those produced by climate change and they might overshadow any real climatic signal in a GSTH. Until recently, borehole temperature depth profiles were not logged to infer past climates, but for heat flow measurements. For heat flow studies, corrections are often small and can be avoided when boreholes are deep and the surface effects become negligible. But for climate studies, the signal is recorded in the shallow part of the profile which is most affected by noise.

It had been hoped that the problem of noise could be alleviated through regional GSTH studies, performed by inverting several borehole temperature profiles within a given region (Beltrami et Mareschal, 1992; Pollack *et al.*, 1996). Such studies assume that variations of air surface temperature trends and thus of ground surface temperatures remain correlated over distances $\approx$ 500 km (Hansen et Lebedeff, 1987; Jones *et al.*, 1999). Two methods can be used to determine a regional GSTH : all the borehole temperature profiles are inverted simultaneously

to obtain the common GSTH, or each profile is inverted separately and the individual GSTHs are averaged. If noise is random and uncorrelated, the simultaneous inversion of a given data-set, either local or regional, should theoretically yield a GSTH with a better signal to noise ratio than an average of individual inversions. This assumes that the noise is uncorrelated and that there is no systematic bias in the perturbations of the temperature profile. This latter condition is unlikely to be met for practical reasons : for instance, boreholes located on the shore of a lake can be (and are) logged, but boreholes in the middle of a lake never are. Boreholes drilled in lakes are normally cemented ; even when they are not, the casing is never left sticking out of the lake and has been pulled out. Some authors (Lewis, 1998) have thus argued that the error associated to GSTH will systematically be biased towards a warming of the ground surface. The argument is that in most cases, human and/or natural effects on the energy balance at the ground surface will cause a gain of energy by the ground (clear-cutting of forested areas, pollution effects on vegetation cover, forest fires, etc.). Previous studies with poorly documented site conditions retained all the boreholes and might have overestimated the warming trend (Beltrami *et al.*, 1992; Beltrami et Mareschal, 1992).

When the conditions at the sites are well documented, one could eliminate the temperature profiles that are perturbed by surface conditions. In general, very few boreholes meet strict criteria, and the majority of the logged boreholes in a region are rejected. For example, in two recent studies only 15 and 50% of the logged boreholes within the study areas were retained (Guillou-Frottier *et al.*, 1998; Gosselin et Mareschal, 2003).

The correlation of individual inversions of temperature profiles is often weak whether they come from the same region (Gosselin et Mareschal, 2003) or cover a wide part of the Earth surface (Harris et Chapman, 2001). Consequently, the GSTH averaging all the individual inversions has very poor resolution (Pollack *et al.*, 1998). It was hoped that the simultaneous inversion of profiles from a region that have recorded the same GSTH would improve resolution because the signal in the GSTH should be correlated and the noise is not (Beltrami et Mareschal, 1992, 1995; Clauser et Mareschal, 1995; Pollack *et al.*, 1996). In practice, this did not turn out to be true (Huang *et al.*, 2000; Gosselin et Mareschal, 2003). There are several reasons that joint inversion did not do much to improve the results.

1. The number of temperature profiles remains small and insufficient to produce a significant improvement in the signal to noise ratio which is $\propto \sqrt{N}$.

2. The assumption that the GSTHs are identical is almost never verified. One would not expect it to hold when the data cover a very wide region of the Earth. Even at the regional scale, visual inspection of the reduced temperature profiles reveals that they have not recorded the same GSTH. Thus, the joint inversion of real data seldom improves signal/noise ratio; sometimes it decreases this ratio.
3. Even when the GSTHs are identical at all sites, the records will be consistent only if the thermal diffusivity at each site is well determined. The danger of adjusting physical properties is that the GSTHs may appear well correlated when they are not.
4. The resolution is limited by the profile with the highest noise level which determines how much regularization is required (Beltrami *et al.*, 1997).
5. Beltrami *et al.* (1997) have emphasized the need to combine profiles with comparable vertical depth in order to avoid bias. The minimum depth sampled varies much between boreholes, because measurements above the water table are extremely noisy and are often discarded. This is an important bias because temperature perturbations are largest near the surface.

Different authors have calculated the GSTH (local or regional) from the raw or the « reduced » temperature depth profiles. The reduced temperature profile is obtained by removing from the data a reference temperature profile, obtained by upward continuation of the lowermost part of the profile, assumed to be near steady state. This preprocessing of data allows to infer warming or cooling by visual inspection of these reduced profiles. But it may also be useful to improve the results of the inversions using the singular value decomposition algorithm to determine regional GSTH.

So far, there is no consensus among researchers on the best procedure to obtain a regional GSTH (simultaneous inversion vs. average of individual inversions, selection of borehole temperature profiles unaffected by non-climatic perturbations vs. « indiscriminate » use of all the borehole temperature profiles, reduced vs raw temperature profiles). No systematic studies were conducted because there were not enough measurements in a given region to make statistically relevant comparisons. During the past 20 years, the GEOTOP-IPGP (Institut de Physique du Globe de Paris) research team has logged 338 boreholes at more than 100 different sites across south-central and south-eastern Canada (Figure 4.1). Because these sites are distributed in three main regions, northern Manitoba and Saskatchewan, north-western Ontario, and eastern Ontario and Quebec, these borehole temperature data are appropriate to conduct regional studies, and

the number of data in each region is sufficient to compare results from the different procedures.

2.4 Theoretical Framework

2.4.1 General formulation. The direct problem.

Usually, the data consist of a few temperature profiles, thermal conductivity, and heat production measurements. Because the temperature profiles are sparse and the boreholes where they were obtained are far apart, it is common to neglect lateral variations in physical properties, and in the boundary conditions. These assumptions are not always satisfied either because the surface boundary condition can vary (effect of lakes, vegetation cover, topography, etc.) or because physical properties vary horizontally and there may be refraction. This is likely to be the case with mining exploration boreholes that target very local mineralized bodies. In general, however, there is not enough information on the 3-D conductivity variations and insufficient data to warrant a three dimensional model.

For a layered earth, the steady-state temperature profile can be written as :

$$\begin{aligned} T_e z &= T_{ref} + q_{ref} R(z) - M(z) \\ R(z) &= \int_0^z \frac{dz'}{\lambda(z')} \\ M(z) &= \int_0^z \frac{dz'}{\lambda(z')} \int_0^{z'} dz" H(z") \end{aligned} \tag{2.1}$$

where λ is the thermal conductivity, H is the heat generation, z is depth, positive downward. The heat flow q_{ref} is taken positive upward. If a temperature perturbation $T_0(t)$ is applied uniformly on the surface $z = 0$, the temperature in a homogeneous half space is given by (Carslaw et Jaeger, 1959) :

$$T_t(z,t) = \frac{z}{2\sqrt{\pi\kappa}} \int_0^t \frac{T_0(t')}{(t-t')^{3/2}} \times \exp\left(\frac{-z^2}{4\kappa(t-t')}\right) dt' \tag{2.2}$$

where the thermal diffusivity κ is assumed constant.

For a jump ΔT in surface temperature at time t before present, the temperature perturbation is given by :

$$T(z) = \Delta T \times \text{erfc} \frac{z}{2\sqrt{\kappa t}} \tag{2.3}$$

If temperature increases linearly from 0 at time t before present to ΔT now, the surface temperature perturbation is given by :

$$T(z) = \Delta T \left((1 + \frac{z^2}{2\kappa t}) \times \mathrm{erfc} \frac{z}{2\sqrt{\kappa t}} + \frac{z}{2\sqrt{\kappa t}} \times \exp \frac{z^2}{4\kappa t} \right) \tag{2.4}$$

For a constant change in surface heat flux Δq starting at time t before present, the temperature perturbation is (Carslaw et Jaeger, 1959) :

$$T(z) = \frac{2\Delta q}{\lambda} \left((\frac{\kappa t}{\pi})^{1/2} \times \exp \frac{-z^2}{4\kappa t} - \frac{z}{2} \times \mathrm{erfc} \frac{z}{2\sqrt{\kappa t}} \right) \tag{2.5}$$

and, in particular, the change in surface temperature is given by :

$$T(z = 0) = \frac{2\Delta q}{\lambda} (\frac{\kappa t}{\pi})^{1/2} \tag{2.6}$$

Such a boundary condition was used by Beltrami (2001).

Figure 4.2 shows the temperature profiles for three different surface boundary conditions leading the same present surface temperature. As one would expect, warming is more rapid after a jump in surface temperature than after a jump in surface heat flow. This is well known, but the point is that the reconstructed history depends on the boundary condition, which is poorly understood. For instance, using a heat flow boundary condition might lead to underestimating the time when the change in surface temperature conditions occurred.

It is possible to account for variations in thermal diffusivity with depth. Formal solutions for the transient temperature in a horizontally layered half space are easily obtained with the Laplace transform (e.g. Carslaw et Jaeger, 1959). It is thus possible to include the variations in thermal diffusivity in the equations but advantages are too small to warrant the additional complications. The « Born approximation » to the general solution of the heat equation for continuously varying physical properties with depth is given in Shen et Beck (1991). Because thermal diffusivity variations are usually small, their effect on the transient temperature profile is a second order perturbation that can safely be neglected in view of all the other sources of error, provided that the average diffusivity is well determined. This does not hold true for the effect of conductivity variations on the steady state temperature profile which must be accounted for.

2.4.2 The inverse problem

For borehole temperature data, the inverse problem consists of determining, from the temperature depth profile, the reference surface temperature and heat flow, and the ground surface temperature history. Determining the reference heat flow requires knowledge of the thermal conductivity variations, usually measured on core samples. Alternatively, the thermal conductivity structure can be introduced as free model parameters through the thermal resistance vs depth in equation (2.1), but in this case the inverse problem becomes non-linear.

Generally, the inverse problem can be expressed as an integral equation :

$$T(z) = \int_{-\infty}^{0} \Delta T(t') K(z, t') dt' \tag{2.7}$$

where the kernel $K(z, t')$ is given in equation (2.2). It turns out that this type of integral equation always describes an ill-posed problem. If T(z) is known approximately, there is no solution to the inverse problem. Furthermore, an approximate solution is useless because the inverse operator is not continuous. The physical meaning of this instability is easy to understand. We can always add to the solution $\Delta T(t)$ a periodic function $N \sin(\omega t)$. Regardless how large N, the effect on the temperature profile $T(z)$ can be made arbitrarily small by increasing the frequency ω. In other words, the difference between the exact and the approximate surface temperatures could be arbitrarily large at almost any time. This is paradoxical, but we do take advantage of this property because we are mainly concerned with long period trends. In inverting temperature depth profiles, we can thus safely neglect the daily or the annual cycles although their amplitudes are at least ten times larger than those of the long term trends that we are trying to detect.

2.4.3 The inverse problem discretized

Because the temperature variations of short duration are filtered out of the temperature profile, any parametrization that allows to reproduce the gross features of the surface temperature history could be used. Many different parameterizations have been proposed for the GSTH : a discontinuous function corresponding to the mean surface temperature during K time intervals Δ_k $(k = 1, ...N)$, a continuous function varying linearly within K intervals Δ_k, a Fourier series, etc.

We shall assume that the GSTH is approximated by a discontinuous function corresponding to the mean surface temperature during K intervals of duration Δ_k (where the Δ_k can be adjusted to the resolution decreasing with time).

For a single temperature profile, the temperature Θ_j measured at depth z_j can be written as :

$$\Theta_j = A_{jl} X_l \tag{2.8}$$

where Θ_j is the measured temperature at depth z_j corrected for the heat production between the surface and that depth, X_l is a vector containing the unknowns $\{T_0, q_0, T_1, ..., T_K\}$, and A_{jl} is a matrix containing 1 in the first column and the thermal resistances to depth z_j, $R(z_j)$ in the second column. In columns 3 to $K+2$ the elements $A_{j,k+2}$ are obtained by calculating the differences between error functions at times t_k and t_{k-1} for depth z_j :

$$A_{j,k+2} = \text{erfc}\left(\frac{z_j}{2\sqrt{\kappa t_k}}\right) - \text{erfc}\left(\frac{z_j}{2\sqrt{\kappa t_{k-1}}}\right) \tag{2.9}$$

where κ is the thermal diffusivity. The other parameterizations mentioned above would yield a system of equations with the same structure.

Because the meteorological trends appear correlated over distances of ≈500 km (Jones *et al.*, 1986; Hansen et Lebedeff, 1987), boreholes from different sites in the same region may have recorded identical GSTH. If this is indeed the case, it is possible to derive this common GSTH from simultaneous inversion of all the temperature profiles that have recorded seemingly consistent climatic signals. For I boreholes, the unknown parameters are the I surface temperatures and heat flow values and the K parameters of the ground temperature history. The data are all the temperature measurements from all the boreholes. If N_i is the number of temperature measurements at borehole i, the matrix has $N_1 + N_2 + ... + N_I$ rows and $K + 2 \times I$ columns. The first N_1 elements of the first column equal 1 and all the others equal 0; the following N_2 elements in the second column are 1 and all the other elements are 0, and so on. The following I columns contain the thermal resistances to depth z_j in borehole i. Finally, the K last rows contain the differences between error functions at times t_k and t_{k-1} for every depth and every borehole. The

resulting equations can be written as (Clauser et Mareschal, 1995) :

$$\begin{bmatrix} \boldsymbol{\theta}^{(1)} \\ \boldsymbol{\theta}^{(2)} \\ \dots \\ \boldsymbol{\theta}^{(I)} \end{bmatrix} = \begin{bmatrix} 1 & 0 & \dots & 0 & \mathbf{R}^{(1)} & 0 & \dots & 0 & \mathbf{A}^{(1)} \\ 0 & 1 & \dots & 0 & 0 & \mathbf{R}^{(2)} & \dots & 0 & \mathbf{A}^{(2)} \\ \dots & \dots & \dots & \dots & \dots & \dots & \dots & \dots & \dots \\ 0 & 0 & \dots & 1 & 0 & 0 & \dots & \mathbf{R}^{(I)} & \mathbf{A}^{(I)} \end{bmatrix} \times \begin{bmatrix} T_0^{(1)} \\ T_0^{(2)} \\ \dots \\ T_0^{(I)} \\ q_0^{(1)} \\ q_0^{(2)} \\ \dots \\ q_0^{(I)} \\ \mathbf{T} \end{bmatrix} \tag{2.10}$$

where $\boldsymbol{\theta}^{(i)}$ denote the vectors of temperature data for borehole i and $\mathbf{R}^{(i)}$ denote the vectors containing thermal resistance to each depth in borehole i; the elements of the matrix $\mathbf{A}^{(i)}$ are the differences between error functions at time t_k and t_{k-1} for each depth of borehole i. Thermal diffusivity is usually assumed constant within each borehole but varies between boreholes. The unknown parameters are the I reference surface temperatures $T_0^{(i)}$, the I reference heat flows $q_0^{(i)}$, and the K parameters of the common ground surface temperature history contained in the vector $\mathbf{T}$. The reference temperature and heat flow determined by this procedure are only relative to the ground surface temperature history that is reconstructed. In Canada where the last glaciation and the glacial retreat are well documented, an adjustment to the heat flow is always made to account for the glacial interglacial history (e.g. Jessop, 1971).

Regularization by Singular Value Decomposition

The system of N linear equations defined by equations (2.8) and (2.10) must be solved for the $M = K + 2 \times I$ unknown parameters. In general, the system is both underdetermined and overdetermined, and it is unstable. If the system of equations $Ax = b$ is mixed-determined, a generalized solution can be obtained by the singular value decomposition (SVD) (Lanczos, 1961; Press *et al.*, 1992). It involves the decomposition of the $(N \times M)$ matrix A as follows :

$$A = U \Lambda V^T \tag{2.11}$$

where superscript T denotes the transpose of a matrix. The matrix U is an $(N \times N)$ orthonormal matrix (i.e. a rotation matrix) in data space, V is an $(M \times M)$ orthonormal matrix in parameter space, and Λ is an $(N \times M)$ diagonal matrix; the only nonzero elements are the L « singular

values » λ_l on the diagonal, $L \leq \min(N, M)$. The generalized solution is given by

$$x = V\Lambda^{-1}U^T b \tag{2.12}$$

where the $(M \times N)$ matrix Λ^{-1} is a diagonal matrix with the L elements $1/\lambda_l$ on the diagonal (for $\lambda_l \neq 0$) completed with zeros. The instability of the inversion results from the existence of very small singular values. In practice, this problem can be alleviated either by retaining only the $P \leq L$ singular values larger than a given "cutoff" or by damping the reciprocals of the smaller singular values. The damping is done by replacing the reciprocals of the smaller singular values λ_l by

$$\frac{1}{\lambda_l} \rightarrow \frac{\lambda_l}{\lambda_l^2 + \epsilon^2} \tag{2.13}$$

where ϵ will be referred to as damping or regularization parameter. The impact of noise can be reduced by selecting a higher value ϵ, which, however, decreases the resolution (Beltrami *et al.*, 1997). For borehole temperature data, the value of ϵ in joint inversion ranges between 0.1 and 0.3. The damping parameter is usually slightly higher than the singular value cutoff ($\approx$0.05). In practice, we make some assumption on the regularity of the solution and select the damping parameter accordingly (Parker, 1994). The procedure consists of selecting a relatively low value of the parameter, and examining the resulting GSTH ; if oscillations of large amplitude appear in the solution, the value of the damping parameter is increased until these oscillations are attenuated (Clauser et Mareschal, 1995). Oscillations in the very recent past are the result of the structure of the eigenvectors in model space and are difficult to eliminate altogether with a sharp cutoff. Although there is no compelling argument to prefer one method over the other, damping usually gives smoother results than the sharp cutoff. In particular, a proper selection of the damping parameter for individual inversions will reduce the amplitude of the oscillations during the 20^{th} century to a level comparable to that found in the meteorological records.

2.5 Description of the Data

The borehole temperature profiles used in this study were obtained by researchers at GEOTOP and at the Institut de Physique du Globe de Paris (IPGP) over the past twenty years. The measurements were made for determining heat flow in the Canadian Shield and are described in a series of papers (Pinet *et al.*, 1991; Mareschal *et al.*, 2000, 2005; Perry *et al.*, 2006).

This study separates in three regions all the borehole temperature depth profiles logged for

heat flow determination in the Canadian Shield by the GEOTOP-IPGP team over the past 20 years (Figure 4.1). In order to give the same weight to deep boreholes in the simultaneous inversion, all boreholes deeper than 550 meters were truncated to that depth. This procedure avoids biasing the inversion toward the GSTH recorded by deeper holes (Beltrami et Mareschal, 1995). Because the LIA affect the temperature profiles to $\approx$ 400m depth, the depth selected allows to detect the variations in ground surface temperature of the past 500 years. Also, since shallow boreholes are very difficult to reduce with accuracy and to invert, they could affect the simultaneous inversions. Therefore, all boreholes shallower than approximately 350 meters were automatically rejected. Between 1100 and 1900 AD, all the proxy data indicate that the variations in ground surface temperature remained relatively small. Their effect on the temperature profile beneath 300m is sufficiently small that the reference heat flow and surface temperature (relative to that period) are well determined. This does not hold for the glacial-interglacial cycle which affects the profile to depths in excess of 2500m (Hartman et Rath, 2005). In Canada, an adjustment accounting for this cycle is routinely made to determine the surface heat flow.

The boreholes located in central Canada between the provinces of Saskatchewan and Manitoba were logged between 1993 and 1999. Table 2.1 shows the location of all these boreholes with their depth and a remark explaining if it was retained for inversion or the reason why it was rejected.

The second region selected in this study covers a large part of north-western Ontario. Most of the boreholes in this region were logged between 2000 and 2005 and their locations, depths and remarks are shown in Table 2.2.

The third region covers the eastern part of Ontario and the western part Quebec. The temperatures measurements were made for heat flow determination between 1987 and 1993. The location, depth and remarks for each borehole are given in Table 2.3. Because at that time the objective of the measurement was not the study of climate change, the surface conditions were not sufficiently documented to select boreholes suitable for inversion. Only, the shallowest boreholes have been eliminated from the study. Analysis of this data-set will allow to compare the trends in three different regions when all the measured boreholes are retained for inversion.

For all profiles, temperature measurements are made at 10 m intervals using an electrical

cable and a probe equipped with a thermistor. The precision of these measurements is of the order of 0.002 K and the overall accuracy is better than 0.02 K. The GEOTOP-IPGP research team is equipped with several cables ranging from 600 m to 2.3 km and with probes capable of measuring temperatures in the range between -15 to 50 degrees Celsius.

For each borehole, core samples were collected to measure their thermal conductivity. Usually, the core is sampled every 80-100 m, and wherever important changes in lithology occur. Thermal conductivity is determined by the method of divided bars (Misener et Beck, 1960). Heat generation is also determined for the heat flow studies. Heat generation is usually low in the Canadian Shield and has little effect on the shallow part of the temperature profiles, and it can be ignored except for very deep boreholes.

Each profile was carefully examined and when necessary erratic data points in the shallow part of the profile were removed. These erratic values are caused by the probe not equilibrating with the groundwater or by water movement near the ground surface. A test was performed to verify that this removal does not affect the GSTH. A synthetic temperature depth profile was inverted using first the complete profile, then the same profile without the first 30 meters, and finally the same profile without the first 60 meters. The results showed almost no difference in the GSTH between the complete and the profile truncated above 30m, while the resolution of the recent past decreases for GSTH obtained from the profile truncated above 60 m. This test shows that the removal of one or two data points in the topmost 20 meters of many boreholes does not strongly affect the recent part of the GSTH.

2.6 Results

2.6.1 Tests with Synthetic Data

The SVD method for simultaneous inversions has been thoroughly tested for regional GSTH by using multiple series of 84 synthetic temperature depth profiles containing a ground surface temperature history signal of 600 years similar to those appearing in recent publications for central and eastern Canada (Guillou-Frottier *et al.*, 1998; Gosselin et Mareschal, 2003; Beltrami et Mareschal, 1992). Each synthetic temperature depth profile had random noise added to it ; this noise had approximately the same level we observe in measured data. We verified

that varying some parameters of the synthetics (noise level, sampling interval, total depth of the profile, reference gradient and surface temperature) does not affect the GSTH.

Most of the parameters mentioned above had little or no effect on the simultaneous inversions. However, we noticed instabilities when the average of all reference temperatures had a value other than 0. Large oscillations appeared in the GSTH as well as a jump in surface temperature at the beginning of the history. We carefully examined and interpreted the resolution matrices as showing a spill-over of the reference temperatures to the rest of the matrix when a large number of profiles were simultaneously inverted.

In order to prevent this « spill-over » of the reference temperatures into the solution, it was simply removed by using the reduced temperature profiles (i.e. the difference between the observed and reference profiles). When properly reduced, a profile only shows the perturbations to the steady-state temperature in the borehole without any information on the reference temperature or gradient. Further tests with series of synthetic temperature depth profiles showed that GSTHs obtained from reduced profiles accurately recover the input.

Although no problems were identified when using observed temperature profiles for individual inversions or simultaneous inversions using a limited number of profiles, it is recommended to use reduced profiles when inverting simultaneously many profiles.

2.6.2 Study with Real Data : Selection of Profiles and Interpretation

Manitoba-Saskatchewan

The first data set analyzed was from the Saskatchewan-Manitoba region (Figure 1), consisting of 106 boreholes logged between 1993 and 1999. First, all boreholes shallower than approximately 200 meters were eliminated. This was necessary because the reference gradient for such shallow profiles is too poorly constrained for the profiles to be reduced. Also these shallow profiles do not provide the desired time window for this study. Another 3 boreholes (9903, 9904 and 9905) from the Kississing Lake site were removed from the dataset because the lake effect was so overwhelming that it overshadowed the signal of the other profiles. This limited to 73 the number of usable boreholes for the regional study in Saskatchewan-Manitoba. From these

73 boreholes, only 13 were considered affected by no other surface condition than a temporal change in the ground surface temperatures. Table2.1 lists all the boreholes in the region with their characteristics and the non-climatic effects that were noted. The reduced temperature profiles for the entire data set show a lot of variability and seem inconsistent; however, the 13 retained profiles are much more similar and consistent with each other. All the profiles are shown in Fig 2.3a. Since most of these profiles are affected by non-climatic factors, the variability is considerable, although an overall warming trend is clearly visible and can also be inferred from the average GSTH. If only the 13 unaffected temperature depth profiles are plotted (Figure 2.3b), the variability decreases dramatically and not only the amplitude of the recent warming, but the onset of the little ice age (LIA) is also apparent. However it is also worth noting that the average of the reduced temperature profiles of the entire and selected datasets are almost identical.

Unless otherwise noted, the same parametrization was used for all the inversions in this study (i.e. 20 year time steps covering 600 years). Thermal conductivity and diffusivity were assumed constant for all inversions in this paper and heat production values were not taken into consideration.

The 73 temperature depth profiles were inverted simultaneously with the same parametrization and a value for regularization parameter, $\epsilon = 0.3$. A larger regularization parameter than for the individual inversions is necessary because the singular values are different and decrease more slowly than those of individual inversions. In order to obtain comparable information between individual and simultaneous inversions, one needs to use approximately the same number of singular values for both. Thus, the cut-off needs to be higher in simultaneous inversions than in individual inversions. The result from the simultaneous inversion was then compared with a simultaneous inversion using only the 13 selected profiles and is shown in Figure 2.4.

One of the problems of most inversion techniques is the occurrence of instabilities due to the inversion. Actually, the main difficulty is the proper tradeoff between stability and resolution. In the case of SVD, the instability affects the larger singular values and thus the recent past in the GSTH; it is seen as marked oscillation at 20-40 years before present. In this study, the inconsistencies between the records of various boreholes are causing these instabilities. It casts serious doubt that any conclusion concerning the very recent past can be derived from the simultaneous inversion of noisy records. In the data space, the corresponding eigen vectors

sample mostly the shallow part of the profile, which is noisiest, i.e. the most affected by non-climatic surface perturbations.

To alleviate the instability problem and to gain perspective on the resolution of the simultaneous inversions, we calculated the averages of inversion for all the individual profiles from the complete and the selected data-sets. Each profile from the complete data-set of 73 profiles was inverted, using the same regularization parameter for all the profiles($\epsilon = 0.05$), but adapting the parametrization for the shallow profiles. These individual GSTHs were then averaged in order to obtain a regional GSTH. For the 13 selected profiles, each inversion was optimized by using the smallest regularization parameter possible while preserving the stability of the inversion. There is a major difference between the results obtained from the entire dataset and those from the selected profiles. It concerns the LIA minimum (ca. 1820 A.D.), which is more pronounced in the selected profiles than with the entire dataset. There are two factors explaining that difference of amplitude. First, as mentioned above, the 13 selected profiles were inverted using unique optimized regularization parameters, meaning each individual inversion was optimized for maximum signal to noise ratio. This optimization is impossible to perform on the complete data-set (73 profiles) because the signal is often non-climatic, and the optimization would amplify the noise. Without even amplifying the noise, the many profiles (60 out of of 73) that recorded non-climatic effects will dominate the average and yield near zero temperature perturbation at the time of the LIA. It is noteworthy that individual inversions are performed independently and that there is no constraint to fit a unique model, whereas a simultaneous inversion does have this constraint. In profiles severely affected by non-climatic perturbations, the climatic signal can be taken into consideration by the simultaneous inversion. So in the case of a simple average of individual inversions, the fact that all GSTHs have the same weight means that random non-climatic perturbations will weight heavily on the overall average.

On the other hand, the average of individual inversions has the advantage of being more stable than a joint inversion. Since these instabilities are usually not correlated to the climatic signal, the average of several GSTH will ultimately cancel most of the instabilities and yield a reasonable value in the interval 20-40 years before present (Figure 2.4).

Northwestern Ontario

The second data-set analyzed for this study was from Northwestern Ontario (Figure 4.1). It consists of 56 boreholes logged between 2000 and 2003. All boreholes shallower than approximately 200 meters were eliminated. All the profiles in the dataset are displayed on Figure 2.5a. Temperature depth profiles from two more sites were removed from the data-set because of the overwhelming effects they had on the inversions. The profiles (0306, 0307 and 0308) from the Junior Lake site where an important forest fire had occurred a few years before measurements were eliminated. We also eliminated the profiles from Seagull (0112 and 0113) because of the overwhelming effect of water and gas rushing out of an over-pressured zone at depth. The perturbed Seagull profiles are easily identifiable on Figure 2.5a. Water was still rushing out of the borehole several weeks after the drilling operations had stopped. The complete dataset of usable boreholes for northwestern Ontario contained 35 boreholes. From this set, 15 were considered unaffected by non-climatic perturbations. The description of the boreholes and the reasons for eliminating some profiles are listed in Table 2.2. The resulting reduced profiles are shown on Figure 2.5b. The complete dataset includes some very noisy profiles. As in central Canada, the selected profiles exhibit more consistent trends than the complete data set, but the average reduced profiles of both datasets are similar.

As for Manitoba-Saskatchewan, we obtained four different regional GSTHs by inverting jointly and by averaging individual inversions of the complete and of the selected datasets (Figure 2.6).

The inversions were performed with the same temporal parametrization as for Manitoba-Saskatchewan (20 year time steps covering 600 years before present). However, because the northwestern Ontario boreholes were generally noisier than those in Saskatchewan-Manitoba a higher value was selected for the regularization parameter of individual inversions ($\epsilon = 0.1$).

The regional GSTH using the complete dataset of 35 temperature depth profiles and the selected dataset of 15 profiles were inverted with a regularization parameter $\epsilon = 0.2$ and 0.15 respectively. Despite the high noise level, the regularization parameter is smaller than the one used for Manitoba-Saskatchewan region mainly because there are less temperature depth profiles (and thus lower singular values) in the complete data set than in Manitoba-Saskatchewan. On

Figure 2.6, the GSTHs are reasonably similar until 100 years before present. But the GSTH for the complete dataset is very unstable in the most recent 100 years, showing a serious warming followed by a sudden 1.0 K drop over a 20 year interval and a 1.25 K jump in the last 20 year step. This clear non-climatic signal is most likely due to the sum of two factors : 1) an effect of the noisier profiles measured in that region, and 2) the inversion instability.

The average of the individual inversions for the region confirms that this oscillation is due to the instability of the inversion. For the individual inversions, each profile contained in the complete dataset was inverted with a regularization parameter $\epsilon = 0.1$; the profiles contained in the selected dataset were all optimized using the best signal to noise ratio possible (smallest regularization parameter). The results are also plotted against the simultaneous inversions on Figure 2.6. This suggests that the large oscillation in the simultaneous inversion of the complete dataset is non-climatic, since none of the averages show such a jump.

The study of western Ontario has also shown that simultaneous inversion of all boreholes in a given region regardless of the site conditions is likely to lead to an erroneous GSTH. A single very perturbed profile has the potential to cause major non-climatic shifts in the final GSTH. This happened with the accidental inclusion of the Seagull site (boreholes # 0112 and 0113) in the data set. The resulting GSTH was very much affected, showing a full degree drop in temperatures with the minimum occurring at the exact time of the LIA minimum (1780 A.D.). This apparent LIA signal was due only to the inclusion of the Seagull site where the temperature profile was extremely perturbed by the gushing out of water and gas that persisted years after drilling. The GSTH without that site contains no LIA signal in western Ontario.

A comparison of the curves obtained by averaging individual inversions of both datasets shows similar GSTHs for the first 300 years and then some divergence in the recent most past, as was observed in the averages of Manitoba-Saskatchewan. As was the case in Manitoba-Saskatchewan, the presence of profiles perturbed by random non-climatic effects in the complete dataset tends to bring the average near zero.

The obvious difference between the first two regions is the absence of any LIA signal from the western Ontario datasets. Regardless of noise level or depth, we could not see a LIA cooling period in the GSTH from any of the profiles and are confident that it is missing in that part of

Canada.

Eastern Ontario and Quebec

The third dataset used for this study contains the oldest measurements taken by the GEOTOP-IPGP research team in Quebec and in eastern Ontario between 1987 and 1992 (Figure 1). As mentioned before in this paper, these measurements were taken solely for heat flow studies and there is very little documentation on the actual measurement sites. Because of this lack of information, the analysis of the data from this region was done only on the complete dataset, as it was impossible to identify non-perturbed sites with certainty. Although a total of 137 boreholes had been measured, the complete dataset consists only of 28 usable boreholes because many of these boreholes are too shallow and/or severely perturbed (Table 2.3). The reduced profiles are displayed on Figure 2.7. Like in the other two regions, these profiles are quite inconsistent, but the average of all the reduced profiles is not very different from those obtained in the other regions. When we revisited some of these sites, we found out that they were affected by non-climatic perturbations. Some of these 28 boreholes would thus be rejected if we could apply the same strict criteria as in the other two regions.

The 28 temperature depth profiles were all individually inverted using the same parametrization as for the other regions and $\epsilon = 0.1$. The regional GSTH for eastern Canada was performed by simultaneously inverting the complete dataset of 28 temperature depth profiles with a regularization parameter $\epsilon = 0.3$. As for the other two regions, an average of individual inversions was also performed in order to compare the two methods as well as the effects of potential instabilities. Both curves are plotted in Figure 2.8. The difference in amplitude of the LIA minimum (1800 A.D.) between the joint inversion and the average is similar to that observed in central Canada and has the same explanation, the weight of the random non-climatic perturbations minimizing the GSTH. Therefore, we think that the LIA signal detected in eastern Canada is real. For the recent past (past 60 years), there are differences between the two curves. The joint inversion yields a very unstable GSTH in the very recent past (recent most 60 years). This is another indication that the shallow section of some of the profiles is dominated by noise (i.e. non climatic effects). The regional GSTH obtained from the average of individual inversions probably yields the best (i.e. most stable) GSTH for that period, as the instabilities are canceling out in the averaging process.

2.7 Discussion

The study was undertaken to compare different procedures to process and invert a regional GSTH from borehole temperature depth profiles, in particular : (1) Is it better to select boreholes that are not affected by non climatic perturbations, or does the noise from these perturbations cancel out ? (2) Is it better to perform a joint inversion of all the temperature depth profiles than to average the results individual inversions? The most important conclusion is that the results obtained by different procedures remain fairly consistent with each other, and the differences between methods are less than the error limits. Provided the inversions are carried out with sufficient care, similar trends will be inferred from all the procedures. This does not mean that they yield identical results. When choosing a particular procedure, we are faced with the standard problem of the tradeoff between resolution and stability of the inversion.

- Whenever possible, i.e. when the sites are well documented, it is much better to select temperature profiles that are not perturbed by non-climatic effects near the surface. Regardless of the method used (joint inversion or averaging of individual inversions), the GSTHs have higher resolution and are more stable than those of the entire dataset.
- Because selected profiles are less noisy than all the profiles from a region and the resolution is determined by the level of noise in the noisiest of the profiles, it is better to invert jointly selected profiles. In other words, the joint inversion of non selected profiles does not improve at all the resolution which is degraded by the level of noise of the noisiest profile. It increases the instability because the eigen vectors in data space that correspond to the large singular values sample the shallow part of the profile that is most affected by the non-climatic perturbations. The resolution is improved by selecting profiles that are not affected by non-climatic signals.
- The average of all the GSTHs from a region has very poor resolution. The individual inversions of all the profiles from a region always yield GSTHs that are very inconsistent with each other. This supports the view that the non-climatic effects are more or less random, but these effects often overwhelm the climatic signal in the individual inversions.
- This study comforted us in the opinion that few good data always yield much better results in terms of resolution and stability than many low quality data. Whenever possible, i.e. when there is a sufficient number of profiles that are well documented, a selection of profiles should be made.
- It is worthwhile to compare the GSTH obtained by averaging individual inversions and by

joint inversion of the selected profiles. When profiles are selected, individual inversions yield consistent results. If each individual inversion is optimized, the resolution of the average of the individual inversions is better than that of the joint inversion of the same profiles. Also, the average of the inversions of selected profiles does not show large amplitude oscillations in the very recent past. It appears that averaging individual inversions yields more stable results than the joint inversion of the same profiles. In particular, the amplitude of the oscillations in the averaged GSTH during the 20^{th} century is comparable to that in the meteorological records.

- The comparison of GSTHs using complete and selected temperature depth profiles, show no systematic warming trend due to non-climatic perturbations. If there were systematic warming effects on these perturbed profiles, these would be apparent in the different comparisons of GSTH techniques presented in this paper. However, contrary to the suggestion by Lewis (1998), there does not seem to be any sign of bias in the data and no systematic warmer trend in the GSTH obtained from all the profiles measured in a region than in that obtained from selected profiles.

Determining the ground surface temperature history from borehole temperature profiles in south-central and southeastern Canada has been the object of many studies (Nielsen et Beck, 1989; Beltrami et Mareschal, 1991, 1992; Wang *et al.*, 1994; Guillou-Frottier *et al.*, 1998) (Majorowicz *et al.*, 1999; Gosselin et Mareschal, 2003). Our results are consistent with previous results, but because different approaches were used to process the data, our study clarifies the problems of resolution and robustness of the regional GSTH. Our results are consistent with each other but differ in resolution with some trends that are well marked only with some methods.

- Regardless of the method used, there seems to be a warming signal ranging between 0.5 and 1.0 K over the past 500 years with some regions experiencing different warming rates. The LIA signatures obtained in Manitoba-Saskatchewan and and in eastern Canada are consistent and appear almost synchronous (with very limited time resolution). This suggests that the LIA occurred simultaneously across the central and eastern parts of Canada.
- On the other hand, the LIA is not found in northwestern Ontario, which is located between these two regions. This point was also discussed by Gosselin et Mareschal (2003). Although the Ontario profiles are in general noisier and shallower than those in Manitoba-Saskatchewan, we do not believe that this explains the absence of the LIA. Regardless of the depth or noise level of the profiles, none of the individual inversions shows the LIA

cooling. Two boreholes (logged by the Geological Survey of Canada in the early 1980s) located in northwestern Ontario but more than 500km to the north of our study area do show a LIA signal. One possibility is that the LIA did not occur near Lake Superior because the the local climate is affected by the lake.

- All regional GSTHs performed with selected temperature depth profiles show either a decrease or a stabilization of the warming rate in the recent past (20-40 years ago) before the most recent warming. This is in agreement with meteorological data from weather stations located in or near Central Canada, (as shown in Figure 10 from Gosselin et Mareschal (2003)). These mean annual surface air temperature data, smoothed by averaging over an 11 year window, show a cooling trend from the 1940s to the 1970s. Despite the 20 year steps used in the regional GSTHs and the difference between surface air and ground surface temperatures, the GSTHs from all three regions appear well correlated with meteorological data.

Overall, the best method to obtain a valid GSTH using temperature depth profiles measured in boreholes seems to be to 1) Carefully select boreholes for which all external perturbations other than climate have been ruled out 2) perform a simultaneous inversion of the selected temperature depth profiles selecting a regularization parameter adjusted to the noise level and number of profiles used in the inversion and 3) in order to confirm the GSTH and remove any instability caused by the inversion, also perform an average of individual inversions done on selected profiles with the lowest possible regularization parameter.

2.8 Conclusion

In general, we find that selecting temperature depth profiles that are not affected by surface conditions yields a GSTH with the highest resolution. When profiles have been selected, simultaneous inversion of all the profiles and averaging of individual inversions yield almost identical results.

Simultaneous inversion of noisy temperature depth profiles usually fails to improve signal to noise ratio and turns out to be very unstable. When profiles that are affected by surface conditions can not be eliminated, it is preferable to average the GSTHs of individual inversions. The resolution is always poor but the average GSTH is stable.

All the temperature profiles and additional tables are available on the GEOTOP website at http ://www.unites.uqam.ca/geotop/geophysique/flux/index.htm

2.9 Acknowledgements

The authors are grateful to two anonymous reviewers for their constructive comments. This work was supported by NSERC (Natural Science and Engineering Research Council of Canada) through a Discovery grant to JCM.

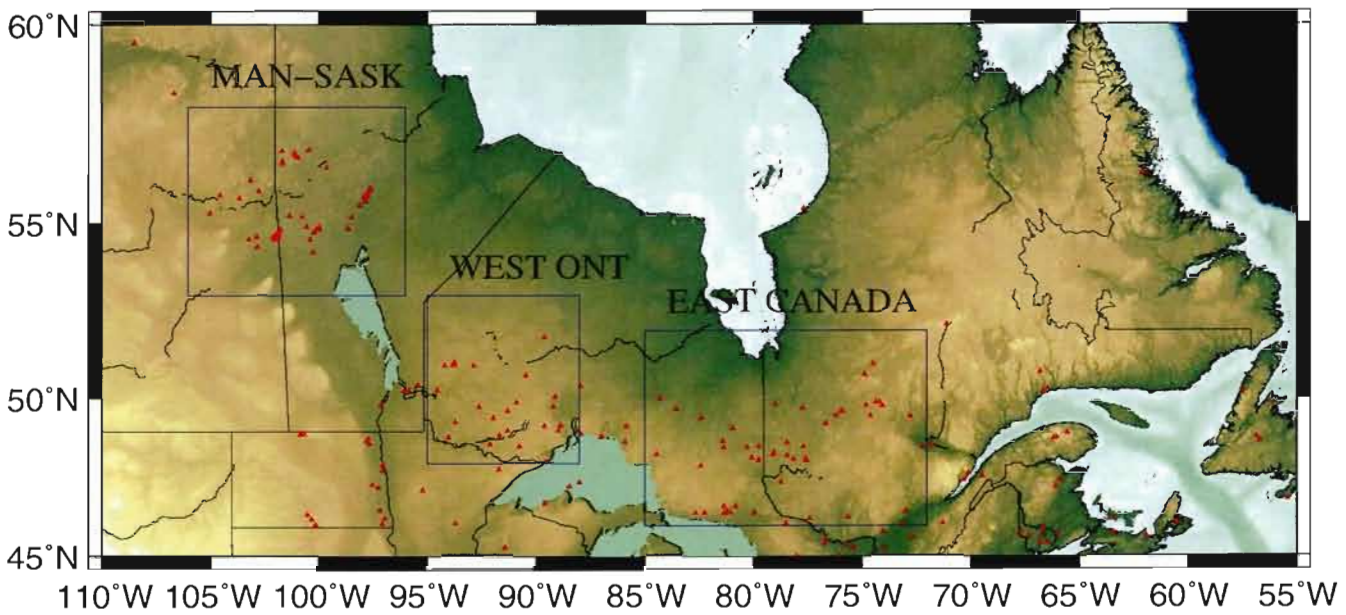

FIG. 2.1: Location map showing the three regions and the data used in this study. The blue rectangles delimits the three regions. The red triangles show all the borehole temperature depth profiles available in central and eastern Canada.

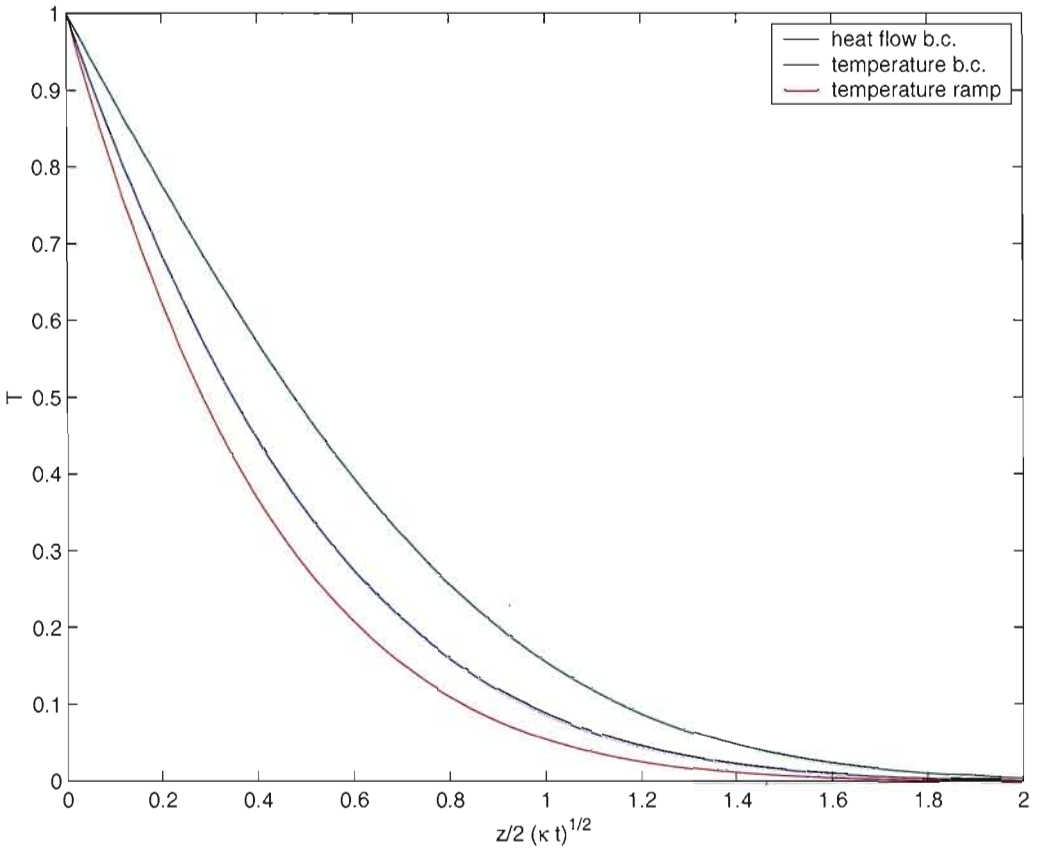

FIG. 2.2: Comparison of temperature profiles corresponding to different surface boundary conditions : Constant temperature, constant heat flux, and linearly increasing temperature.

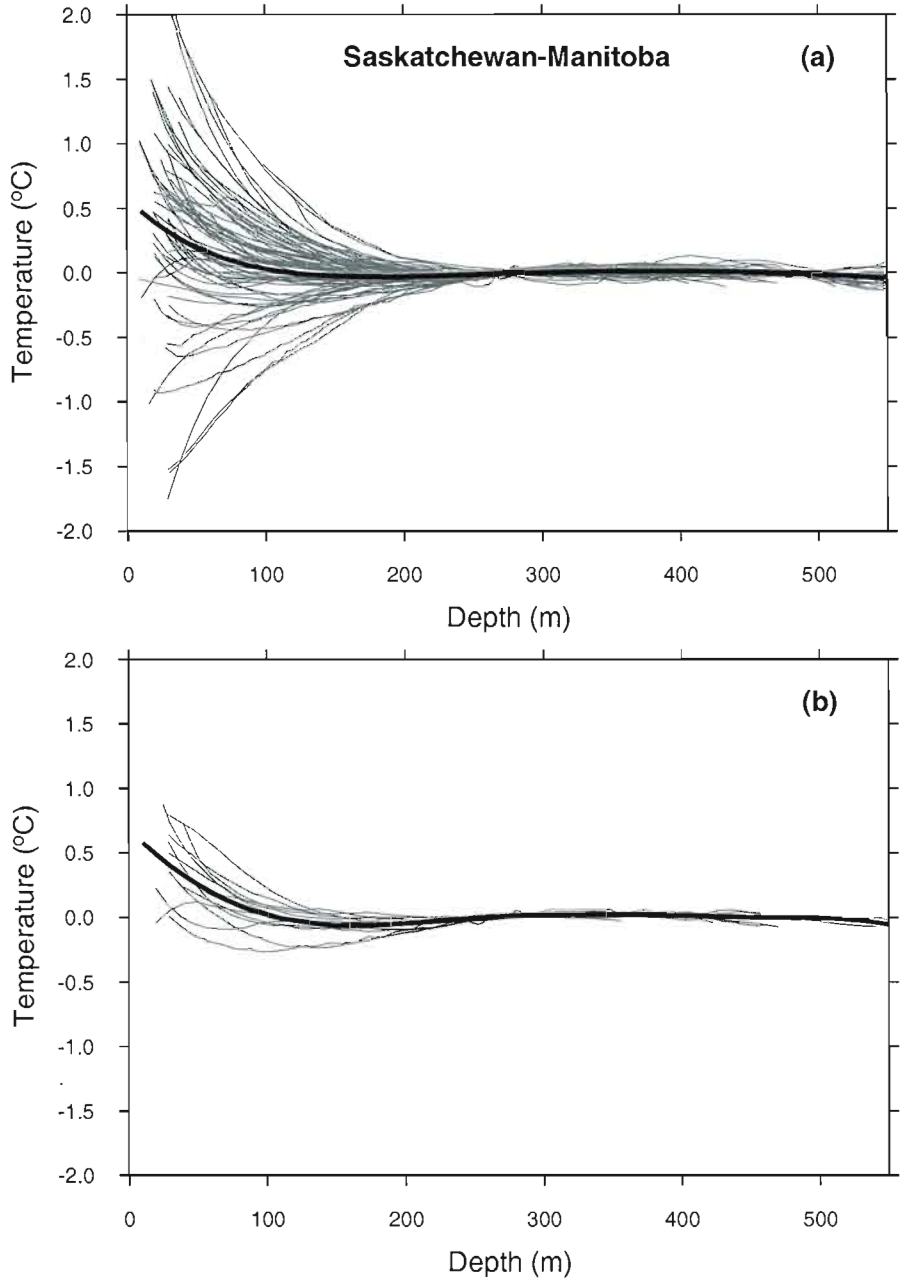

FIG. 2.3: Reduced temperature-depth profiles measured in northern Manitoba and Saskatchewan : (a) all the profiles recorded; (b) selected profiles not affected by non-climatic surface perturbations. The thick lines represent the average of all the temperature depth profiles.

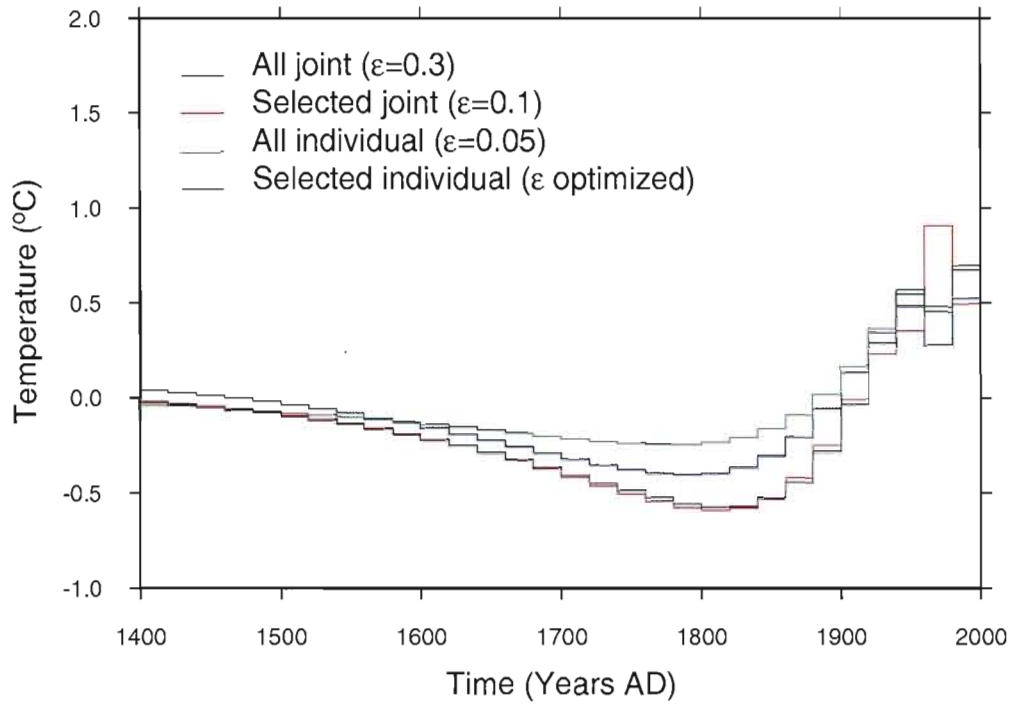

FIG. 2.4: Comparison of ground-surface temperature histories obtained using different methods for the Saskatchewan-Manitoba region.

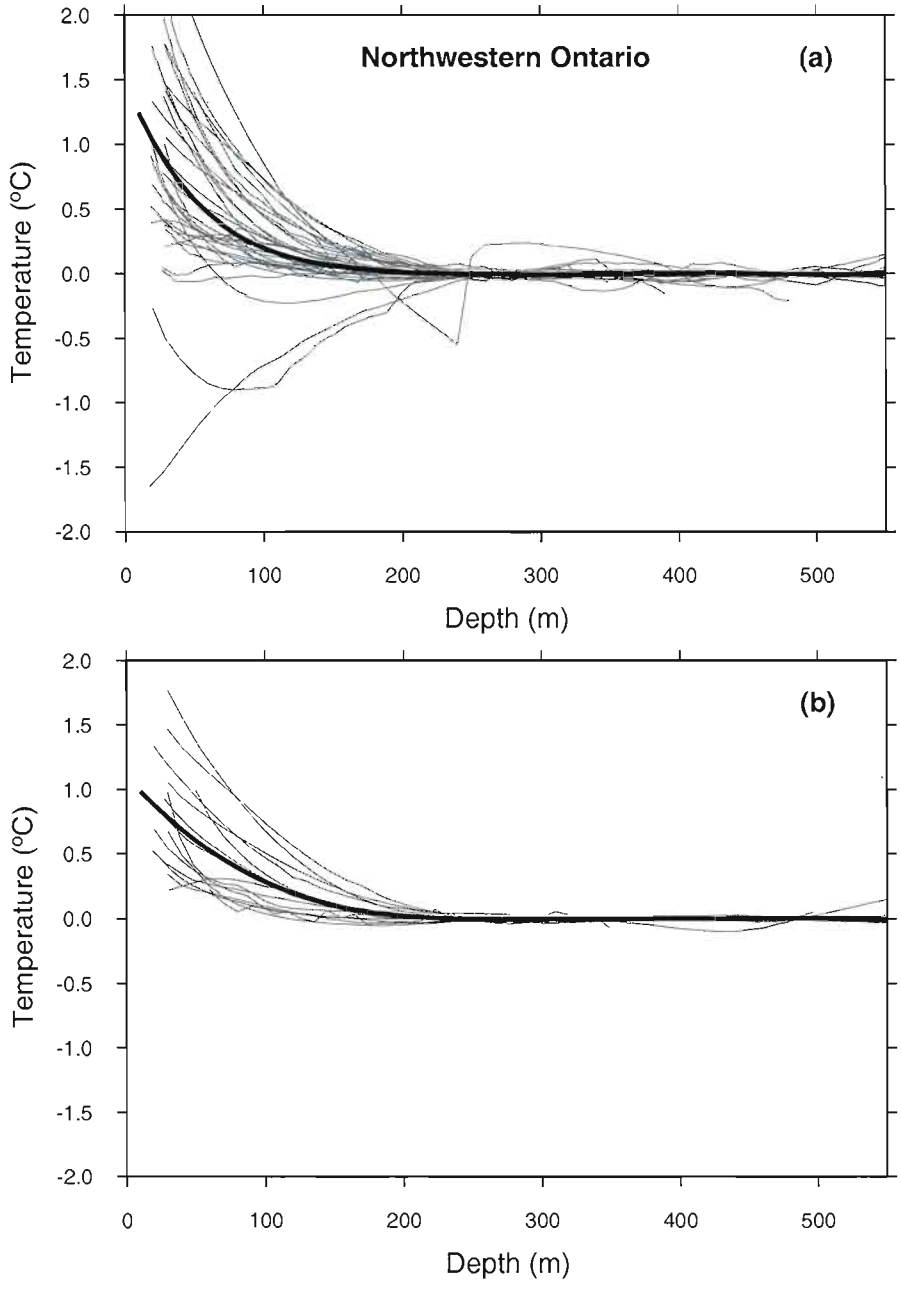

FIG. 2.5: Reduced temperature-depth profiles measured in northwestern Ontario : (a) all the profiles recorded; (b) selected profiles not affected by non-climatic surface perturbations. The thick lines are the averages of all the profiles.

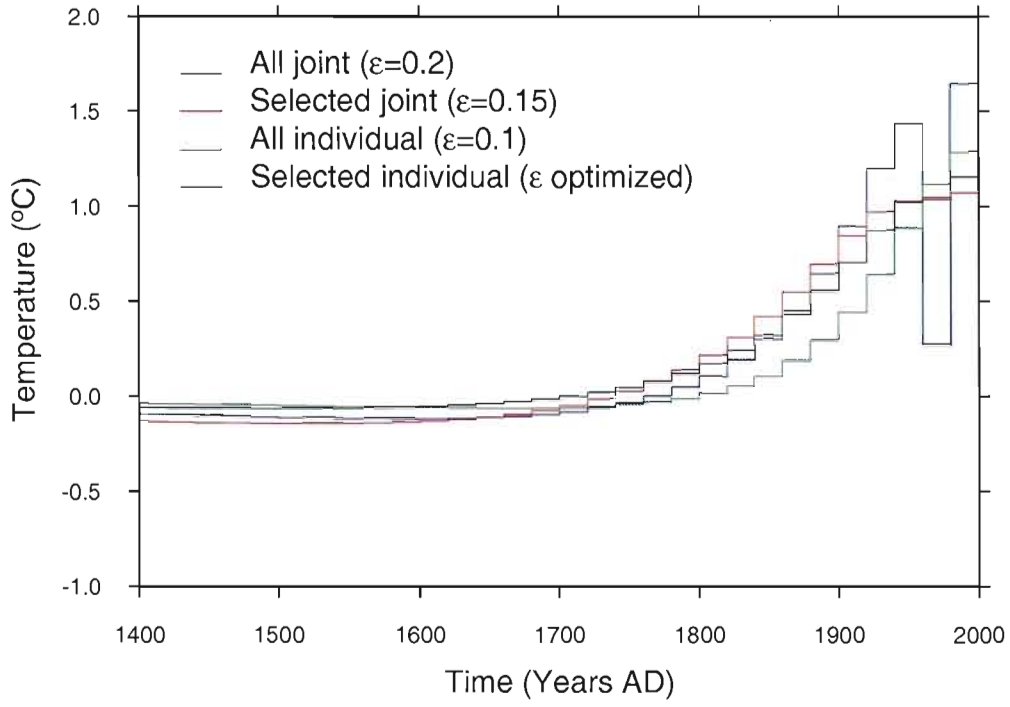

FIG. 2.6: Comparison of ground-surface temperature histories obtained using different methods for the northwestern Ontario region.

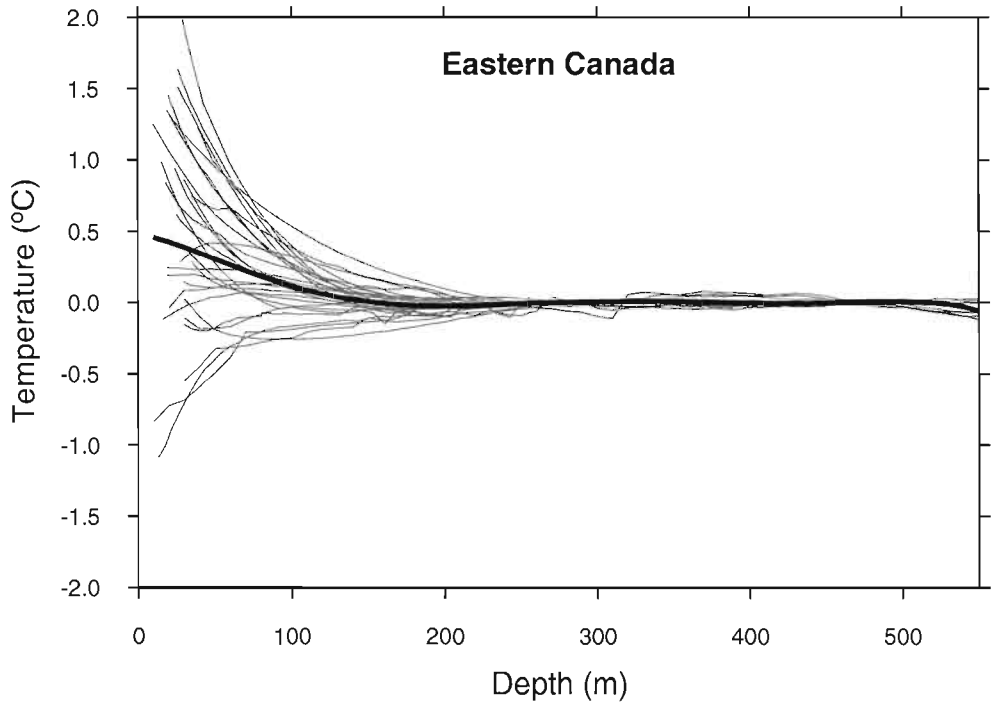

FIG. 2.7: Reduced temperature profiles measured in eastern Ontario and western Quebec. The thick line represents the average of all the profiles. Surface conditions were not documented to eliminate « noisy » profiles.

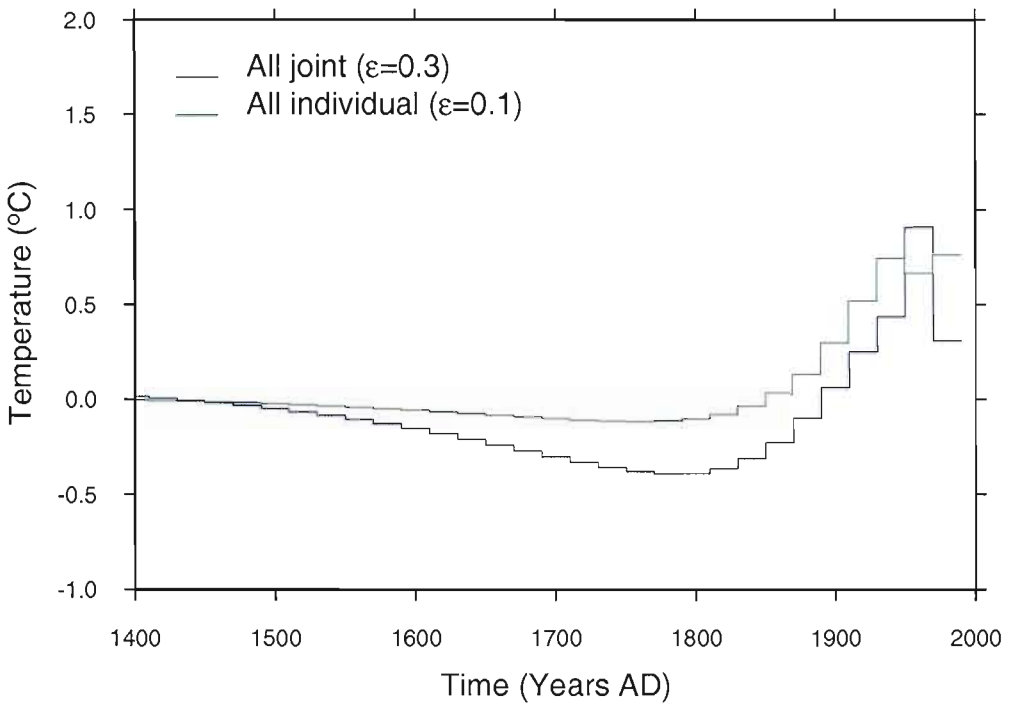

FIG. 2.8: Comparison of ground-surface temperature histories using two different methods for the eastern Canada region.

TAB. 2.1: Saskatchewan-Manitoba temperature profiles. For each borehole deeper than 300m, we give the location, the log identification number, the geographic coordinates, the vertical depth measured (Δh) and either that it was selected or the identified cause of non climatic perturbation.

Site	Log i.d.	Latitude	Longitude	Δh,m	Selection Comment
Wabowden	9301	54°52'29"	98°38'39"	810	Lake
Wabowden	9302	54°52'29"	98°38'39"	810	Lake
Flin Flon	9303	54°47'00"	101°53'00"	507	Steep topography
Flin Flon	9304	54°47'14"	101°53'10"	542	Steep topography
Schist Lake	9305	54°43'11"	101°49'57"	870	Lake
Reed Lake	9306	54°34'15"	100°22'50"	433	Lake
Flin Flon	9307	54°47'14"	101°53'17"	577	Steep topography
Snow Lake	9308	54°52'04"	99°58'52"	645	Selected for GSTH
Snow Lake	9309	54°51'16"	99°57'15"	686	Selected for GSTH
Birchtree Mine	9405	55°41'59"	97°53'50"	521	Refraction
Thompson Station	9407	55°44'25"	97°49'22"	991	Refraction
Moak Lake	9408	55°54'21"	97°40'06"	267	Selected for GSTH
Moak Lake	9409	55°53'53"	97°40'41"	470	Selected for GSTH
Pipe Mine	9410	55°29'17"	98°07'50"	386	Large tree clearing
Pipe Mine	9411	55°29'10"	98°07'54"	840	Large tree clearing
Pipe Mine	9412	55°29'17"	98°07'50"	938	Large tree clearing
Thompson Station	9413	55°44'46"	97°48'48"	555	Refraction

Site	Log i.d.	Latitude	Longitude	Δh,m	Selection Comment
Ruttan Mine	9414	56°29'07"	99°36'21"	415	Water flow
Ruttan Mine	9415	56°28'50"	99°37'09"	821	Water flow
West Arm	9501	54°38'13"	101°50'51"	1180	Steep topography
Cormorant Lake	9502	54°12'49"	100°13'47"	352	Lake, steep topography
Cormorant Lake	9503	54°13'05"	100°13'32"	290	Lake, steep topography
Bigstone Lake	9504	54°34'31"	103°11'59"	244	Lake
Tartan Lake	9505	54°51'28"	101°44'23"	568	Lake, steep topography
Bigstone Lake	9506	54°34'31"	101°11'59"	616	Lake
Wasekwan Lake	9514	56°44'04"	100°57'01"	376	Selected for GSTH
Farley Lake	9516	56°34'84"	100°26'07"	589	Permafrost
Farley Lake	9517	56°34'84"	100°26'07"	558	Permafrost
Fox Mine	9519	56°37'52"	101°38'02"	423	Selected for GSTH
Farley Lake	9520	56°54'34"	100°26'18"	580	Permafrost
Waden Bay	9601	55°17'31"	105°01'11"	880	Steep topography, water flow
Brabant	9603	56°07'47"	103°42'24"	570	Selected for GSTH
Brabant	9604	56°07'54"	103°42'01"	541	Selected for GSTH
Brabant	9605	56°07'51"	103°42'16"	464	Selected for GSTH
McIlvenna Bay	9607	54°38'16"	102°49'42"	947	Lake, steep topography
McIlvenna Bay	9608	54°38'09"	102°49'42"	560	Lake, steep topography
Denare Beach	9609	54°39'29"	102°03'31"	585	Steep topography
Denare Beach	9610	54°39'28"	102°09'27"	534	Steep topography

Site	Log i.d.	Latitude	Longitude	Δh,m	Selection Comment
Frances Lake	9614	56°49'38"	101°06'08"	419	Lake
Frances Lake	9615	56°49'29"	101°06'25"	437	Lake
McWhirter Lake	9616	56°35'04"	101°39'36"	383	Lake
Batty Lake	9617	55°09'52"	100°45'34"	308	Selected
Missinipe	9618	55°44'55"	104°33'21"	282	Steep topography
Missinipe	9619	55°44'52"	104°33'29"	257	Steep topography
Missinipe	9620	55°44'48"	104°33'25"	265	Steep topography
Missinipe	9621	55°44'42"	104°33'10"	188	Steep topography
Missinipe	9622	55°44'50"	104°33'10"	247	Steep topography
Soab Mine	9701	55°11'30"	98°24'40"	568	Shallow part of hole not logged
Soab Mine	9702	55°10'14"	98°27'28"	680	Selected for GSTH
Chisel Lake	9801	54°50'44"	100°06'35"	715	
Chisel Lake	9802	54°50'48"	100°06'24"	765	Topography
Mystic Lake	9803	54°36'57"	101°58'09"	291	Lake
Batty Lake (9617)	9804	55°09'52"	100°45'34"	308	Selected for GSTH
Limestone Bay	9805	54°12'43"	100°13'43"	145	Lake
Leo Lake	9806	54°47'24"	101°34'11"	499	Steep topography
Leo Lake	9807	54°47'24"	101°34'12"	447	Steep topography
Knife Lake	9808	55°52'08"	102°44'25"	420	Topography
Knife Lake	9809	55°52'17"	102°44'13"	278	Too shallow
Mystery Lake	9812	55°49'40"	97°45'40"	898	Selected for GSTH

Site	Log i.d.	Latitude	Longitude	Δh,m	Selection Comment
Mystery Lake	9813	55°49'40"	97°46'36"	672	Unstable measurements
Pipe Mine	9814	55°29'10"	98°07'35"	345	Over-representation
Pipe Mine	9815	55°29'10"	98°07'42"	348	Over-representation
Pipe Mine	9816	55°29'20"	98°07'53"	380	Over-representation
Pipe Mine	9817	55°29'12"	98°07'47"	220	Over-representation
Morgan Lake	9818	54°45'34"	100°12'23"	668	Lake
Morgan Lake	9819	54°45'51"	100°12'53"	268	Lake
Callinan Mine	9901	54°47'00"	101°51' 30"	606	Clearing near highway
Kississing Lake	9903	55°12'08"	101°21'25"	380	Lake
Kississing Lake	9904	55°11'58"	101°21'34"	280	Lake
Kississing Lake	9905	55°11'53"	101°21'26"	300	Lake
Flin Flon	9906	54°46'23"	101°50'15"	1418	Lake and topography
Loonehead Lake	9907	54°55'54"	100°33'"48	523	Topography
Leo Lake	9909	54°47'25"	101°34'19"	469	Topography
Missinipe (9622)	9912	55°44'48 "	104°33'10"	255	Steep topography
Missinipe	9913	55°44'53"	104°33'97"	276	Steep topography
Missinipe	9915	55°45'26"	104°33'45"	255	Steep topography
Missinipe	9916	55°44'48"	104°33'25"	262	Steep topography
McCollum Lake	9917	56°08'48"	103°08'28"	225	Lake, forest fire
McCollum Lake	9918	56°09'34"	103°06'57"	394	Lake, forest fire
McCollum Lake	9919	56°08'55"	103°08'35"	254	Lake, forest fire

Site	Log i.d.	Latitude	Longitude	Δh,m	Selection Comment
McCollum Lake	9917	56°08'48"	103°08'28"	225	Lake, forest fire
McCollum Lake	9918	56°09'34"	103°06'57"	394	Lake, forest fire
McCollum Lake	9919	56°08'55"	103°08'35"	254	Lake, forest fire
Cluff Lake Mine	9920	58°22'36"	109°32'28"	330	Close to open mine pit
Shea Creek	9921	58°13'46"	109°31'05"	250	Water flow
Shea Creek	9922	58°13'43"	109°31'05"	730	Water flow
Shea Creek	9923	58°13'49"	109°31'12"	400	Water flow
Pipe Mine	0015	55°29'17"	98°07'50"	377	Over-representation
Moak Lake	0016	55°55'32"	97°37'09"	860	Large tree clearing
Owl	0017	55°40'17"	97°51'35"	916	Selected for GSTH
Barbara Lake	0018	56°53'20"	101°04'16"	385	Lake
Barbara Lake	0019	56°53'26"	101°04'55"	672	Lake
Pipe Mine	0020	55°29'16"	98°08'11"	326	Over-representation
Pipe Mine	0021	55°29'09"	98°07'54"	343	Over-representation
Pipe Mine	0022	55°29'30"	98°07'51"	375	Over-representation
Pipe Mine (9815)	0114	55°29'10"	98°07'42"	1610	Over-representation
Pipe Mine	0115	55°29'20"	98°07'54"	335	Over-representation
Owl	0116	55°40'17"	97°51'35"	1568	Same as 0017

TAB. 2.2: Northwestern Ontario Sites. For each borehole deeper than 300m, we give the location, the log identification number, the geographic coordinates, the vertical depth measured (Δh) and either that it was selected or the identified cause of non climatic perturbation.

Site	Log i.d.	Longitude	Latitude	Δh,m	Selection Comment
Red Lake	0001	51°00'47"	93°48'50"	805	Selected for GSTH
Balmertown	0002	51°09'59"	93°42'56"	1724	Selected for GSTH
Ben Lake	0003	50°53'26"	93°06'26"	338	Selected for GSTH
Ben Lake	0004	50°52'43"	93°06'15"	496	Selected for GSTH
Garnet Lake	0005	50°59'49"	92°49'27"	925	Lake
Mattabi Mine	0006	49°52'36"	90°59'45"	653	Steep topography, rail road, tree clearing
Mattabi Mine	0007	49°53'39"	90°59'51"	896	Selected for GSTH
Lac des Iles	0008	49°10'17"	89°36'18"	675	Selected for GSTH
Lac des Iles	0009	49°10'19"	89°36'19"	781	Topography
Thunder Bay South	0010	48°10'40"	89°29'04"	480	Steep topography, water flow
Thunder Bay South	0011	48°11'44"	89°28'58"	470	Steep topography, water flow
Geco Mine	0012	49°10'00"	85°49'29"	956	Steep topography
Geco Mine	0013	49°09'30"	85°48'36"	1435	Steep topography
Rainy River	0102	48°49'54"	94°00'46"	723	Selected for GSTH
Cameron Lake	0104	49°17'35"	93°43'11"	638	Selected for GSTH
Rainy River	0106	48°49'44"	94°00'54"	460	Selected for GSTH
Thunder Lake	0107	49°45'24"	92°36'53"	734	Selected for GSTH

Site	Log i.d.	Longitude	Latitude	Δh,m	Selection Comment
Thunder Lake	0108	49°45'27"	92°36'36"	770	Selected for GSTH
Big Whopper	0111	50°15'49"	94°33'57"	304	Too shallow
Seagull	0112	49°01'39"	88°57'27"	800	Water flow
Seagull	0113	49°01'39"	88°57'30"	890	Water flow
Chukuni River	0201	51°03'03"	34°44'02"	2028	Selected for GSTH
Abino Point	0203	51°06'16"	93°	575	Lake
Seagull	0206	49°01'35"	88°57'23"	800	Water flow
Pigeon River	0207	48°03'13"	89°31'36"	740	Noisy data
Seagull (Repeat of 0113)	0208	49°01'39"	88°57'30"	890	Water flow
Samuels Lake	0209	48°37'15"	92°05'43"	370	Selected for GSTH
Samuels Lake	0210	48°37'16"	92°05'47"	280	Lake
Lumby Lake	0301	49°02'09"	91°18'24"	573	Water flow
Lumby Lake	0302	49°02'38"	91°18'23"	412	Topography
Ardeen Mine	0303	48°32'24"	90°46'10"	597	Topography
Ardeen Mine	0304	48°32'35"	90°46'04"	587	Topography
Disraeli	0305	49°07' 49"	88°58' 01"	291	Steep topography
Junior Lake	0306	50°22'55"	87°56'58"	352	Forest fire
Junior Lake	0307	50°22'51"	87°56'59"	370	Forest fire
Junior Lake	0308	50°22'57"	87°57'09"	423	Forest fire
Gull River	0309	49°45'07"	89°11'16"	810	Selected for GSTH
Norwood	0310	50°03'47"	89°05'22"	390	Topography, Lake
Spruce River	0311	49°11'07"	88°52'23"	349	Selected for GSTH
Nipigon Bay	0312	48°55'11"	87°55'12"	423	Lake

TAB. 2.3: Eastern Canada temperature profiles : For each borehole deeper than 300 meters, we give the location, the log identification number, the geographic coordinates, the vertical depth measured (Δh) and the reason for not retaining the profile when it was not used. 59 out of the 127 logged boreholes are included in this table.

Site	Log i.d.	Longitude	Latitude	Δh,m	Selection Comment
Évain	8706	48°16'47"	79°05'49"	590	
Évain	8707	48°16'53"	79°05'25"	590	
Val d'Or	8708	48°05'57"	77°33'33"	357	
Val d'Or	8709	48°05'49"	77°33'22"	335	
Mont Vallières de St-Réal	8719	48°49'50"	65°57'35"	599	Topography
Mont Vallières de St-Réal	8720	48°49'53"	66°00'48"	600	Topography
Mont Vallières de St-Réal	8721	48°49'17"	66°01'17"	500	Topography
Dôme de Lemieux	8723	48°48'49"	66°07'48"	520	Topography
Dôme de Lemieux	8724	48°47'23"	66°10'54"	571	Topography
Dôme de Lemieux	8725	48°47'08"	66°08'55"	350	Topography
Desmaraisville	8736	49°36'54"	75°50'50"	335	Topmost 50m missing
Desmaraisville	8740	49°37'11"	75°52'12"	306	
Chapais	8742	49°47'19"	74°48'34"	519	
Chapais	8743	49°47'49"	74°48'33"	504	
Matagami	8744	49°42'58"	77°44'03"	600	
Matagami	8745	49°42'48"	77°44'03"	600	
Matagami	8746	49°42'56"	77°44'20"	600	

Site	Log i.d.	Longitude	Latitude	Δh,m	Selection Comment
Renfrew	8801	45°25'23"	76°42'17"	372	Noisy
Belleterre	8810	47°24'03"	78°42'41"	420	
Belleterre	8811	47°24'06"	78°42'37"	387	
Belleterre	8812	47°24'08"	78°42'43"	357	
Belleterre	8813	47°24'08"	78°42'46"	389	
Madoc	8814	44°30'14"	77°27'06"	330	Measurements in open pit
Cordova Mine	8820	44°32'00"	77°47'16"	377	
Darlington	8901	43°52'05"	78°43'00"	300	Industrial site
Snowdon	8905	44°51'24"	78°30'02"	318	Water flow
Snowdon	8907	44°51'27"	78°30'12"	300	Water flow
Limerick	8910	44°52'15"	77°43'18"	340	Noisy
Limerick	8911	44°52'17"	77°43'25"	425	Top 80m missing
Copper Cliff	8925	46°26'24"	81°03'56"	560	
Copper Cliff	8926	46°26'"	81°03'"	600	
Copper Cliff	8927	46°26'"	81°03'"	473	
Bourlamaque	9001	48°06'54"	77°44'58"	417	
Selbaie Mine	9005	49°49'19"	78°57'48"	387	Water flow
Selbaie Mine	9006	49°48'53"	78°57'05"	407	Water flow
Selbaie Mine	9007	49°49'02"	78°56'40"	397	Water flow
Ile Marguerite	9008	49°53'36"	74°10'28"	593	Island
Ile Marguerite	9009	49°53'55"	74°10'12"	571	Island

Site	Log i.d.	Longitude	Latitude	Δh,m	Selection Comment
Lac aux Dorés	9010	49°52'50"	74°20'00"	440	
Lac aux Dorés	9012	49°52'50"	74°20'01"	317	
La Malbaie	9013	47°41'43"	70°05'42"	490	
Les Éboulements	9014	47°29'05"	70°19'43"	430	Water flow
Mine Belmoral	9101	48°07'45"	77°34'56"	316	
Mine Belmoral	9103	48°08'20"	77°35'57"	360	
Mine Dumagami	9105	48°15'04"	78°26'13"	430	
Holloway Lake	9114	48°31'11"	79°43'07"	420	
Holloway Lake	9116	48°31'13"	79°43'16"	374	
Lebel-Grevet	9201	49°14'13"	76°39'12"	681	
Lebel-Grevet	9202	49°14'32"	76°39'13"	880	
Lebel-Grevet	9203	49°14'40"	76°39'12"	880	
Boyvinet	9204	49°36'12"	75°58'49"	511	
Boyvinet	9205	49°35'22"	75°59'10"	425	
Coniagas	9206	49°29'34"	79°10'22"	450	
Coniagas	9207	49°29'40"	76°10'22"	610	
Gamache	9209	49°28'46"	74°36'40"	486	
Gamache	9211	49°29'02"	74°37'04"	480	
Barraute	9212	48°31'50"	77°41'36"	370	
Barraute	9213	48°31'45"	77°41'08"	640	
Barraute	9214	48°31'50"	77°41'26"	620	

CHAPITRE 3

RECENT CLIMATE VARIATIONS IN THE SUBARCTIC INFERRED FROM THREE BOREHOLE TEMPERATURE PROFILES IN NORTHERN QUEBEC, CANADA

Publié dans *Earth and Planetary Science Letters* (2007), vol.263, pages 355-369.
doi : 10.1016\j.epsl.2007.093017

3.1 Résumé

Trois profils de température provenant de forages creusés dans le pergélisol du nord du Québec, au Canada, ont été utilisés afin de reconstruire l'histoire de la température à la surface du sol (HTSS) de la région. Les mesures ont été effectuées dans un désert rocheux à une altitude de plus de 600 m sur le plateau Katinniq, près de la pointe nord de la péninsule d'Ungava. Les forages ont été mesurés plus de 3 ans après avoir été forés, garantissant ainsi leur retour à l'équilibre thermique. Des mesures de conductivité thermique ont été faites sur des échantillons de carottes. La production de chaleur radiogénique est faible et peut être négligée. Les profils de température présentent de fortes déviations par rapport à l'état stationnaire dans les premiers 200 m. Nous supposons que ces déviations ont été causées par les variations récentes (moins de 300 ans) des températures de surface. Les reconstructions de l'HTSS obtenues par l'inversion des profils de température montrent un réchauffement systématique de 2.5 K, mais divergent de manière significative lorsque l'on s'attarde aux détails. Un des profils est considéré comme étant peu affecté par les effets topographiques ainsi que par les changements de conductivité thermique en profondeur et est analysé en détail en utilisant différentes méthodes d'inversions. Des méthodes directes ont également été utilisées afin de vérifier le potentiel des données à reconstruire adéquatement l'HTSS. Les résultats montrent un réchauffement marqué ($\approx$ 1.4 K) entre le milieu du 18^e siècle et 1940, suivi d'un épisode de refroidissement ($\approx$ 0.4 K) qui dura 40-50 ans, suivi d'un réchauffement très marqué de $\approx$ 1.7 K au cours des 15 dernières années. Les mesures de températures dans le forage indiquent que la plus grande partie du signal de réchauffement a bien eu lieu au cours des 15 dernières années. Les résultats obtenus

sont en accord avec les données météorologiques disponibles et les données provenant de différents proxies.

3.2 Abstract

Three temperature depth profiles recorded in permafrost in Northern Quebec, Canada, were used to infer the ground surface temperature history (GSTH) of the region. The site is located in a barren rock desert on the Katinniq plateau at an elevation of 600 m, near the northern tip of the Ungava Peninsula. The boreholes were logged more than three years after drilling was completed, insuring that the holes had returned to thermal equilibrium. Thermal conductivity measurements were made on core samples. Radiogenic heat production is small and can be neglected. The temperature depth profiles show marked deviations from steady state in the upper 200m that are assumed to be caused by recent (<300 years) variations in ground surface temperature. The GSTH's obtained by inversion of the three temperature profiles consistently show warming by $\sim$ 2.5 K, but differ significantly in the details. One profile which is least affected by topographic effects and thermal conductivity changes was analyzed in great details with different inversion methods; direct methods were also used to verify how well the GSTH can be resolved by the data. The results show a marked warming ($\approx$1.4 K) between the mid-1700s and 1940, followed by a cooling episode ($\approx$0.4 K) which lasted 40-50 years, followed by a sharp $\approx$ 1.7 K warming over the past 15 years. The borehole temperature measurements suggest that most of this warming occurred over the past 15 years. These results are in agreement with the available meteorological records and proxy data.

Keywords : Climate change, Arctic, Permafrost, Borehole temperature profile, Ground surface temperature history, Little Ice Age.

3.3 Introduction

Global circulation models (GCMs) predict that, under a scenario of global warming due to an increase in atmospheric greenhouse gases, the higher latitudes of the Northern Hemisphere will be warming more rapidly than regions at lower latitudes due to multiple feedback mechanisms (Houghton *et al.*, 1996; Flato *et al.*, 2000; Serreze *et al.*, 2000; Moritz *et al.*, 2002; Serreze et Francis, 2006). Using a multi-proxy approach, Overpeck *et al.* (1997) showed that

high-latitude regions have been warming since the end of the Little Ice Age (LIA), about 150 years ago. Direct measurements of surface air temperature (SAT) show that over the past century this warming has not been constant, with most Arctic regions exhibiting a cooling period between the 1940s and the 1970s (Jones et Kelly, 1983; Przybylak, 2000; Serreze *et al.*, 2000; Moritz *et al.*, 2002), a feature not observed in the proxies used by Overpeck *et al.* (1997). Changes in the Arctic have never been uniform since the last deglaciation and the fairly synchronous and uniform warming signal of the recent past is unprecedented for the region (Kerwin *et al.*, 2004). Therefore, all Arctic regions do not respond uniformly to climate change even if the average SATs are increasing. For example, using SAT records, Przybylak (2000) showed that between 1950 and the mid 1990s, temperatures have decreased or remained stable everywhere in the Arctic except in the Pacific region. Global estimates of climate change in the entire Arctic are important ; however, we need to assess the spatial patterns of abrupt climate change in order to identify and understand the responsible forcing mechanisms (Rind et Overpeck, 1993).

The absence of long term SAT records in the Arctic and subarctic makes it difficult to gain perspective on the actual amplitude of recent climate change. In northern Quebec (Figure 3.1), the earliest SAT measurements date back to the early 1920s on the coast of Hudson Bay (Inukjuak and Kuujjurapik), and the late 1940s on the coast of Ungava Bay (Kuujjuaq). The meteorological station at Iqaluit on Baffin Island in Nunavut (Figure 3.1) started recording SATs in the late 1940s. These two stations indicate moderate cooling between 1940 and 1980, followed by strong warming starting in 1990 (Figure 3.2). These records are much too short to yield information on the amplitude of the warming that followed the LIA, and also on the full amplitude of the cooling episode experienced by several regions in the Northern Hemisphere and the Arctic in the mid-20^{th} century.

Because of the absence of long records, paleoclimate studies have been performed with different proxies. Long-term reconstructions by Fallu *et al.* (2005) and Kerwin *et al.* (2004) using paleolimnological methods provide long term trends in surface temperature evolution for the past 6000-8000 years, but little information on recent climate evolution because the response of the lake ecosystems is slow and the proxy records are much too coarse. Permafrost evolution studies north of Kuujjuarapik in subarctic Quebec show continuous degradation during the past 50 years (Laberge et Payette, 1995; Payette *et al.*, 2004). Although this degradation suggests warming of ground temperatures, the reported increases in snow accumulation over the studied

period which started in 1957 could have counterbalanced the effect of decreasing or stable SATs. Indeed, SAT records at Kuujjuarapik show that after a drop between 1950 and 1960, average SATs remained constant from 1960 to 1990. By studying the growth and decay of ice-wedges near Salluit, Kasper et Allard (2001) produced a 3400-year reconstruction of climatic intervals including the recent cooling episode (1940-1990) also inferred from permafrost temperature studies in this region (Wang et Allard, 1995; Allard *et al.*, 1995). On Baffin Island, across Hudson Strait from the northern tip of the Ungava peninsula, Hughen *et al.* (2000) found a 2K increase in June temperatures during the 20^{th} century affecting the formation of varve sediments in summer. The absence of a cooling episode in the 20^{th} century could be attributed to the fact that, even though June temperature remained stable over the past 50 years for the entire Arctic (Przybylak, 2000), the effect of possibly longer and/or colder winters has been ignored by this analysis of proxy data (Allard *et al.*, 1995; Serreze *et al.*, 2000).

Borehole temperature depth profiles can be interpreted to infer changes in ground surface temperature on time scales from decades to millennia (see papers in Lewis, 1992). Temperature measurements in permafrost are particularly useful because they are not affected by ground water flow (Lachenbruch et Marshall, 1986; Romanovsky *et al.*, 2002). Unlike results from other proxy data, the inferred ground surface temperature history (GSTH) does not require calibration. The heat conduction equation is used to directly infer temperature changes at the ground surface from the measured temperature anomalies.

Several studies have been performed elsewhere in the Canadian Arctic. Majorowicz et al. [2004; 2005] used 61 temperature profiles measured in the 1970s and 1980s to infer a GSTH suggesting a warming of 2K between the mid-1850s and the 1970s with a cooling period between the 1940s and 1970s. The majority of the profiles used in this study are very noisy and they appear affected by several non-climatic perturbations, such as proximity to water bodies (lakes or seas), convection in the wide boreholes (petroleum exploration), and changes in thermal conductivity with depth. These noisy profiles were used for inversion because no other boreholes were available to infer GSTH in the Arctic. Through the Canadian Arctic Permafrost Observatories research program, Taylor *et al.* (2006) used three ~800 m deep boreholes drilled between 1960 and 1990 to infer a 500 years GSTH for Ellesmere Island. Their study suggests a 3 K warming since the LIA minimum, between 1730 and 1860 depending on borehole. The uncertainty is related to important changes in thermal conductivity at depth which can be attributed to the

heterogeneous nature of the sedimentary rocks forming this area.

In this paper, we present three temperature depth profiles measured in mining exploration boreholes located at the Raglan mine in northern Quebec. We inverted the three profiles to determine their GSTH's. The three GSTH's show similar trends, but they differ in the details. We suspected that two of the profiles are perturbed by several non-climatic effects and, thus we retained only one to analyze in details and to get the maximum resolution in the inverted GSTH. We have used different methods and parameterizations to infer the GSTH and obtained very consistent results. The GSTH inferred from this profile can be compared with ~60 years of instrumental recording of SATs at Iqaluit, located on Baffin Island ~350 km northeast of the study site, and at Kuujjuaq, located ~500 km southeast of the study site (Figure 3.1). The length and precision of the results allows a comparison of amplitudes between the cooling signals of both the LIA and mid-20^{th} century cooling episode and the warming trend of the past 15 years.

3.4 Theoretical Framework

3.4.1 Direct model

In a horizontally layered conductive half space with uniform variations in surface temperature, the temperature T at depth z can be written as :

$$T(z) = T_{ref} + q_{ref} \int_0^z \frac{dz'}{\lambda(z')} + T_t(z) \tag{3.1}$$

where T_{ref} is the reference surface temperature, q_{ref} the reference heat flow, λ the thermal conductivity, and $T_t(z)$ the perturbation caused by the past variations in surface temperature. Heat sources are neglected, but they could be included in the reference temperature profile. Thermal conductivity is usually measured on core samples. The transient term $T_t(z)$ is obtained by solving the one dimensional heat equation with time varying surface boundary condition. If the ground surface temperature is approximated by its average value during K time intervals, the transient term can be written as (Carslaw et Jaeger, 1959) :

$$T_t(z) = \sum_{k=1}^{K} \Delta T_k (\mathrm{erfc}\frac{z}{2\sqrt{\kappa t_k}} - \mathrm{erfc}\frac{z}{2\sqrt{\kappa t_{k-1}}}) \tag{3.2}$$

where κ is the thermal diffusivity, erfc denotes the complementary error function, and ΔT_k is the surface temperature perturbation between times t_k and t_{k-1} (i.e. the difference between

the average ground surface temperature during that time interval and the reference surface temperature).

3.4.2 Inversion methods

Singular value decomposition

The standard method used to determine the GSTH requires choosing a parametrization, (i.e. selecting the times $t_k; k = 0, 1, ...K$, with usually $t_0 = 0$, when the surface temperature varies in stepwise manner). For N temperature depth measurements, we obtain from equations 4.1 and 4.2 a set of N linear equations with $K + 2$ unknowns : the surface temperature perturbations ΔT_k, the reference surface temperature, and the reference heat flow. This linear system of equations is ill-conditioned, and its solution is unstable; a very small change in the data will induce a very large change in the solution (Lanczos, 1961). One method to stabilize the solution of such unstable systems is the singular value decomposition (SVD) (Lanczos, 1961). The application of SVD to the ground surface temperature history has been described in several papers (Mareschal et Beltrami, 1992; Clauser et Mareschal, 1995). The linear system of equations can be written as :

$$Ax = U\Lambda V^T x = b \tag{3.3}$$

where A is a $(N \times K+2)$ matrix, x and b are column vectors of length $K+2$ and N respectively, U and V are orthogonal matrices (rotation in data and parameter space) and Λ is a diagonal matrix of singular values. The instability, which stems from the presence of very small singular values, can be eliminated by replacing the reciprocals of the singular values λ_k by :

$$\frac{1}{\lambda_k} \rightarrow \frac{\lambda_k}{\lambda_k^2 + \epsilon^2} \tag{3.4}$$

where ϵ is referred to as the damping or regularization parameter (Clauser et Mareschal, 1995; Chouinard et Mareschal, 2007). After this regularization, the solution is approximate. The larger the regularization parameter, the more stable the solution. This stability is obtained at the expense of resolution. Because of the diffusive character of the heat equation, resolution is always very limited in the inversion of GSTH.

Monte Carlo method

In order to determine the range of GSTH, reference surface temperature, and heat flow compatible with the data, we have also used a Monte Carlo method (Mareschal *et al.*, 1999). The Monte Carlo method (Press *et al.*, 1992; Mosegaard et Tarantola, 1995; Sambridge et Mosegaard, 2002) consists of exploring systematically or randomly the space of model parameters, for each set of model parameters, $\mathbf{m}$, predicting the observations, and calculating the misfit $S(\mathbf{m})$ between the data and the predictions. The parameters to be determined are the reference heat flow and temperature and mean ground surface temperatures during K time intervals. In order to reduce the computation time, the number of parameters must be small. The time intervals are chosen accordingly to the resolution of the data. The misfit is usually calculated in the L_2 norm. Because of physical constraints or *a priori* information, it is usually sufficient to explore some limited region in the space of model parameters $\mathbf{m_i} < \mathbf{m} < \mathbf{m_s}$. The objective is to determine numerous sets of model parameters such that the misfit is less than a fixed value $S(\mathbf{m}) < S_0$. In the Monte Carlo method, the sets of model parameters are generated randomly. The Monte Carlo method is useful to estimate the range of model parameters consistent with the data.

3.5 Description of Data

We have obtained temperature depth profiles in three boreholes at the Raglan property, owned by Xstrata Nickel. This property is located on the Katinniq plateau in the Cape Smith foldbelt of the Ungava Peninsula in Northern Quebec (Figure 3.1). The measurements were made in three drill-holes that are less than 1000m apart (see Table 3.1 for exact location and characteristics of the holes). The measurements are taken at 10m interval with a calibrated thermistor with a precision better than 0.005K. Studies of the resolution of the inversion have shown that this sampling interval is sufficient and that finer sampling does not improve resolution (Beltrami et Mareschal, 1995). In order to avoid any perturbation caused by the probe, the measurements are made when the probe is lowered. We collected core samples from the different lithologies to measure the thermal conductivity and heat production. For each sample, thermal conductivity was measured with the divided bar apparatus. Each core sample was cut into five disks of different thicknesses. The thermal resistance of each disk was measured and thermal conductivity calculated by a least squares linear fit to the resistance/thickness data. This procedure eliminates isolated heterogeneities and yields a truly representative conductivity which

characterizes large-scale crustal heat transport. The accuracy of the conductivity measurements is better than 3%.

One borehole was fitted immediately after drilling (August 2003) with a capped steel casing filled with silicon oil. The steel casing has a length of 415 meters and an internal diameter of 25.4 mm (1 inch). This system was installed in order to allow repeat measurements of permafrost temperatures at depth long after drilling, i.e. after diffusion of the thermal effects resulting from the drilling operation and complete freezing of water in the borehole. Repeat temperature measurements in permafrost show that the thermal perturbation due to drilling may take more than one year to diffuse away (see for example the measurements at Lac de Gras reported in (Mareschal *et al.*, 2004)). We logged twice this borehole (0501-0613), in August 2005 and in September 2006 to verify that the temperatures had returned to equilibrium. This borehole is located on the south bank of a 2-3 m deep dried river bed whose channel follows the path of a $\approx$ 50 m wide valley. This dried river bed has only been observed in late summer/early fall and is probably an actual stream or river during the thawing season in late spring/early summer. The location of the borehole is lower than the surrounding area ($\approx$ 10 m).

We were also able to measure temperature in two other holes that had not been fitted with special equipment for hole reentry. During drilling in cold regions, a solution of calcium chloride (CaCl) is used as drilling fluid. The brine left in the holes after drilling is sufficiently concentrated to remain unfrozen at the coldest underground temperatures measured in the area (-7.2 °C at 50 m), provided that it has not been diluted by either fresh surface water or underground deep water flows. Among 30 boreholes inspected, two were found to be unfrozen. Beneath a thin cap of freshwater ice, the top 120 m of the boreholes were filled with a slushy brine, while the lowermost parts of the holes were filled by liquid brine. The first of these holes (0614) is located 134 m southwest from hole 0501, on the upper portion of the small valley. The other open borehole (0615) is located 930 m southwest from 0501, with flat topography nearby.

All four profiles consistently show marked departures from equilibrium above $\approx$150 m (Figure 3.4). The temperature gradients are reversed near the surface and suggest very strong recent warming. Below 150 m, the profiles in holes 0501 and 0614 show marked variations in the temperature gradient that are absent in the log of hole 0615 (Figure 4.3). The lithology logs show that the former two profiles intersect a 40 m thick argillite zone. Thermal conductivity

measurements performed on samples selected from all boreholes show lower thermal conductivity in the argillite than in the surrounding rocks (Table 3.2). The drop in conductivity is also consistent with the increase in gradient in the argillite zone (Figure 4.3). Because the layers are strongly dipping, a correction accounting for the variations in conductivity (as in equation 4.1) cannot be introduced.

3.6 Results

We have used the standard SVD inversion methods to infer GSTH's for the past 400 years for the three profiles. We have then applied several different methods to analyze in detail one profile which is not affected by noise and to estimate error bars for the inverted temperatures. We have also used direct models to ascertain the robustness (or the lack of it) of some of our conclusions.

3.6.1 Individual and joint inversion of the three temperature profiles

We have first tried to invert all the temperature depth profiles including those that are affected by conductivity variations and surface topography. We have inverted the three profiles separately and simultaneously to determine their common trends.

Individual inversions

We have first inverted the three temperature profiles with the SVD to obtain their GSTH's. The three profiles were inverted with the same parametrization (50 time intervals of 8 years), and the same value for the regularization parameter ($\epsilon = 0.02$) Although there are strong similarities between profiles, the only common trend between these three inversions is that they indicate that total ground surface warming exceeded 2.5 K (Figure 3.5a). However, the GSTH's for profiles 0501 and 0614 show variations with large amplitude that are not synchronous. The inversion of 0615 shows cooling by $\approx$2 K at 1850, followed by warming until 1960, while the inversion of 0501 does not indicate the cooling episode but only warming relative to the reference temperature. Both 0501 and 0615 indicate 1-1.5 K cooling starting 40-60 years ago, followed by marked warming in the past 15 years. The inversion of the temperature data from 0615 does not include variations of such amplitude. It shows warming by 1K until 1920, followed by moderate

cooling by 0.4K between 1940 and 1970, followed by very strong warming. The oscillations in the two former inversions (0501, 0614) are characteristic of noisy temperature profiles, the source of the noise being the geology (thermal conductivity variations) or surface effects (topography). The impact of noise on those two GSTH's could be reduced by using a higher value for ϵ but only at the expense of also decreasing the resolution of the true climatic signal.

Joint inversion

It has been argued that combining noisy borehole temperature profiles could yield a GSTH that is less affected by noise than the individual profiles. This can be done in two ways, either by inverting simultaneously different profiles that have recorded the same GSTH (Beltrami et Mareschal, 1992; Clauser et Mareschal, 1995) or by averaging the ground temperature histories inverted from individual profiles (Pollack *et al.*, 1996). The argument is that the trends due to the common temperature history would be reinforced and that, if the noise is random, it would cancel out. The two methods (joint inversion and averaging of the inversions) yield relatively similar results for the three profiles but also some significant differences for the GSTH of the past 100 years (Figure 3.5b), in particular regarding the amplitude and duration of the 1940-1980 cooling episode. The amplitude of this cooling episode ($\sim$1 K) is much larger than in the meteorological records. Whether the resolution of the GSTH can be improved by combining noisy temperature profiles has been questioned. The improvement in the signal/noise ratio is small as it is proportional to $\sqrt{N}$ (N number of profiles). In a recent study using all the borehole temperature profiles available in central and eastern Canada, we have shown that, regardless of the method used, combining noisy profiles fails to improve the GSTH and that it always results in loss of resolution. A few noise-free borehole temperature data allow much better resolution than many noisy profiles. Whenever possible, the best method to obtain a reliable GSTH is to eliminate profiles where noise has been identified and to only invert profiles without known non-climatic perturbations (Chouinard et Mareschal, 2007).

3.6.2 Inversion of the unbiased temperature profile

The hole 0615 does not intersect the argillite zone above 400 m and is not affected by surface topography which is almost flat at that location. Because there is no evidence for thermal perturbation other than climate, we have thus carefully analyzed this temperature profile and

used different approaches to determine the GSTH. Above 400m, this hole intersects only gabbro and peridotite with the same average conductivity.

The GSTH was first obtained by SVD inversion of this temperature profile. We have then used Monte Carlo inversion in order to better assess the uncertainties on the estimated parameters of the GSTH.

Singular value decomposition

The SVD inversions were performed using 8-year time intervals. This was necessary to fit the very recent changes (<15 years) in ground surface temperature. With time intervals longer than 10 years, the solution seems to become unstable, i.e. oscillations appear in the GSTH. A damping parameter value of ϵ=0.02 was used for the inversions. We have first obtained a solution for the past 400 years to analyze in detail the recent warming. We have also tried a 800 year GSTH to detect the cooling episode of the LIA.

For both parameterizations, we have obtained the same values for the reference surface temperature (−8.63 °C) and the reference gradient (0.0147 K m^{-1}).

The 400 year GSTH indicates continuous warming from 1600 to 1940, followed by 0.45 K cooling until 1975 followed by strong warming, most of which occurred during the past 10 years (Figure 4.4b).

The 800 year GSTH shows the LIA temperature decrease, but the amplitude of the cooling seems to be low (Figure 4.4a). It is important to note that cooling starting 500 years ago would have affected the profile down to 400 m. A pre-LIA reference temperature profile can not be determined because the profile is not deep enough and consequently, the amplitude of the LIA cooling will be seriously underestimated from a 400 m profile. The minimum temperature during the LIA was 0.2 K below reference temperature in the mid-18^{th} century. The most recent part of this GSTH is almost identical to that of the 400 year GSTH. The warming signal following the LIA minimum is constant until ~1925, when the surface temperature reached a value of 0.8 K above reference temperature and then dropped by 0.25 K over the next 40 years until the mid 1970s. This cooling episode is followed by a dramatic increase of 1.8 K in the past 30 years

to a present value of 2.35 K above the reference ground surface temperature.

Monte Carlo simulations

The GSTHs obtained from SVD do not fit exactly the data, and many other model parameters for the GSTH would fit the temperature profiles equally well. We performed Monte Carlo simulations in order to obtain the confidence region for the estimated parameters. In order to keep the computing time down and to avoid , we used a parametrization with fewer time intervals than for SVD and with variable duration (i.e. with shorter time intervals for the very recent than for the remote past). For the 400-year GSTH, we used 15 parameters; for the 800-year, we used 17 parameters (reference temperature, reference gradient and 13 or 15 temperature jumps). The search in model parameter space was around the reference temperature and gradient obtained from SVD inversion and zero temperature perturbation during each time interval. The reference and surface temperature perturbations were allowed to vary within ± 8 K and the gradient within ± 0.01 K m^{-1}. The reference surface temperature and gradient were varied around the values obtained by SVD inversion. The perturbations varied around a value of 0, to avoid any bias. For both sets of parameters, we performed six simulations each one sampling 10^{10} models in parameter space. For the 800-year GSTH, an average of 2762 models was retained from each simulation and the average values for the reference temperature and gradient were -8.485 ± 0.017 °C and 14.42 ± 0.041 mK m^{-1}. For the 400 years GSTH, an average of 3348 models per simulation were retained and the average values for the reference temperature and gradient were -8.576 ± 0.009°C and 14.60 ± 0.024 mK m^{-1}. The averaged GSTHs and the standard deviations on temperature perturbations are given in Figure 3.7.

The 800-year GSTH clearly shows the onset of the LIA with a net > 0.2 K drop in ground surface temperatures at the turning of the 16^{th} century.

The 400 years GSTH begins near the LIA minimum of 0.42 K below reference temperature between 1650 and 1700. The subsequent warming, from 1750 to 1900, reaches a value of 0.9 K above reference temperature between the mid-1890s and mid-1920s and then decreases by 0.3 K between the mid-1940s and mid-1960s. This period seems to be the coldest of the past 100 years for the area. The warming of the ground surface temperatures then resumes at a rate comparable to post-LIA warming until the time step covering the past 10 years, where it undergoes a

dramatic increase to a value of 2.3 K above reference temperature, corresponding to a 2.7 K increase in ground surface temperature from the LIA minimum.

Comparison with direct models

In general, the GSTH obtained by SVD inversion shows strong oscillations in the very recent past (see for instance the oscillations of the GSTHs obtained by Beltrami et Mareschal (1992)). These oscillations are due to the structure of the eigenvectors in model space, a linear combination of which is used to fit the GSTH. We have thus used direct models to ascertain that the 20^{th} century cooling event is real and it is not an artifact of the inversion procedure.

We estimated the reference temperature gradient as the mean value of the gradient in the deepest section of the borehole (between 300 and 400 m) which is near steady state. We obtained a value of 0.0145 K m^{-1} close to the value obtained by inversion. The reference surface temperature (i.e. the temperature at the ground surface used as a baseline from which all changes in surface ground temperatures are calculated) is estimated by extrapolating the temperature depth profile between 400 and 300 m to the surface. We obtained a reference surface temperature value of -8.54 °C (compared with -8.63 °C for the inversion). The residual temperature profile which is due to variations in surface temperatures is the difference between the observed and the reference temperature profile.

For the direct models, we have used only 5 or 6 temperature changes (Figure 3.8a). We fitted the data with two models, one including warmer surface temperature between 1900 and 1940 than between 1940 and 1970, and one without cooling and with a constant temperature between 1900 and 1970. We have adjusted the parameters by trial and error for the first model until we observed a reasonable fit between the predicted and observed temperature profiles. For the second model we used the same parameters as obtained in the first but replaced the 1900-1940 and 1940-1970 temperatures by the average of their values.

For both models, the predicted reduced temperature profiles are close to the experimental data (Figure 3.8b). The RMS misfits are 0.225 and 0.295 K for the models with and without cooling episode in 1940-1970 respectively. Although the RMS misfit is marginally lower for the model with a cooling episode than for a model without, the misfits of both models to the data

are much larger than the difference between the two model predictions. We prefer the GSTH with the $20th$ century cooling episode because between 100 and 150 m, the misfit of this model is clearly lower than that of the model without cooling (Figure 3.8c). The $20th$ century cooling episode is just at the resolution threshold for the borehole temperature data, but the direct models suggest that the cooling episode is indeed recorded in the borehole temperature data.

The large ground surface temperature jump of $\sim$ 1.1 K around 1850 actually approximates a gradual increase between 1700 and 1900; this approximation was necessary to keep a small number of parameters.

3.7 Discussion

The temperature profiles recorded in three different boreholes have in common a very conspicuous trend : the warming of the ground surface temperature was $\sim$2.5 K over the past 200-300 years. Because of the noise (i.e. non climatic perturbations in the temperature profiles), the detailed GSTHs of the three profiles are quite different. Joint inversion of the three profiles yield their common trends but does not eliminate completely the effect of noise. Profile 0615, which is least affected by noise, allows better resolution of the GSTH. We have thus carried out in very great details the analysis of that profile and used three different methods to reconstruct the GSTH for the northern Quebec region. For practical reasons, these methods require different parameterizations of the GSTH. Nevertheless, they yielded very consistent results for the recent changes in ground surface temperatures (past 250 years). These results are consistent with the trend inferred from the joint inversion of the three profiles.

The total warming of the ground surface is $\approx$2.5 K between the end of the LIA and present. The two inverse methods suggest that this warming took place at relatively constant rate between 1800 and 1920, and that it was followed by a moderate cooling 0.3-0.4 K episode between 1940-1980. It was followed by very strong warming 1.7 K, most of which occurred during the past ten years.

When we extended the GSTH to include the LIA period, we found a weak cooling 0.3 K that may have started *ca.* 1500. This cooling was inferred both from the SVD and the Monte Carlo method. It is important to note that ground surface temperature changes that occurred 500 years

ago affect the profile down to 400 m. Therefore, it is impossible to simultaneously determine the reference surface temperature and the amplitude of the LIA cooling. Both inversion methods are thus likely to underestimate the amplitude of the LIA cooling. Both methods show an onset of the LIA around 1500 and a marked cooling during the 16^{th} century lasting until the middle of the 18^{th} century. The reconstruction of the LIA also appears to be consistent with the two other profiles that were not retained for inversion. This suggests that the LIA and the subsequent warming might have started approximately 100 years earlier than in southern Canada (Chouinard et Mareschal, 2007).

The three models describe a similar average warming from the end of the 1700s until the early 1900s. The ground surface temperatures reached a peak during the mid-1920s before a drop between 0.25 and 0.45 K by the mid-1970s. This cooling episode is followed by strong warming by 1.8 K over the past 20 years.

The $\sim$ 0.3 K cooling around the early 1940s until the late 1980s corresponds to the cooling signal inferred by Allard *et al.* (1995) and Kasper et Allard (2001) studying permafrost temperatures and ice wedges growth rates in northern Quebec. The GSTH of the past 65 years can also be compared to SAT measurements from meteorological stations located at Kuujjuaq and Iqaluit (Figure 3.2). These two stations, more than 600 km apart, have recorded fairly consistent trends. For both stations, the long-term SAT trends (11-year running average) show details that were not resolved by the GSTH. Surface air temperatures decreased from 1950 to 1975, then seem to stabilize in the late 1970s and to increase until the early 1980s when, during a 7-8 years span, SATs dropped rapidly. Since the early 1990s, SATs have been increasing rapidly in northern Quebec. This sudden drop in SATs during the 1980s is absent from both GSTHs obtained from inversion (Figures 4.4 and 3.7). Also the amplitude of the cooling in the SAT record is larger than that of the GSTH. The difference is likely due to the loss of resolution. It is also important to note that ground and air surface temperatures are always different, although studies show that they track each other (Putnam et Chapman, 1996; Harris et Chapman, 1998). One reason for the difference between GST and SAT is the thermal insulation effect of the snow cover (Bartlett *et al.*, 2004). For the present study, the effect of snow is minor because the Katinniq plateau is a barren desert without vegetation and the surface is free of snow in winter due to the strong winds blowing away the precipitations. Our GSTH reconstructions suggest that the cooling actually began in the 1920s, with the minimum temperatures being reached

in the 1960s. Unfortunately, the SAT measurements only started in the late 1940s and it is impossible to confirm that the cooling had already begun before. Nevertheless, the timing of the cooling period and subsequent warming of all our GSTH reconstructions correlate well with SAT measurements. It is worth noting that the recent climate history in the Canadian Arctic is quite different from that inferred for Alaska where the cooling episode has not been observed.

The most recent warming (1.8 K during the past 15 years) has an amplitude greater than that of the total warming following the LIA. Keeping this in perspective of the decreasing resolution with time of the GSTH, it still appears that such a high rate of warming is unprecedented since the termination of the LIA.

3.8 Conclusion

Three temperature depth profiles measured in boreholes located at the Raglan mine in northern Quebec have been used to infer the ground surface temperature history of the region. The permafrost environment offers the best conditions to reconstruct the GSTH because there is no thermal perturbation due to groundwater flow. All three profiles show that ground temperature has increased by ~2.5 K since the little ice ages. Differences between profiles are due to noise, i.e. variations in thermal conductivity and effects of surface topography. We have used one of the profiles unaffected by these perturbations to infer detailed GSTHs for the past 400 and 800 years. Three methods were used independently, an inversion based on a singular value decomposition algorithm, a Monte Carlo simulation, and forward modeling. The three methods yielded very similar results. The onset of the LIA occurred between 500 and 600 years before present, the ground surface temperatures dropping by at least 0.3 K at the time of the LIA minimum, ~300 years ago. The subsequent warming brought ground temperatures well above their pre-LIA level, reaching a maximum value in the 1920s. This warming was interrupted by the mid-20^{th} century cooling event, when ground surface temperatures dropped by more than 0.3 K in a 40 year period. This cooling event was then followed by extremely strong warming in the past 10-15 years. The present ground surface temperatures is 2.3 K warmer than before the LIA.

3.9 Acknowledgments

The authors wish to acknowledge the very generous support given by Xstrata Nickel (formerly Falconbridge), operator of the Raglan mine, and the help of their staff, especially P. Lessard, J.-F. Tremblay and C. Champagne. Many thanks to Gerard Bienfait (Institut de Physique du Globe de Paris) who prepared a special thermal probe for this study and made the thermal conductivity measurements. The manuscript has been substantially improved by very constructive comments by three reviewers and editor Peggy Delaney. Part of this work was supported by the Natural Sciences and Engineering Research Council of Canada through Discovery Grants to RF and JCM.

The temperature profiles and physical properties measurements are available at the following address :
(http ://www.unites.uqam.ca/geotop/geophysique/flux/data.htm).

TAB. 3.1: Summary information on the three logged boreholes at the the Raglan mine.

identification	UTM coordinates (NAD27)		elevation	total length	length logged	dip at collar	average dip	end of drilling
	eastings	northings	(m)	(m)	(m)	^{o}	^{o}	yyyy/mm/dd
0501	575074.87	6841211.09	614.73	545	10-440	75	75	2003/08/29
0614	575050.87	6841079.26	622.93	539	10-530	77	73	2004/06/13
0615	574475.13	6840501.00	612.78	420	10-420	75	74	2003/09/02

TAB. 3.2: Thermal conductivity for the main lithologies measured on drill core samples. Note that the conductivity of each sample is determined from five different measurements.

lithology	conductivity $W\ m^{-1}\ K^{-1}$	N samples
basalt	3.1	5
argillite	2.4	3
peridotite/gabbro	2.8	7

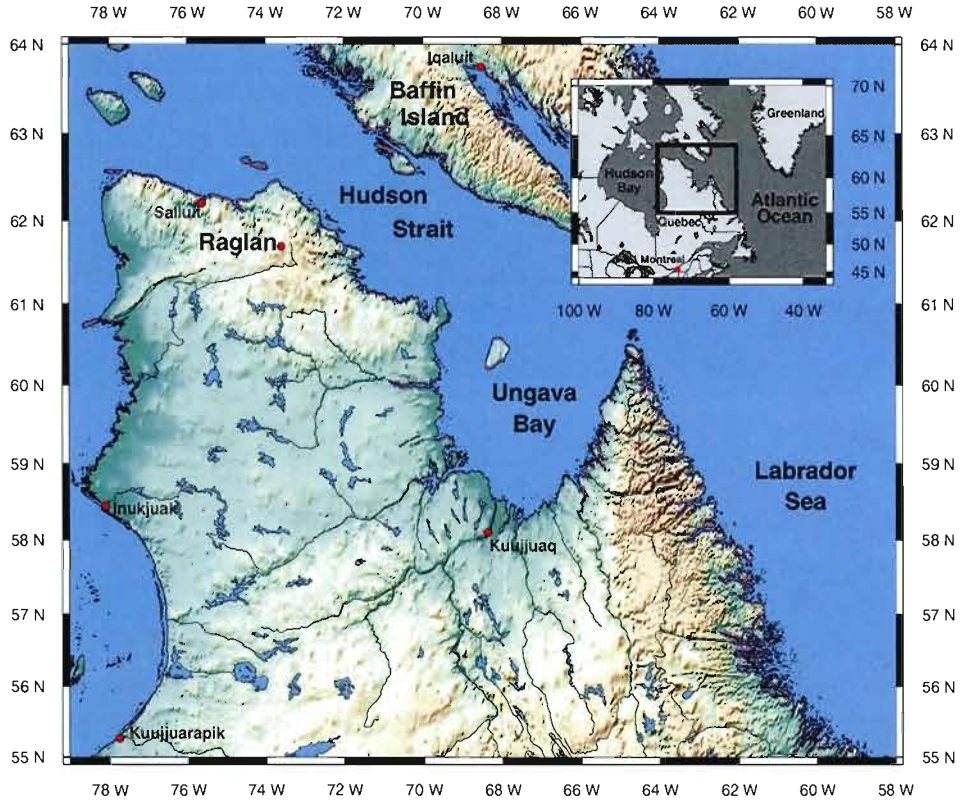

FIG. 3.1: Location map of the study area. The Inuit villages where meteorological data are available or where other climate studies have been undertaken are also identified. For this study, the ground surface temperature histories (GSTH) are compared with data from meteorological stations at Kuujjuaq and Iqaluit (Figure 3.2).

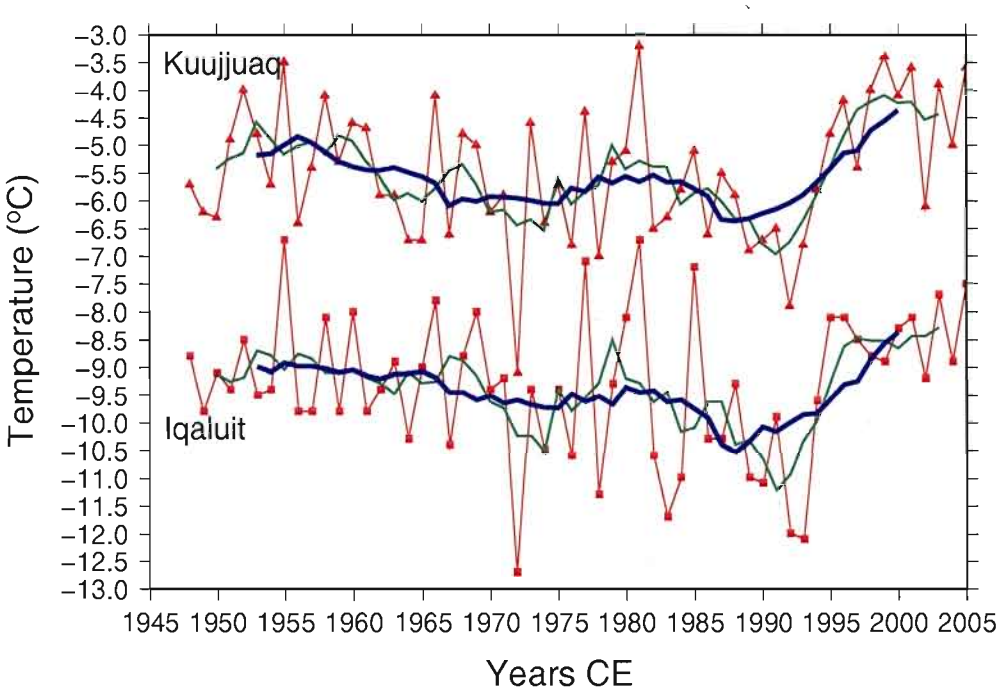

FIG. 3.2: Meteorological data from stations located at Kuujjuaq and Iqaluit. The red markers and line represent the annual mean surface air temperature (SAT) for each station, the green line the 5-years running average and the blue line the 11-year running average.

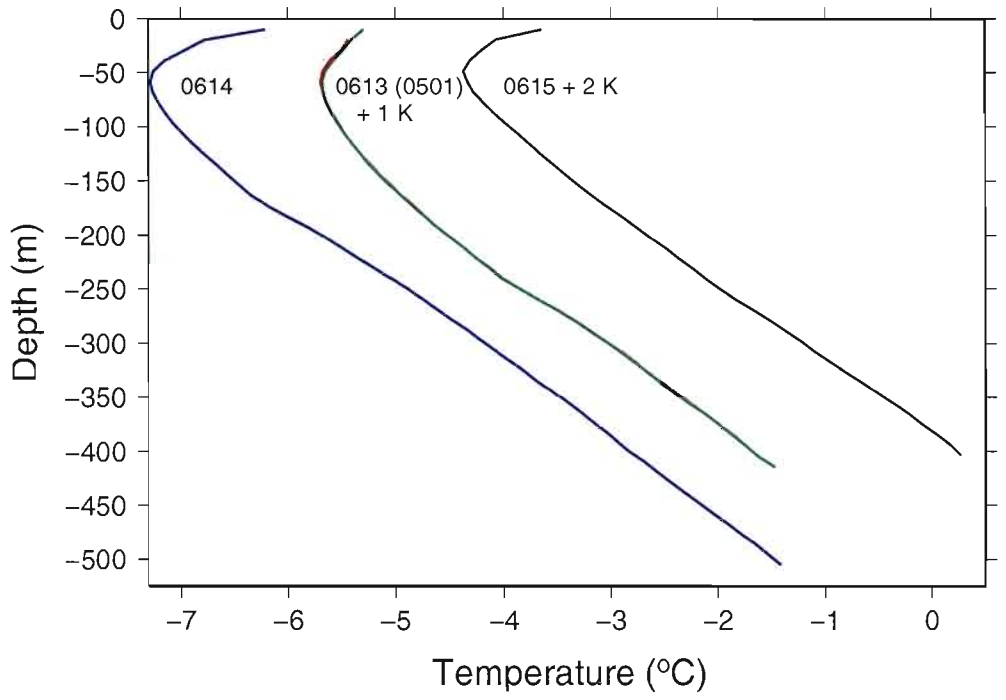

FIG. 3.3: Measured temperature depth profiles of the three Raglan boreholes. One borehole was logged in 2005 (0501, red) and 2006 (0613, green). The profile 0615 is less affected by thermal conductivity variations and topography effects than 0501 and 0614.

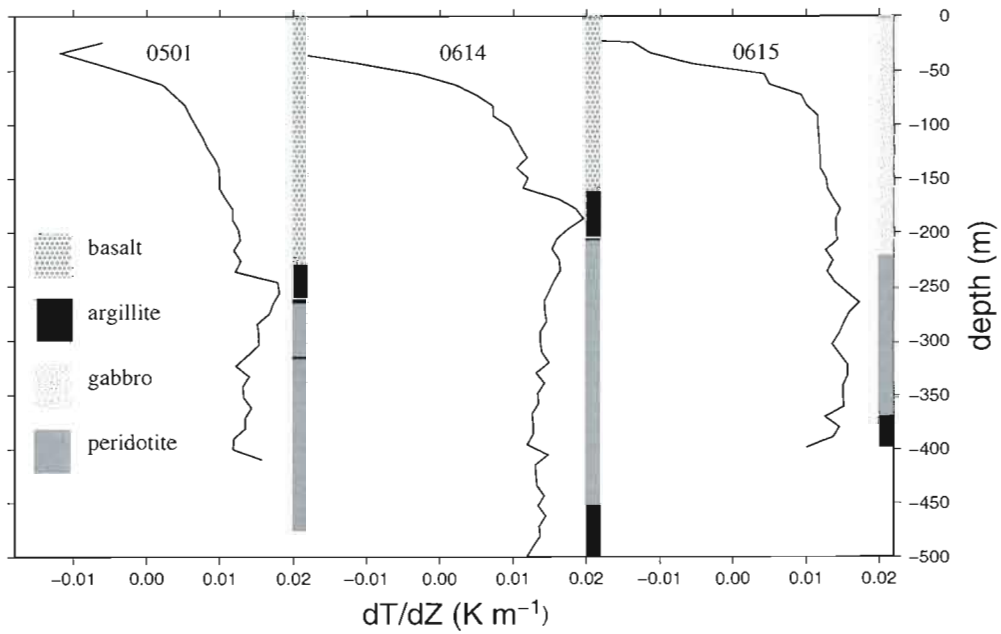

FIG. 3.4: Vertical temperature gradient and summary lithological log for the three Raglan boreholes. In boreholes 0501 and 0614, a strong variation in gradient is associated with the layer of argillite at about 200m. There is also a difference in conductivity between the basalt and the peridotite. Borehole 0615 does not intersect the argillite horizon above 400m and the unperturbed temperature profile above 400m can be inverted with high resolution. Gabbro and peridotite samples had the same average conductivity.

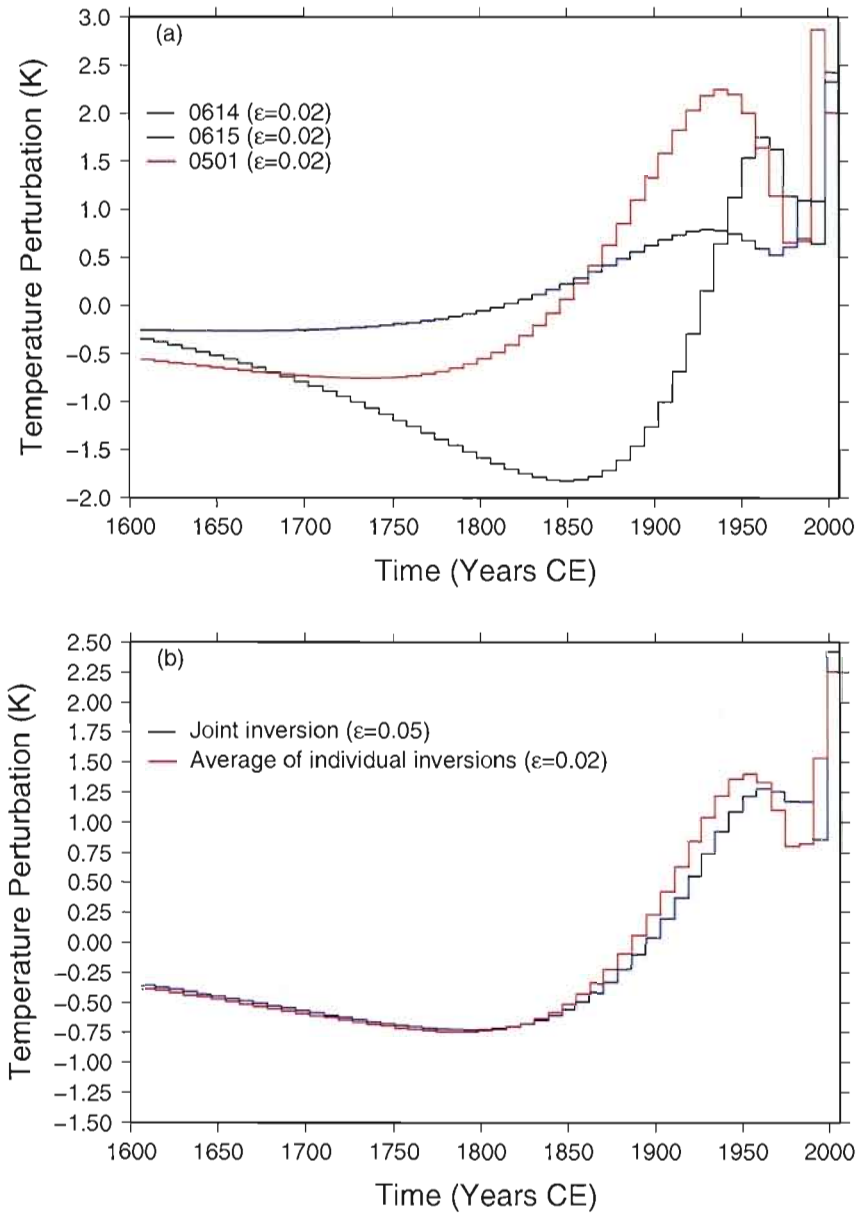

FIG. 3.5: (a) Individual SVD inversion of the three temperature profiles. For comparative purpose, the same value $\epsilon = 0.02$ was used for the regularization parameter of the three profiles. The large amplitudes of temperature variations in 0501 and 0614 are partly caused by the perturbations due to conductivity changes; (b) Composite GSTH for the three profiles obtained either by simultaneous inversion of the three profiles or by averaging the GSTHs of individual profiles.

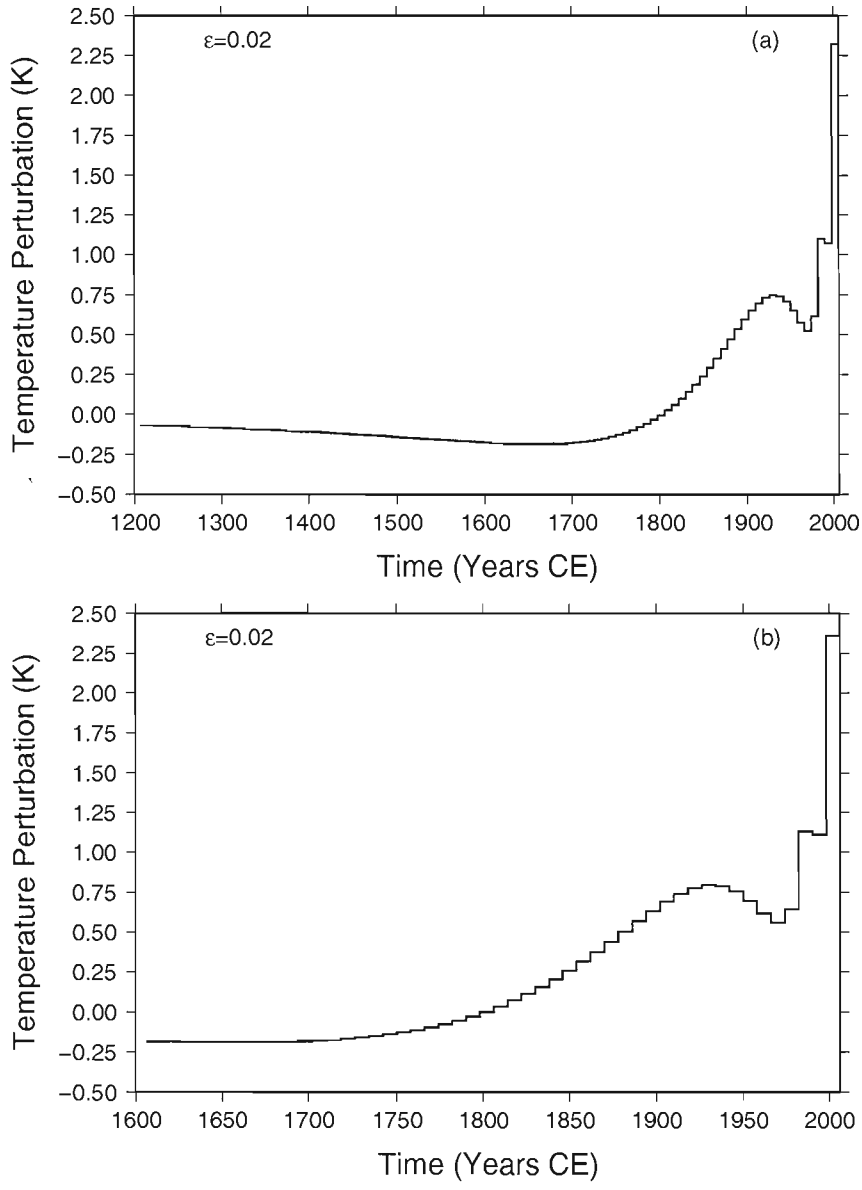

FIG. 3.6: Results of the SVD inversions for the temperature profile in borehole 0615 for a 800-year GSTH (a) and a 400-year GSTH (b). The two inversions were carried out using different parameterizations. The LIA cooling appears but its amplitude is weak. The mid-20^{th} cooling event is clearly identified on these GSTH reconstructions.

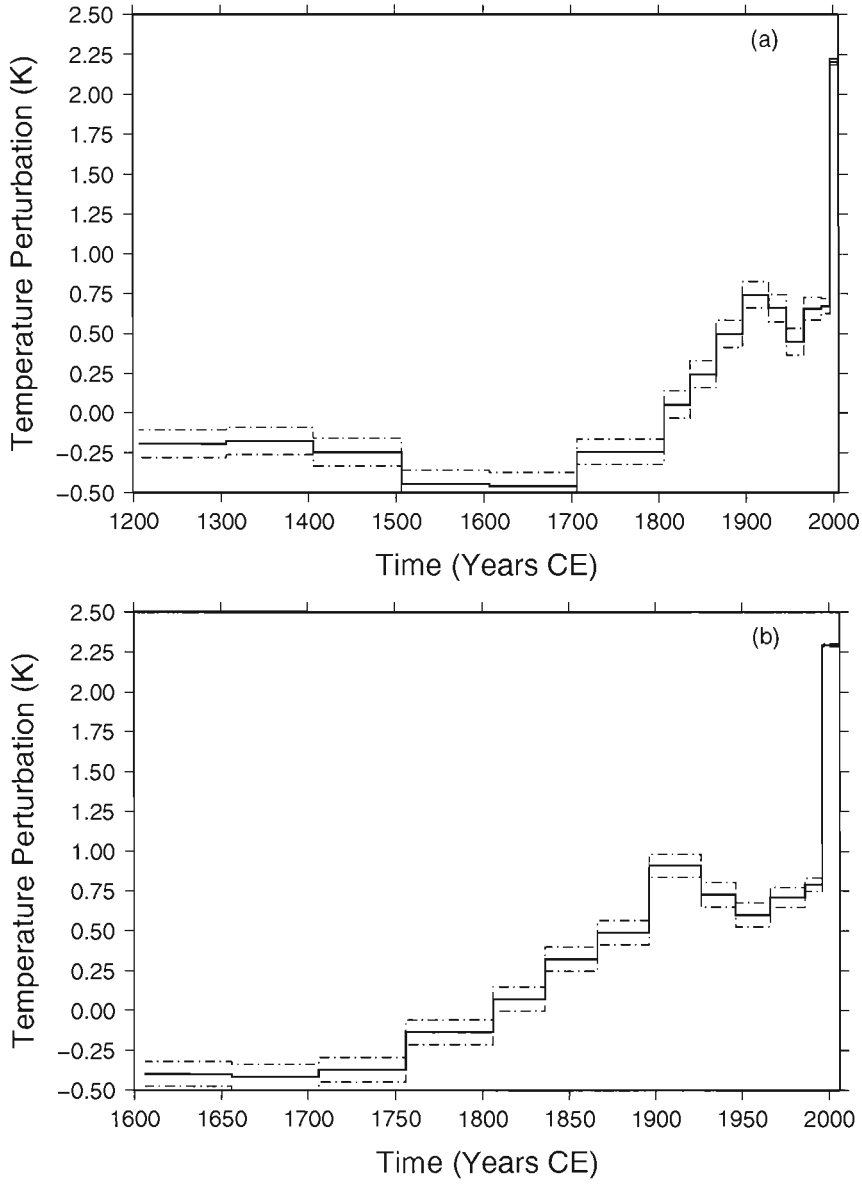

FIG. 3.7: Results of the Monte Carlo inversion for the temperature profile in borehole 0615 for a 800-year GSTH (a) and a 400-year GSTH (b). Note that the parametrization is different for the two inversions. The solid line represents the average of all temperatures retained for each time interval and the dashed lines represent the average ± one standard deviation. The LIA cooling period is just within one standard deviation. The amplitude of the mid-20^{th} cooling event is slightly above the standard deviation.

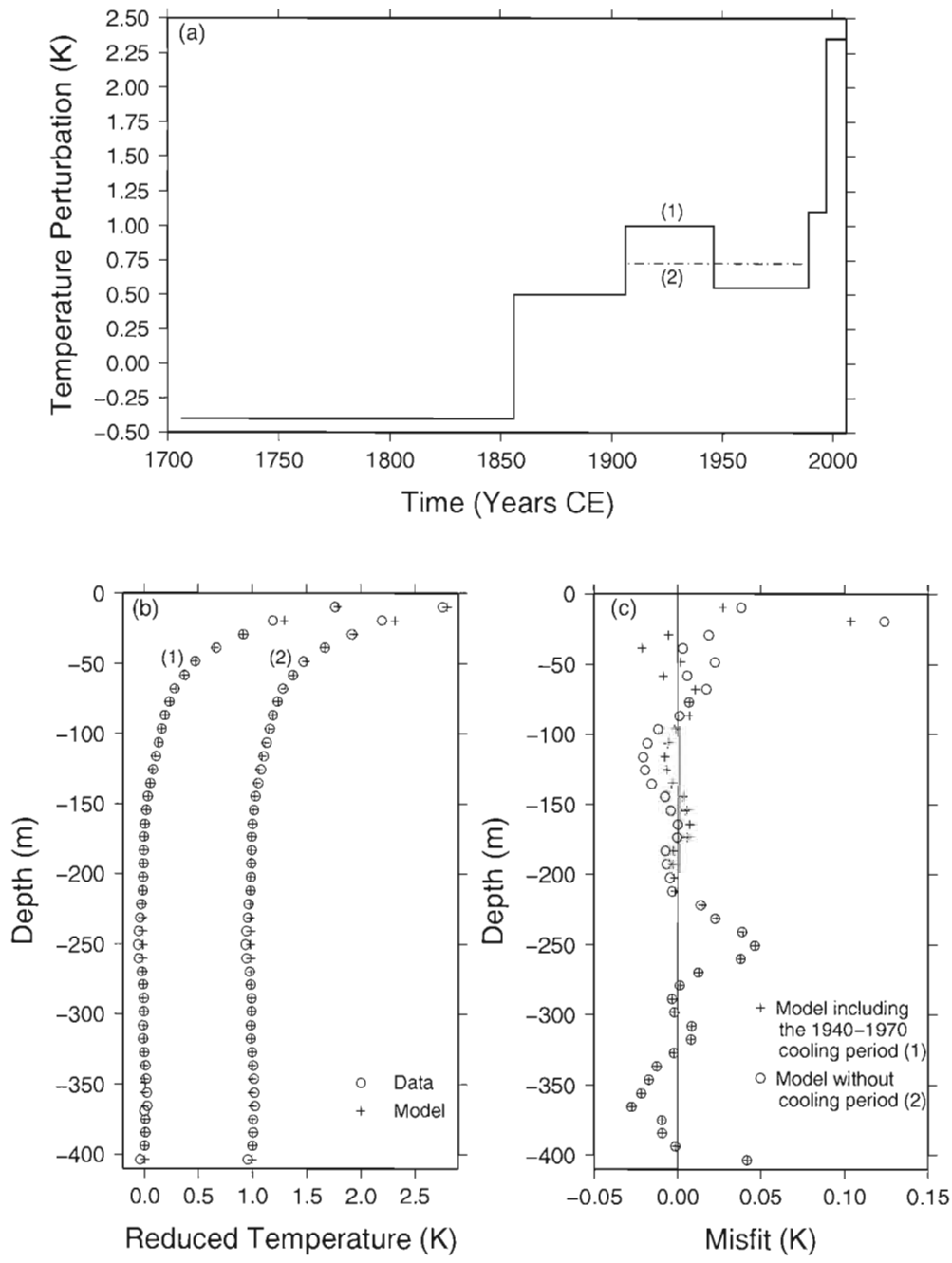

FIG. 3.8: Results of forward modeling. (a) The two GSTH's were used to calculate temperature depth profiles for borehole 0615, with cooling (solid line) and without (dashed line); (b) Calculated and measured reduced temperature profiles; (c) Misfits of the two models with the data.

CHAPITRE 4

30000 YEARS GROUND SURFACE TEMPERATURE HISTORY FROM DEEP BOREHOLES ACROSS CANADA : FROM LAST GLACIAL MAXIMUM BASAL TEMPERATURES TO HOLOCENE CLIMATE OPTIMUM

4.1 Résumé

Nous utilisons les profils de température provenant de 4 forages très profonds (plus de 2000 m) situés dans l'est du Canada et les combinons à 4 profils préalablement étudiés afin de reconstruire les histoires de la température à la surface du sol au dernier maximum glaciaire (DMG) ainsi que pendant le réchauffement subséquent de l'Holocène. L'inversion des profils de température ne montre aucune différence géographique significative de la température sous la portion sud du glacier Laurentidien au DMG. Au DMG, les températures basales étaient égales ou inférieures au point de fusion de la glace. Ces résultats améliorent la résolution spatiale existante des températures basales et sont en accord avec les observations géologiques de surface et les prédictions de modèles qui suggèrent que les vitesses de flux de la glace basale devaient être élevées au dessus des régions étudiées. Ces nouvelles données de températures basales fournissent des contraintes quantitatives pour la dynamique des glaciers. La chronologie du retrait de la calotte glaciaire est évaluée pour chacun des sites et comparée à des études basées sur différents proxies. La chronologie et l'amplitude de température de l'optimum climatique de l'Holocène sont également présentées et comparées aux valeurs obtenues par différents proxies.

4.2 Abstract

We use temperature profiles from 4 very deep (>2000m) borehole located in eastern Canada and 4 previously studied deep boreholes across Canada to infer ground surface temperature histories throughout the Last Glacial Maximum (LGM) and the subsequent warming of the Holocene. Inversions of the temperature profiles show no significant geographic differences in basal temperatures of the southern Laurentide ice sheet at LGM. At LGM, basal temperatures were

at or slightly below the melting point of ice. These results add some spatial resolution to existing basal temperature results and are consistent with field observations and model predictions suggesting high velocity basal flows above the studied regions. These new basal temperatures will provide better quantitative constraints on glacier flow dynamics. We compare ice-sheet retreat chronology of our inversions at each site with other proxies. Chronologies and temperature amplitudes of the Holocene climate optimum are also presented and compared with proxies from previous studies.

4.3 Introduction

In order to model the future of climate change, we must first fully understand how climate evolved in the past. The last major global climatic event to occur on Earth was the last ice-age, which reached its climax during the Last Glacial Maximum (LGM), 20000 years ago. If models successfully reproduce the climate and geomorphology of the Earth during that period and the subsequent deglaciation and Holocene, we will assume their predictions for future climate change to be robust (Mix *et al.*, 2001). Such models need physical data to better constraint their parameters.

The major feature of the last ice age was the presence of large ice-sheets over the planet's continents. Today, the only remaining large low-altitude ice-sheets are the Greenland and Antarctic ice-sheets. Since the climate system has been closely linked to the formation, evolution and eventual retreat of present and past ice-sheets through numerous feedback mechanisms (Manabe et Broccoli, 1985; Imbrie *et al.*, 1992), it is important to fully understand the dynamics of these ice-sheets (Clark *et al.*, 1999).

Ice-sheet dynamics are strongly connected to their underlying geology and processes (Clark *et al.*, 1999). Basal temperatures (i.e. the temperature at the base of ice-sheets) are important parameters of ice-sheet evolution models since their values control the presence and velocity of basal flow (flow of ice at the base of ice-sheets), a crucial parameter of ice thickness reconstructions within dynamic ice-sheet models (Licciardi *et al.*, 1998; Clark *et al.*, 1999; Marshall *et al.*, 2000, 2002; Marshall et Clark, 2002). Basal temperatures are often modeled for ice-sheet evolution models because of the lack of substantial data on thermal conditions at the base of past ice sheets. Some of these models use heat flow measurements as a lower boundary in order to better

constraint basal temperatures (Tarasov et Peltier, 1999, 2004; Peltier, 2004). Based on isostatic models (Peltier, 2004), the south-central portion of the Laurentide ice sheet had to be thinning subsequent to LGM. This thinning can be confirmed by surface geological observations (Hicock et Dreimanis, 1992; Dyke *et al.*, 2002) and implies that fast basal flows had to occur at the base of the ice sheet in order to remove ice mass, thus basal temperatures were likely near the pressure melting point of ice. Such conditions are not only possible, but are actually presently observed under the West Antarctica ice-sheet (Clark *et al.*, 1999).

For obvious reasons, the different methods most often used to infer continental paleoclimates (i.e. palynology, micro-paleontology, dendrochronology, sedimentology, etc.) all have one common shortcoming, they can offer no information on conditions that occurred at the base of an ice-sheet. Relict landscapes offer information on whether the bed of an ice-sheet was frozen or not, but not on the actual temperatures. The dating of moraines will yield information on the chronology of retreats or re-advances of glaciers, but very little on ground surface conditions before such retreats, although ribbed moraines have been used to infer some information on processes taking place below glaciers (Kleman et Hättestrand, 1999).

Temporal variations in ground surface temperatures propagate downwards in the bedrock and are recorded as perturbations to the steady-state thermal regime of the upper crust. These perturbations are analyzed through an inversion of the steady-state temperature depth profile measured in a borehole to yield a reliable ground surface temperature history (GSTH) (Vasseur *et al.*, 1983; Shen et Beck, 1992; Mareschal et Beltrami, 1992). Very deep boreholes (temperature depth profiles deeper than 1800 meters) can be used to infer temperature variations that occurred more than 30000 years before present. The use of very deep boreholes to determine long-scale variations in ground surface temperatures is the only method that can reliably infer basal temperature evolution of long-disappeared ice-sheets such as the Laurentide (Mareschal *et al.*, 1999; Rolandone *et al.*, 2003) or Fennoscandian ice-sheets (Kukkonen et Jõeleht, 2003).

In this study, we consider four very deep boreholes measured in Sudbury and Manitouwage. In order to properly compare these new datasets to the existing Canadian deep borehole dataset we revisit previously studied boreholes in Sept-Iles (Mareschal *et al.*, 1999; Rolandone *et al.*, 2003), Flin Flon (Sass *et al.*, 1971; Rolandone *et al.*, 2003), Balmertown and Thompson (Rolandone *et al.*,

2003)(Figure 4.1). Located between the Sept-Iles borehole and the other three boreholes, the two new sites bring some improvement to the poor spatial resolution of basal temperatures inferred from deep boreholes across Canada. The systematic analysis of all temperature profiles using the same inversion algorithms yields a more consistent determination of the southern Laurentide ice-sheet basal temperature distribution.

GSTHs inferred from deep boreholes also offer information on the Holocene climate optimum (HCO) that followed the deglaciation and during which most regions throughout the continental interiors of Eurasia and North America experienced warmer temperatures than at present. This warm period, which lasted ~2-3 ky, peaked at 6 ky B.P. with summer temperatures ranging from 2 to 4°C higher than at present (Anderson *et al.*, 1988). Numerous studies using different proxies have described surface conditions during the Holocene near our study sites (Mott, 1973; Saarnisto, 1974; Ritchie, 1983; Björck, 1985; Ritchie, 1987; Govaire et Gangloff, 1989; Woods et Davis, 1989; Liu, 1990; de Vernal *et al.*, 1993; Patterson *et al.*, 1997; Davis *et al.*, 2000; Boudreau *et al.*, 2005). We compare our results with these studies and offer our own temperature amplitudes and chronology of the HCO at our study sites. Even if our temporal resolution is poorer than most proxies, an advantage of our method is that, unlike most proxies, the inferred temperatures are independent of the hydrological conditions that occurred during the Holocene.

4.4 Theoretical Framework

For such long-term paleoclimate reconstructions, the temperature at depth in the boreholes must be exactly at the same temperature as the surrounding rocks. As they propagate downwards, the perturbations caused by important variations in ground surface temperatures are dampened to the point where they become almost indistinguishable from the unperturbed steady-state thermal regime. The amplitude of these perturbation is measured in millikelvins. A non-climatic temperature perturbation such as residual drilling heat or water pumping from a nearby mine will completely ruin the climatic signal. Even if systematic, such a non-climatic perturbation voids the model used to infer the ground surface temperature history since the critical assumption is that heat transport in the bedrock is purely vertical conductive. Ideally, a few years should separate drilling from temperature logging in order to insure that no residual temperature perturbation caused by drilling remains.

4.4.1 Direct model

In a conductive half space experiencing horizontally uniform variations in surface temperature, the temperature T at depth z is given by :

$$T(z) = T_{ref} + q_{ref} \int_0^z \frac{dz'}{\lambda(z')} + T_t(z) \tag{4.1}$$

where T_{ref} is the reference surface temperature, q_{ref} the reference heat flow, λ the thermal conductivity and $T_t(z)$ the perturbation caused by the variations in ground surface temperature. Radiogenic heat production at depth is determined using core samples, however it is usually found to be negligible for our analysis. The variations in thermal conductivities at depth are determined by the method of divided bars (Misener et Beck, 1960) on selected representative core samples. The transient term $T_t(z)$ is obtained by solving the one dimensional heat equation with varying surface boundary conditions. By approximating the ground surface temperature by its average value during K time intervals, the equation becomes Carslaw et Jaeger (1959) :

$$T_t(z) = \sum_{k=1}^{K} \Delta T_k (\mathrm{erfc}\frac{z}{2\sqrt{\kappa t_k}} - \mathrm{erfc}\frac{z}{2\sqrt{\kappa t_{k-1}}}) \tag{4.2}$$

where κ is the thermal diffusivity, erfc the complementary error function and ΔT_k the surface temperature perturbation between times t_k and t_{k-1} (i.e. the difference between the average ground surface temperature during that time interval and the reference surface temperature). The inputs for this model are the ground surface temperature variations at different times before present in the form of a step function.

4.4.2 Inverse model

Singular value decomposition

We use singular value decomposition (SVD) to solve an inverse problem which consists in using the temperature depth profile T_z in order to determine T_{ref}, q_{ref} and the step function GSTH (equations 4.1 and 4.2). The use of SVD to infer GSTH has been discussed extensively in past papers (Mareschal et Beltrami, 1992; Beltrami *et al.*, 1992; Clauser et Mareschal, 1995; Chouinard et Mareschal, 2007). In short, for N temperature depth measurements, we evaluate equation 4.2 at each depth where data exists, forming a system of N linear equations with $K + 2$ unknowns defined by the surface temperature perturbations ΔT_k, the reference surface

temperature T_{ref}, and the reference heat flow q_{ref}. Such a linear system of equation is ill-conditioned, and its solution is unstable. This instability is induced by the presence of very small errors in the data, which become amplified in the solution (Lanczos, 1961). In order to stabilize the solution of this unstable system, we use the singular value decomposition method (Lanczos, 1961). Our linear system of equations can be written in the generalized form :

$$Ax = U\Lambda V^T x = b \tag{4.3}$$

where A is a $(N \times K + 2)$ matrix, x is a column vector of length $K + 2$, b is a column vector of length N, U and V are orthogonal matrices (rotation in data and parameter space) and Λ is a diagonal matrix of singular values λ_k. Our solution being vector x, we must therefore multiply our orthogonal matrices by Λ^{-1}. Small errors in the data will yield very small singular values λ_k. The instability of the solution stems from the presence of the reciprocal of these very small singular values $(1/\lambda_k)$. For very small values of λ_k, the reciprocal becomes very large. Being error related, these small singular values can be either cut off or damped. Damping will usually yield a smoother result and is done by replacing the reciprocals of the smaller singular values of λ_k by :

$$\frac{1}{\lambda_k} \rightarrow \frac{\lambda_k}{\lambda_k^2 + \epsilon^2} \tag{4.4}$$

where ϵ is referred to as the damping or regularization parameter (Clauser et Mareschal, 1995; Beltrami *et al.*, 1997; Chouinard et Mareschal, 2007). Because of this damping, the solution becomes approximate. The larger the regularization parameter, the lesser the importance of smaller singular values and thus the more stable the solution. However, with the damping of the smaller singular values we also reduce the resolution of the solution. Thereby, the diffusive nature of the heat equation limits the resolution of a GSTH inversion.

Monte Carlo method

In order to determine the range of GSTH, reference surface temperature, and heat flow compatible with the data, we have also used a Monte Carlo inversion (Mareschal *et al.*, 1999; Chouinard *et al.*, 2007). The Monte Carlo method (Press *et al.*, 1992; Mosegaard et Tarantola, 1995; Sambridge et Mosegaard, 2002) consists in exploring systematically or randomly the space of model parameters and to calculate the misfit, S($\mathbf{m}$), between the data and the temperature profile predicted for each set of model parameters, $\mathbf{m}$. Because of physical constrains or *a priori* information, it is usually sufficient to explore some limited region in the space of model

parameters $\mathbf{m_i} < \mathbf{m} < \mathbf{m_s}$. The objective is to determine sets of model parameters such that the misfit $S(\mathbf{m}) < S_0$. In the Monte Carlo method, sets of model parameters are generated randomly.

A set of parameters is retained when the distance ($\mathbf{L_2}$ norm) between the data and the calculated temperature profile is such that the mean difference between the two profiles is below a given threshold. The parameters to be determined are the reference heat flow and temperature and mean ground surface temperatures during K time intervals, which are chosen accordingly to the resolution of the data [e.g. Beltrami et Mareschal (1995)]. In our Monte Carlo simulations, the reference temperature are allowed to vary between $-5°C$ and $+5°C$ of the initial model value, the reference gradient is allowed to vary between $-0.01°C/m$ and $+0.01°C/m$, and surface temperature perturbations are initially allowed to vary between $-8°C$ and $+8°C$. The thermal diffusivity is assumed constant at $1.0 \times 10^{-6} m^2 s^{-1}$.

4.5 Description of Data

All the sites used to infer GSTHs in this paper are identified on the map shown in Figure 4.1. The addition of the Sudbury and Manitouwadge sites (in red) adds spatial resolution to the existing dataset (in blue).

This section gives details on the sites and additional information on all the unpublished deep borehole measurements. The detailed technical information on each borehole is given in Table 4.1. A previous study by Chouinard et Mareschal (2007) has shown the importance of carefully selecting suitable borehole measurement sites when performing a GSTH, thus we give detailed information on site conditions for all deep boreholes and reasons for either selecting or rejecting them for a 50000 years GSTH.

Unless indicated otherwise, all boreholes were logged at 10 meter intervals using a calibrated probe attached to an electrical cable. The precision of the measurements is of the order of 0.002 K and the overall accuracy is better than 0.02 K. The temperature depth profiles made using the borehole temperature measurements are all shown in Figure 4.2.

4.5.1 Sudbury boreholes

Three deep boreholes (>2000 meters) were logged for temperature in the Sudbury region (Figure 4.1). The ongoing exploration for deep ore bodies in this region makes it an ideal site for deep borehole temperature measurements. The temperature profiles generated are especially good for GSTH studies since the rock formation is very homogeneous at depth (successions of gabbro and granite porphyry horizons), making important variations in thermal conductivity unlikely and measurements very stable. Thermal conductivity values for these boreholes were almost all within a 2.5 to 3.4 W/m·°C range. All boreholes were near vertical. The first borehole, 0316, was logged in September of 2003 and is located northeast of Sudbury, near the community of Falconbridge. This borehole is located in a wooded area next to a steep cliff dropping approximatively 35 meters. Although there is a major topographic effect on the temperature profile, the perturbation is mainly located in the first few hundred meters of the borehole and does not pose a problem when performing a GSTH of the order of tens of thousands of years. Therefore, this borehole was selected to perform a 50000 years GSTH for the Sudbury region. However, any information on the recent GSTH (1000-2000 years) from this borehole should not be trusted.

Borehole 0401 was logged in May of 2004 and is located northwest of Sudbury, south of the municipality of Chelmsford. The borehole is located in a wooded area approximately one kilometer from Xstrata's Lockerby Mine. At the time of measurement, a small beaver pond existed close to the borehole casing. This small lake was very recent (less than a year old) and any effects on the temperature profile are negligible. The main problem with this borehole was the fact that the core shack burned down a few years earlier, so any precise determination of thermal conductivity at depth is impossible. However there were piles of discarded core segments dispersed around the borehole casing and using the lithologic log and a trained geologist we matched the different rock types found at the surface with their description at depth and brought back several samples for thermal conductivity and radioactivity measurements. Since the entire borehole was very homogeneous, the small error associated with the conductivity depth uncertainty can also be neglected. This borehole was selected to perform a 50000 years GSTH for the Sudbury region.

Borehole 0402 was also logged in May of 2004 and is located northwest of Sudbury at the

Craig mine site, near the municipality of Levack. This borehole was unfortunately located near the mine, a lake and a road, and most likely affected by the surrounding topography. A simple visual inspection of the temperature profile reveals major non-climatic effects when compared with the other two deep boreholes logged in the region (Figure 4.2). The major effect is most likely water pumping at the mine, which affects the thermal regime of the entire surrounding area. This borehole was not selected to perform a long term GSTH of the Sudbury region.

In Figure 4.2, the temperature depth profiles of boreholes 0316 and 0401 are both shifted by 20°C, but they do not superimpose because surface conditions were different when the reference temperatures were established. Being located on higher ground with a thinner organic layer and sparser forest cover, the ground above borehole 0316 experiences higher surface temperatures than the ground above borehole 0401, which is located in lowlands, near marches. This does not affect the GSTHs since it is inferred independently from the surface temperatures. In order to infer absolute surface temperatures after our inversions, these surface temperatures must be added to the GSTHs.

4.5.2 Manitouwadge boreholes

Two deep boreholes were logged for temperature in the Manitouwadge region (Figure 4.3) in May of 2006. Both boreholes are located northeast of Manitouwadge near the old Geco mine. Borehole 0610 was drilled in the middle of a small marsh surrounded by forest. This borehole is near vertical down to 1100 meters, at which point it wedges to lower angles. This borehole was tentatively selected to perform a 50000 years GSTH of the Manitouwadge region.

Borehole 0611 is located in a wooded area close to the old mine and a couple hundred meters from a tailings pond. This borehole is near vertical for the entire length of the hole. There is a significant shift in the gradient of this borehole starting near 500 meters below surface. This shift seems to be too marked to be a climatic signal. However, the depth of this perturbation makes any man-made changes in surface conditions highly improbable since it would pre-date the colonization of North America. The proximity to the old Geco mine could possibly explain this perturbation. Since there are no irrefutable reasons to reject this borehole for inversion, it was tentatively selected to perform a 50000 years GSTH of the Manitouwadge region.

4.5.3 Previously studied boreholes

The other boreholes used in this study (9820, 0002, 0114 and the Flin Flon borehole) have been described in previous studies (Mareschal *et al.*, 1999; Rolandone *et al.*, 2003).

Boreholes 0002 and 0114, logged in Balmertown in 2000 and Thompson in 2001 respectively (Figure 4.2) are most likely under the depth limit required to infer ground surface temperatures at LGM. This factor is combined with important variations in thermal conductivities at depth (Rolandone *et al.*, 2003) and lower reference temperatures due to higher latitude, thus a small difference between the reference temperature, the temperature at the base of the glacier and present temperatures. All these factors make the determination of a reliable minimum temperature in ground surface temperatures before the holocene nearly impossible.

Borehole 9820, logged in Sept-Iles in 1998 (Figure 4.2), is only $\sim$ 100 meters deeper than 0002, but the deglaciation signal is much clearer on the profile. Combined with the added depth, the clearer signal may be due to the fact that the borehole is located where the edge of the glacier would have been and probably experienced lower basal temperatures at LGM than the reference or present temperatures.

The Flin Flon borehole was logged in 1970 and results for heat flow and an estimate of the LGM ground surface temperature were first published in Sass *et al.* (1971). These measurements were taken at 50 feet intervals. Reaching almost 3200 meters deep, this borehole is the deepest used in this study (Figure 4.2). Two important variations in thermal conductivities occur at depth around 1900 and 2300 meters (see (Rolandone *et al.*, 2003)). By calculating the thermal resistances at depth and multiplying these value by a representative thermal conductivity of 3.51 W/m·°C to obtain adjusted depths, we corrected the measured temperature depth profile in order to take these variations into account.

4.5.4 Temperature gradients

In Figure 4.3 we plot the gradients of all the selected temperature depth profiles presented in Figure 4.2. This visual tool helps to illustrate different features that appear in the raw data. If we look at a low noise level borehole such as Sudbury borehole 0401, three tendencies appear.

First, there is a relatively stable zone between 1900 and 2200 meters, related to the temperatures at the base of the glacier at and before LGM. Then, one can observe a net reduction in gradient values between 1900 and 900 meters which is due to the strong deglaciation signal, with ground surface temperatures rising towards the end of the last Ice Age and the subsequent rise in temperatures up to the Holocene climatic optimum (Anderson *et al.*, 1988). The third section (200-900 meters) is related to the relatively stable climate of the past 2000 years. The extremely large gradient variations in the shallowest portion of the boreholes are not shown in this figure and are caused by the recent warming of ground surface temperatures.

The other three new boreholes (0316, 0610 and 0611) show the same general tendencies. By looking closely at the gradient of the Sudbury borehole 0316 on Figure 4.3, a discontinuity appears at approximately 1000 meters. This discontinuity is due to an equipment problem, a cable reel broke halfway into the borehole temperature measurements and the cable had to be reeled-in, repaired and redeployed. The Manitouwadge boreholes (0610 and 0611) are located a few kilometers apart, but show a marked difference in the amplitude of gradient variations. As previously mentioned, it is possible that the old Geco mine could have affected the temperature regime at depth, however it would be quite a coincidence that this non-climatic perturbation kept a temperature signature identical as a climatic perturbation.

The four previously published profiles (in blue in Figure 4.3), are not all consistent with the four new profiles (in red). The Thompson (0114) borehole is the noisiest of all selected boreholes. This noise level, combined with important non-uniform variations in thermal conductivities at depth (see values in Rolandone *et al.* (2003)) makes it very difficult to extract a clear climate signal. Upon a visual inspection of its gradient, the Balmertown (0002) borehole does not seem to have recorded any climatic signal. This could be in part due to variations in thermal conductivities at depth (see Rolandone *et al.* (2003)). This lack of long-term climatic signal in a deep borehole has been observed in other regions with inhomogeneous rock horizons at depth displaying high variations in thermal conductivities (i.e. the Matagami (Quebec) region).

When compared with the gradients from the new borehole measurements (in red), the Sept-Iles (9820) borehole seems to exhibit a very late deglaciation signal. It even seems that temperatures started to warm following LGM, then cooled before warming up to Holocene temperatures. The Flin Flon borehole does not show a marked climate signal, however the same general ten-

dencies observed in the new profiles and in 9820 are still present. As previously mentioned, the variations in thermal conductivity were uniform at depth and were taken into account.

4.6 Results

All the GSTHs in this study were performed using both SVD and Monte-Carlo methods. For the SVD inversions, an 18-step 50000 years GSTH using a regularization parameter of $\varepsilon = 0.08$ was used on all profiles to be consistent with the study of (Rolandone *et al.*, 2003). The same regularization parameter could be used on all boreholes since they all have approximately the same number of eigenvalues.

For the Monte-Carlo simulations, a total of 10 billion models were explored for each temperature depth profile with a maximum quadratic error allowed for each simulation adjusted between a value of 1 and 2 so between 1000 and 3000 models would be retained for each simulations. This number of models yielded excellent reproducible statistics. Generally, the result of the SVD inversion was used as an initial model for the simulation. We do not think this induces a bias and tested this assumption by performing Monte-Carlo simulations on different profiles using both the result of a SVD inversion and a null hypothesis (GSTH with values of 0 for each time step) as initial models. As expected, the result using the SVD inversion as an initial model did produce more models within the fixed maximum quadratic error, however both methods yielded very similar results for all profiles.

We plotted the results of the SVD inversions in Figure 4.4 and of the Monte-Carlo simulations in Figure 4.5. For all sites, the general trends between the two methods are practically identical, with most sites exhibiting strong deglaciation signals and clear Holocene optimum temperatures. The main difference between the two methods is found in the actual amplitude of the climate signals. A recent study by Chouinard *et al.* (2007) showed that the SVD method is generally more conservative with regards to temperature amplitudes when reconstructing GSTH than the Monte-Carlo simulations. This feature can also be observed in these results.

The main features of the GSTHs for each temperature depth profile are detailed in Table 4.2 for the SVD inversions and Table 4.3 for the Monte-Carlo simulations. In these tables, the minimum temperature near LGM for each sites is given for each method, along with the time interval

during which this minimum occurred. The same has been done for the maximum temperatures that occurred during the Holocene climatic optimum.

4.7 Discussion

One striking feature of Figure 4.4 and Figure 4.5 is that all sites do not show a clear LGM minimum temperature signal, however they all show signs of the important subsequent Holocene warming. It seems the shallowest boreholes (0002 and 0114) did not capture a clear LGM minimum temperature signal. In the section discussing the gradients of selected boreholes, we already mentioned that on top of having important variations in thermal conductivity at depth, the 0002 borehole did not seem to have recorded a deglaciation signal and that 0114 was very noisy (Figure 4.3), making climate estimates very difficult in both cases. The fact that these were also the two shallowest boreholes was also raised as a possible partial explanation for the lack of signal. We tested this theory by truncating one of the deeper boreholes (0401) by increments of 100 meters and inverting the resulting profiles using SVD. The results showed the expected loss of resolution with shallower depth. However, the pattern of this loss of resolution is interesting, the minimum and maximum values decreasing in amplitude while being shifted towards more recent times. In Figure 4.6 we compare the GSTH of the complete 0401 profile with GSTHs made with the 0401 profile truncated at 1800 and 1400 meters. The shorter profiles yield GSTHs that are similar to the GSTHs of 0002 and 0114 (Figure 4.4), the main difference being a lower Holocene maximum value for 0002 and 0114 due in part to the loss of signal and to the fact that they are located further North than the 0401 profile. If we also take into account the much deeper Flin Flon borehole which is located in the same region as 0114, but shows minimums and maximums of much higher amplitudes, it would be safe to say that even if a deglaciation signal would have appeared in their gradients, the two shallow boreholes are simply not deep enough to have captured the full LGM and deglaciation signal. Thereby, contrary to the statement of Rolandone *et al.* (2003), boreholes shallower than 1800 meters should not be used to infer LGM surface temperatures.

The shallowness of the 0114 borehole also partly explains the low reference temperature inferred from the inversions. Instead of being related to the average ground surface temperature of the past 500000 years and it's multiple glaciation-deglaciation periods (Harris et Chapman, 1995; Mareschal *et al.*, 1999), it ends up being heavily affected by the last glaciation and thus

exhibits a very low value.

4.7.1 Comparison with previous studies

When compared with the previous study by Rolandone *et al.* (2003) using the SVD method to infer the GSTHs, the results of the previously studies boreholes (flinflon, 9820, 0002 and 0114) are of course very similar. We did not use the same temporal parametrization, choosing not to resolve the past 100 years in order to cut down on the number of temporal parameters to be resolved. We also opted not to parameterize the period ranging from 50000 to 100000 years before present since none of the boreholes are deep enough, nor have enough climatic signal remaining to capture these GSTHs (Harris et Chapman, 1995; Mareschal *et al.*, 1999). Using the same regularization parameter with fewer parameters probably explains the small gain in resolution in our results.

If we compare the Sept-Iles site (9820) with the results from the paper of Mareschal *et al.* (1999) in which they used the Monte-Carlo method to infer the GSTH, we find significant differences with our results in both absolute temperatures and amplitudes. Some of these differences could be due to the lower number of models explored and thus retained in their study. In their paper, they found absolute temperatures of -5 to -6°C at LGM and 6 to 7°C for the Holocene climatic optimum, yielding an amplitude of approximately 12 degrees between the two events. Our Monte-Carlo results Table 4.3 suggest a minimum of -1.6°C and a maximum of 6°C for a total amplitude of approximately 7.6°C. Also, their reference temperature is identified at between 0 and 1°C, whereas ours is of 2.1°C regardless of the method used. Since our Monte-Carlo result is consistent with both our SVD result and the SVD result of the Rolandone *et al.* (2003) study, we think our GSTH of the Sept-Iles region is better constrained.

4.7.2 Laurentide Ice Sheet basal temperatures and retreat

There seems to be inconsistencies with some of our results when looking at the T_{min} column in Table 4.2 and Table 4.3. As expected the values are invariably lower for the ground surface temperatures obtained using the Monte-Carlo method (Chouinard *et al.*, 2007) and to identify reliable absolute temperatures, we think these values are probably more reliable.

The Flin Flon temperature depth profile is subject to important changes in thermal conductivity at the depth where the major portion of the LGM ground surface temperature signal is located (~1900 meters). Even though we made corrections to account for this change, these corrections are of the order of the signal we try to extract so the uncertainty becomes higher for this profile at these depths. Because of this, the T_{min} value of -1.9°C obtained in the 10-15 ky B.P. interval using the Monte-Carlo method might not be as reliable as some of the other T_{mins} inferred in this paper. If we focus on the subsequent warming and the ice sheet retreat, the results show that the 0°C threshold was crossed between the 8-10 and 10-15 ky B.P. intervals, which correlates perfectly with the dates shown on deglaciation maps from Dyke *et al.* (2003), with an ~10ky B.P. ice sheet retreat and a ~9ky B.P Lake Agassiz retreat at Flin Flon.

Following glacial retreat, the Sept-Iles site (9820) remained submerged and rebounded above sea-level ~6 ky B.P. (Hillaire-Marcel, 1979). Our results show that ground surface temperatures were approximately at 0°C between 6 and 8ky B.P.. This result suggests that following relatively low ground surface temperatures during the past ice age (~-1.6°C), permafrost may have formed below the ice sheet in this region and lasted approximately until the period this region rebounded above sea-level. Permafrost occurrence in this region at the time of glacial retreat is not uncommon (Govaire et Gangloff, 1989).

The sites of Balmertown (0002) and Thompson (0114) have already been identified as unlikely to yield any useful information regarding basal temperatures at LGM. The very high basal temperature values obtained using both inversion methods confirm this (Table 4.3).

The two selected Sudbury temperature depth profiles (0316 and 0401) are probably the best suited to perform this type of study because of their combination of great depth and few variations in thermal conductivities. Our GSTHs of this area show that basal temperatures were between -0.7 and -0.9°C between 20 and 25 ky B.P. (Figure 4.5), coinciding with the timing of the LGM. The 0°C was reached during the 10-15 ky B.P. interval for borehole 0316 and during the 15-20 ky B.P. interval for borehole 0401. Although seemingly different, these results show that this temperature was most likely reached near the 15 ky B.P. mark. The fact that time is poorly constrained in our models at those ages (~4000 years uncertainty), may explain the difference between our results and the ~12.5 ky B.P. glacier retreat date from the Dyke *et al.* (2003) maps. However, ground surface temperatures could actually have been slightly above 0°C

during the few thousand years preceding the total retreat of the glacier, as basal flow velocities over this region have been predicted to be quite high during this period (Clark *et al.*, 1996; Licciardi *et al.*, 1998; Clark *et al.*, 1999; Dyke *et al.*, 2002; Peltier, 2004).

The Manitouwadge boreholes (0610 and 0611) present a great interpretation challenge because of the striking differences between the two temperature depth profiles and their inversions. By looking at Figure 4.5, one can notice the difference in the profiles of 0610 and 0611, especially when compared to the profiles 0316 and 0401 of Sudbury. The Sudbury profiles are fairly identical whereas the Manitouwadge profiles are not, the 0611 profile exhibiting a curvature not seen on profile 0610. We currently have no explanation for this feature. Because of this, it is very difficult to interpret the GSTHs inferred from those profiles, with T_{mins} of 1°C for 0610 and -3.82°C for 0611 (Table 4.3). The signal seems to be damped for 0610 and amplified for 0611. Thermal conductivity measurements are not yet completed on theses boreholes, so a definite answer will only be possible once every possible measurable parameter has been taken into account. The GSTH of borehole 0611 still presents a plausible 0°C timing, with surface temperatures going from negative to positive values between the 8-10 and the 10-15 ky B.P. intervals. This result would be in agreement with the ~10.2-10.7 ky B.P. ice sheet retreat dates estimated for this area (Saarnisto, 1974; Dyke *et al.*, 2003).

4.7.3 Holocene Climate Optimum

As explained in the previous section, there are some discrepancies in the T_{max} values between the SVD and Monte-Carlo results. Again, since the SVD results tend to be a bit conservative, we will use the Monte-Carlo results when discussing the results. In order to compare the dates and duration of event from our results with dates from other proxies studies using uncorrected ^{14}C dates, we calibrated them using a tool based on the (Fairbanks *et al.*, 2005) calibration curve.

The Flin Flon results (Figure 4.5) show a warm period occurring between the 2-3 and the 4-6 ky B.P. time intervals. In Table 4.3, we can see that a maximum temperature of almost 6°C was reached during the 3-4 ky B.P. interval. These results correlate well with proxies from other studies performed in this region and for which the Holocene climate optimum (HCO) is fixed between 2 and 6.8 ky B.P.(Ritchie, 1983), with a maximum occurring ~6.2 ky B.P.(Mott, 1973; Ritchie, 1983, 1987; Patterson *et al.*, 1997).

As previously discussed, the lack of a clear climatic signal for the Thompson (0114) and Balmertown (0002) boreholes, partially due to large variations in thermal conductivities at depth, combined with their relatively shallow depths, produces results that are biased towards low and late HCO values. To eliminate this problem and try to isolate only the Holocene GSTH, we tried truncating the temperature depth profiles to even shallower depths in order to minimize the effect of the last glaciation. Not only did this method not produce any improvements, but it eliminated part of the HCO signal. The part of the boreholes containing the HCO signal being indivisible from the deglaciation signal, it is therefore impossible to establish reliable HCO temperature amplitudes or chronologies using these boreholes.

The Sept-Iles (9820) GSTH yields an HCO that occurs between 1.5 and 3 ky B.P. (Figure 4.5), with a maximum value over 6°C during the 2-3 ky B.P interval (Table 4.3). This HCO signal happens later and is shorter than for the other regions because, as previously mentioned, the site was submerged prior to ~6 ky B.P. (Hillaire-Marcel, 1979). However, even the part of the region that rested above sea level remained relatively cool for an extended period of time because of catabatic winds coming from the residual Quebec-Labrador ice dome (Richard et Labelle, 1988). These winds most likely kept regional ground surface temperatures lower than surrounding water temperatures and would have caused the late afforestation of the north shore of the Gulf of St. Lawrence. These cool air and land conditions are not recorded in the marine environment offshore Sept-Iles (HCO signal at ~6.5 ky B.P.) because of water mass homogenization (de Vernal *et al.*, 1993).

For the Sudbury boreholes (0316 and 0401), we will rely exclusively on the results from the 0401 borehole for HCO temperature determinations since, as previously mentioned, the 0316 borehole is affected by severe topography which could be inducing a non-climatic effect up to 2 ky B.P.. This effect is visible on the inversion results (Figure 4.5), where the 0316 GSTH is the only one exhibiting a continuous cooling in the past 2000 years up to 200 years ago. The results of the Monte-Carlo inversion for the 0401 borehole (Figure 4.5) reveal a HCO signal between the 2-3 and 6-8 ky B.P. time intervals, with a maximum value of 8.4°C during the 4-6 ky B.P. interval. This is in agreement with palynological analysis performed in northeastern Ontario (Liu, 1990; Boudreau *et al.*, 2005), showing a HCO signal occurring between 3 and 7.8 ky B.P., with maximum values found between 4.4 and 6.8 ky B.P.. At sites located in northern Michigan, 430km east of Sudbury, Davis *et al.* (2000) have shown maximum Holocene

temperatures occurring between 4.4 and 6.8 ky B.P., again in good agreement with our Sudbury results.

The determination of absolute temperatures at the Manitouwadge sites (0610 and 0611) is not possible because of the problems presented in the previous section. However, even in the amplitude of the GSTHs are not well constrained, the timing of the successive climatic events should still be relatively well resolved. We will use the results of borehole 0611 to compare timing with other proxies since the signal is much clearer than for borehole 0610. From Figure 4.5, a clear HCO is apparent between 2-3 and 6-8 ky B.P., with maximum values reached during the 4-6 ky B.P. interval. These intervals are the same as for the Sudbury region and thus correlate well with the results from the studies mentioned in the previous paragraph. A study from Björck (1985) performed in northwestern Ontario puts the HCO at ~6.8-7.4 ky B.P., a bit earlier than our results and from similar studies in northeastern Ontario, but still within the incertitude of our temporal resolution.

4.8 Conclusion

The ice-sheet basal temperatures inferred from our inversions show that basal temperatures probably never reached values below -2°C under the ice sheet at any of our studied sites during the past 30000 years. Although we can not stress enough that the temporal resolution of our results decreases greatly as we go further back in time. Because of this, the temperature values end up being averaged over a very long time period and basal temperatures could have reached lower, or higher, temperatures during the 5000 to 15000 years time-steps we present in this study.

The inferred ground surface temperatures presented in this study are all at or near the pressure melting point and would allow the occurrence of fast flowing ice streams that is either predicted (Peltier, 2004) or deducted through observations (Dyke *et al.*, 2002) over the Canadian prairies and north of the Great Lakes in Ontario.

In order to gain a better understanding of possible permafrost presence and its thickness at different locations under the ice-sheet, our basal temperature results should be combined with a permafrost evolution model.

Overall, our results yield maximum ground surface temperatures between 6 and 8.4°C occurring at different periods between 2 and 8 ky B.P. (relative to the HCO chronology in each region) over central and eastern Canada.

The agreement of our LGM basal temperature values with observations and predictions, combined with the agreement of our Holocene climate optimum results with other proxies validates that the long-term ground surface temperature histories inferred in this study are robust and reliable.

4.9 Acknowledgments

We wish to thank C.Jaupart, G.Bienfait, C.Gosselin, H.K.C.Perry, P.Audet and R.Lapointe who all helped with field measurements and core sample analysis. Part of this work was supported by the Natural Sciences and Engineering Research Council of Canada through a Discovery Grant.

TAB. 4.1: For each borehole selected to perform a GSTH in this paper, we give the location, the log identification number, the geographic coordinates, the vertical depth measured (Δh), and the elevation of the site.

Site	Log i.d.	Latitude	Longitude	Δh,m	Elevation,m
Flin Flon	flinflon	54°43'	102°00'	2865	333
Sept-Iles	9820	50°12'46"	66°38'19"	1820	70
Balmertown	0002	51°01'59"	93°42'56"	1724	359
Thompson	0114	55°29'10"	98°07'42"	1610	224
Sudbury	0316	46°39'05"	80°47'30"	2121	321
Sudbury	0401	46°26'00"	81°18'55"	2206	283
Manitouwadge	0610	49°09'07"	85°43'46"	2068	320
Manitouwadge	6011	49°10'16"	85°46'31"	2279	325

TAB. 4.2: Results of the SVD inversions for every borehole used in this study. The table highlights the major features of the GSTHs for each borehole, which are their reference temperatures T_{ref}, the temperature gradient ∇ (related to the regional heat flow) and the minimum (T_{min}) and maximum (T_{max}) temperatures reached along with their corresponding chronology.

Profile	T_{ref}(°C)	∇(°C/m)	T_{min}(°C)	Time (kyear BP)	T_{max}(°C)	Time (kyear BP)
flinflon	4.04	0.0114	-0.20	8.9-12.6	5.71	3.2-4.5
9820	2.07	0.0167	-1.49	12.6-17.7	5.76	1.6-2.2
0002	2.49	0.0098	2.02	6.3-8.9	3.41	1.6-2.2
0114	0.67	0.0159	0.53	17.7-35.5	0.68	6.3-8.9
0316	3.06	0.0166	-0.32	17.7-25	6.04	3.2-4.5
0401	4.07	0.0174	0.31	25-35.4	7.65	4.5-6.3
0610	2.28	0.0130	1.14	17.7-25	4.02	2.2-3.2
6011	1.60	0.0135	-3.26	17.7-25	6.52	3.2-4.5

TAB. 4.3: Results of the Monte-Carlo simulations for every borehole used in this study. The table highlights the major features of the GSTHs for each borehole, which are the number of retained models for the simulation, their average reference temperatures T_{ref}, the average temperature gradient ∇ (related to the regional heat flow) and the minimum (T_{min}) and maximum (T_{max}) temperatures reached along with their corresponding chronology.

Profile	#models	T_{ref}(°C)	∇(°C/m)	T_{min}(°C)	Time (kyear BP)	T_{max}(°C)	Time (kyear BP)
flinflon	1389	4.27	0.0113	-1.91	10-15	5.99	3-4
9820	2075	2.11	0.0167	-1.59	10-15	6.06	2-3
0002	2482	2.64	0.0098	1.61	6-8	3.80	2-3
0114	1183	0.72	0.0159	0.32	20-35	0.78	6-8
0316	2457	3.17	0.0166	-0.69	20-35	6.51	3-4
0401	1624	4.13	0.0174	-0.90	20-35	8.38	4-6
0610	2644	2.18	0.0131	1.04	15-20	4.25	2-3
0611	1480	1.72	0.0135	-3.82	20-35	7.98	4-6

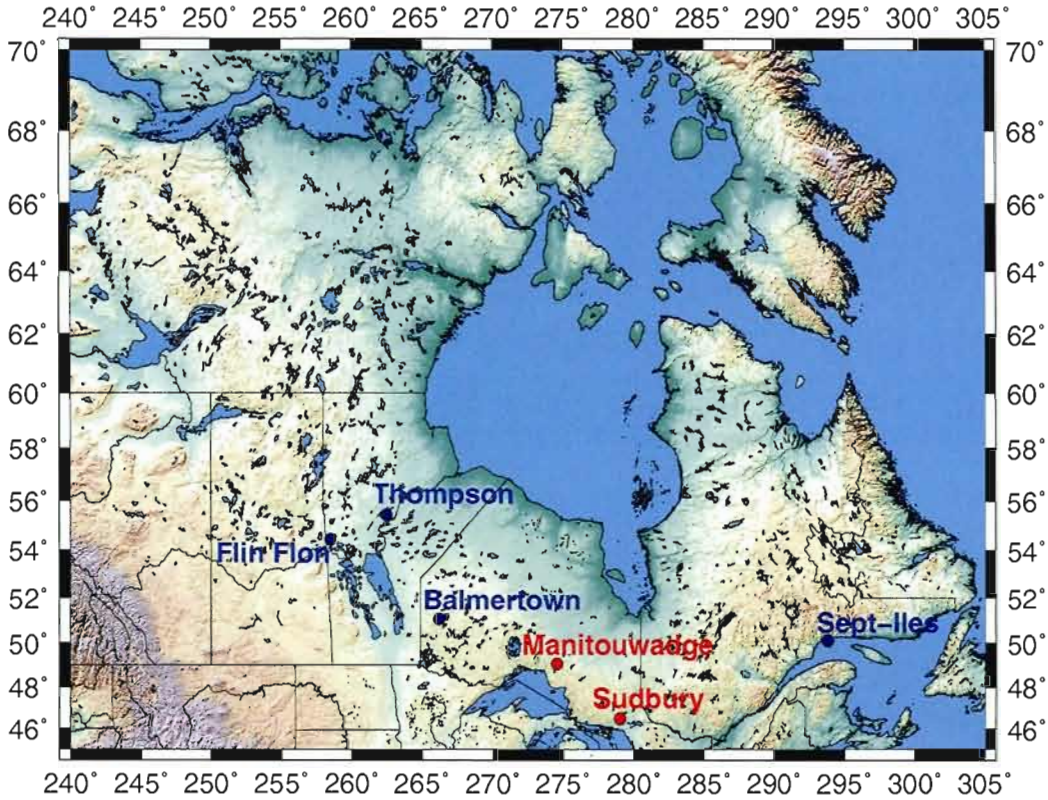

FIG. 4.1: Map of Canada showing the location of all the boreholes used to infer GSTHs in this study. The sites in blue were discussed in previously published papers, the sites in red are the new boreholes presented in this paper.

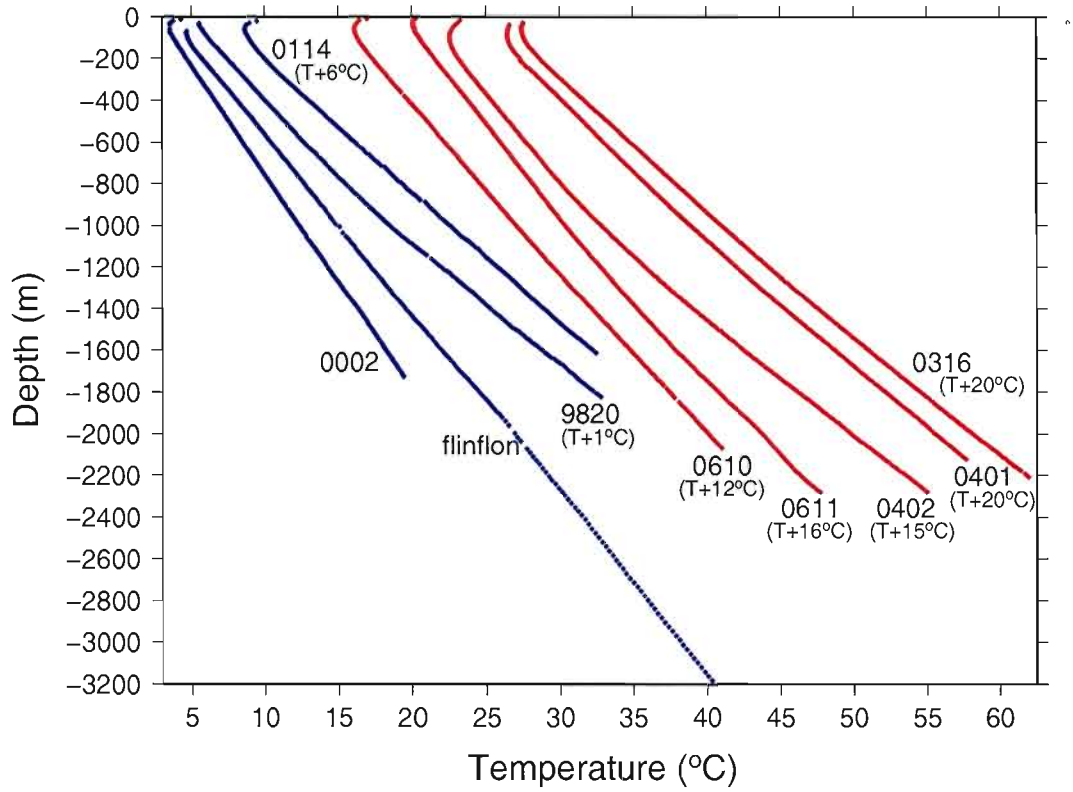

FIG. 4.2: Temperature depth profiles of all boreholes mentioned in this study. The profiles in blue were presented in previous papers, the profiles in red are the new measurements presented in this paper.

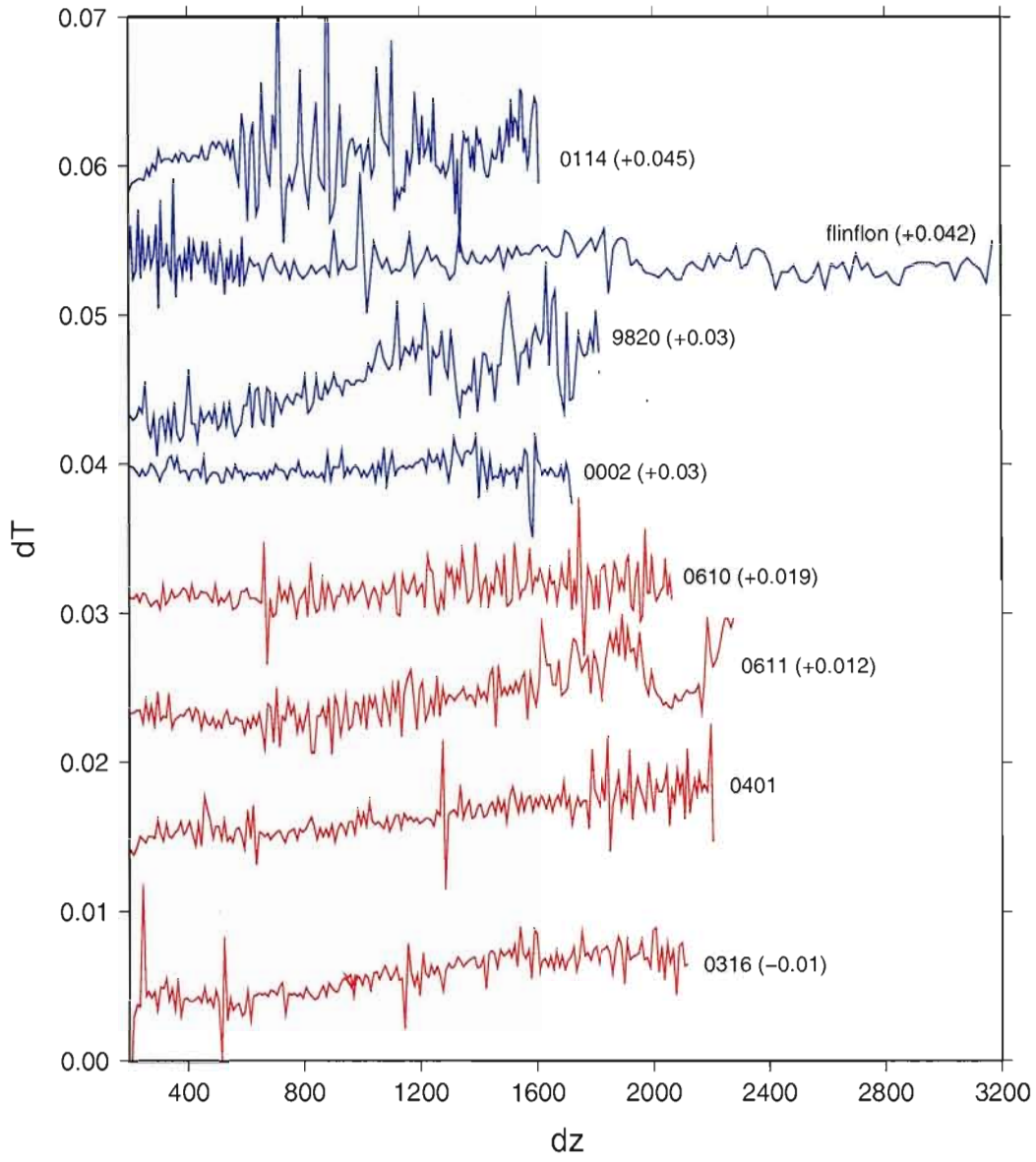

FIG. 4.3: Gradients of all boreholes selected to perform a GSTH in this paper.

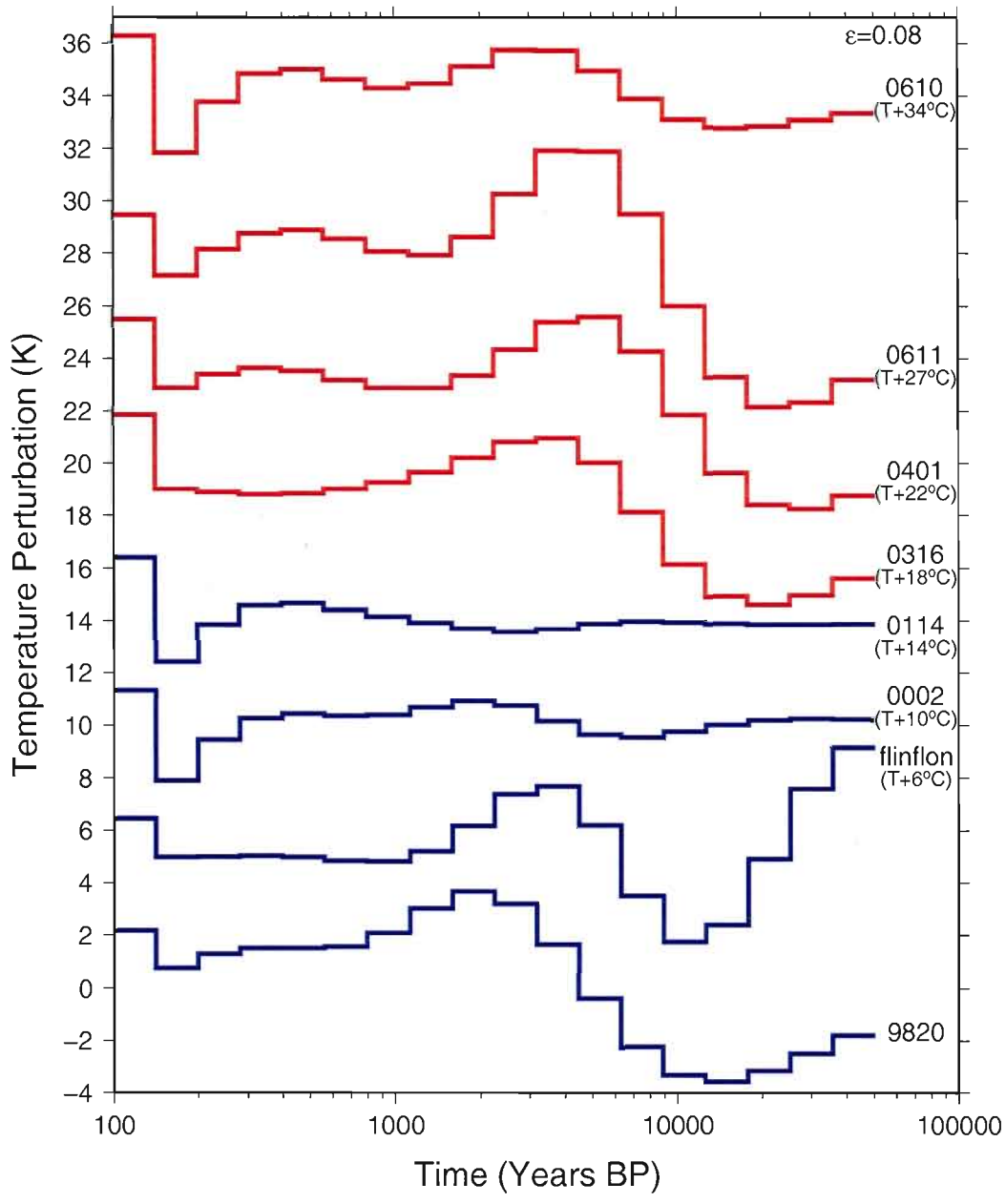

FIG. 4.4: Ground surface temperature histories inferred from the temperature profiles presented in Figure 4.2 using a singular value decomposition algorithm.

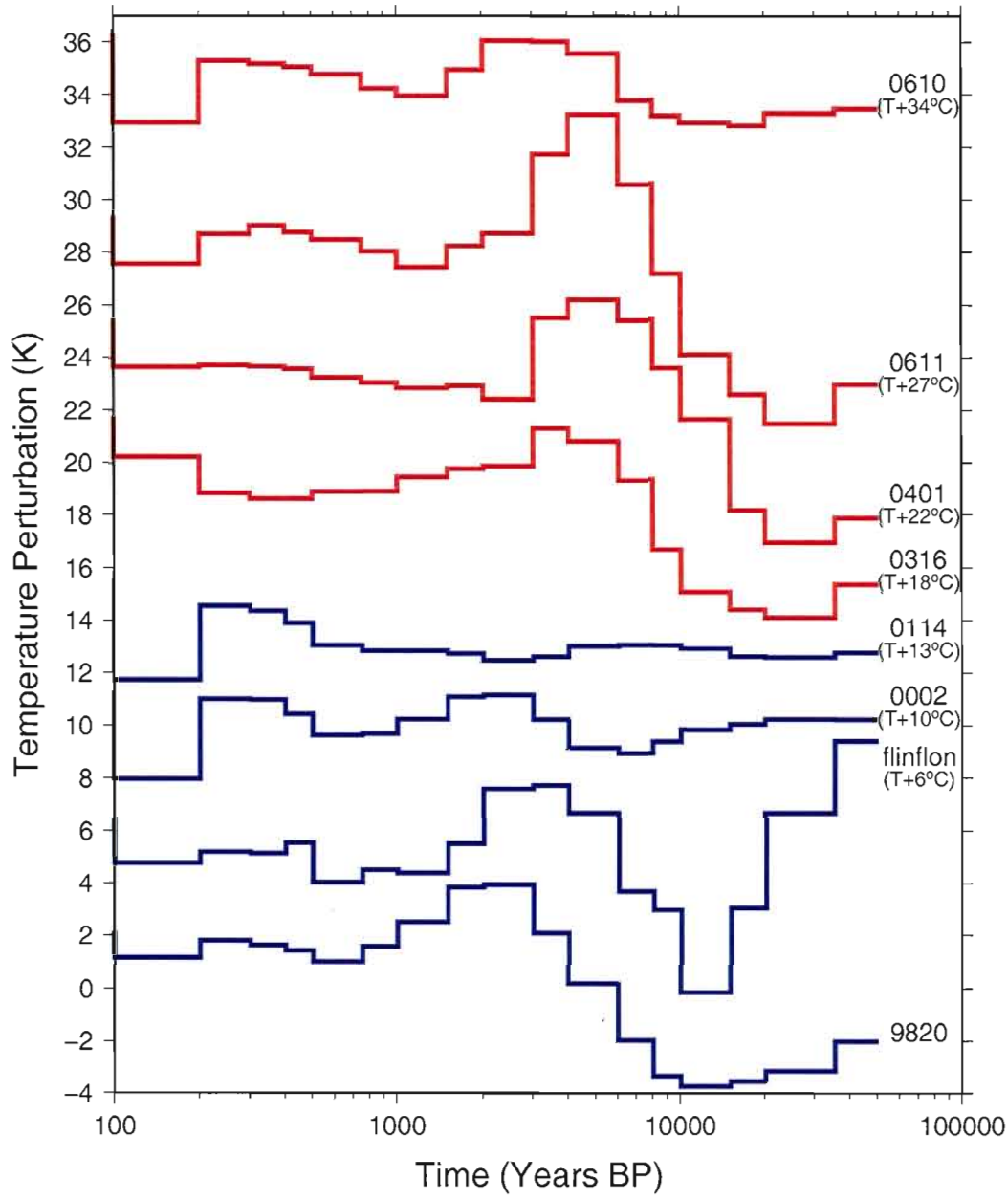

FIG. 4.5: Ground surface temperature histories inferred from the temperature profiles presented in Figure 4.2 using a Monte-Carlo simulation.

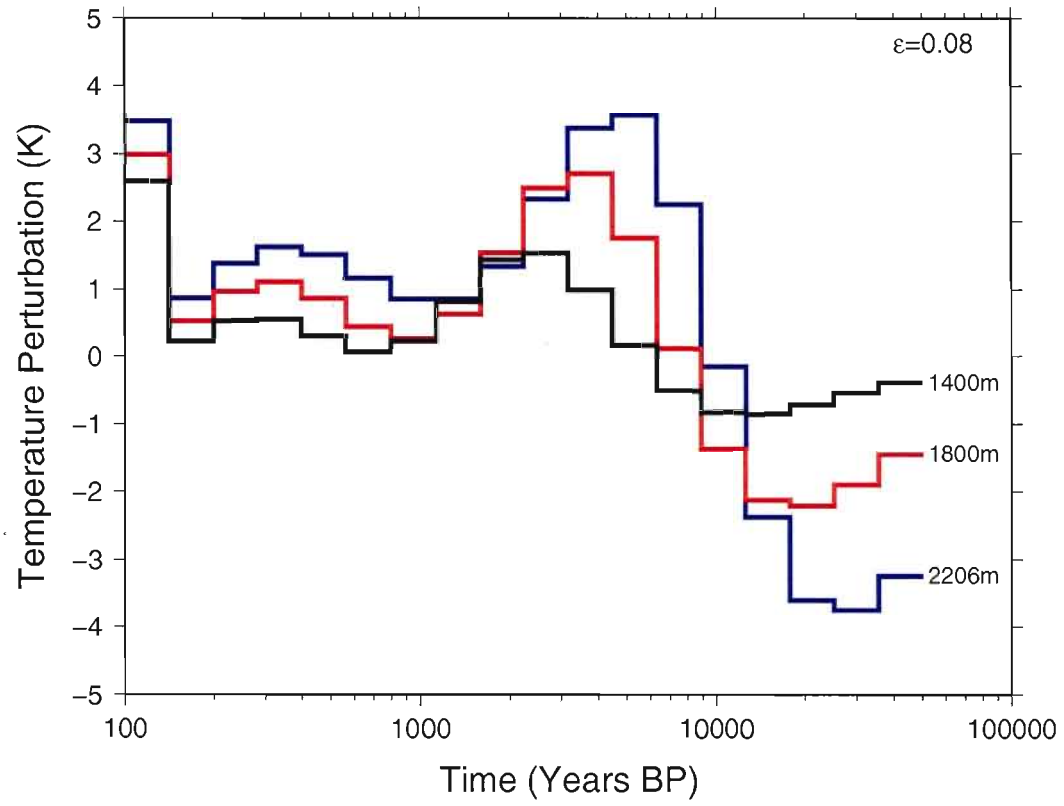

FIG. 4.6: Test performed on GSTHs based on the temperature profile of borehole 0401. The profile was cropped at 1800 and 1400 meters and inversions of the profile were performed. The results show a loss in resolution for the LGM basal temperatures and for the values of the HCO.

CHAPITRE 5

CONCLUSION

Le manuscrit de cette thèse regroupe les résultats de trois études portant sur l'amélioration de la méthode de reconstitution de l'histoire des température à la surface du sol (HTSS) ainsi que sur son application à des problèmes environnementaux touchant aux changements climatiques passés à courte et à longue échelle temporelle. Les objectifs généraux de cette thèse étaient de faire avancer les connaissances sur la méthode de reconstitution de l'HTSS ainsi que de fournir des données reliées aux changements climatiques qui contribueront à accroître notre compréhension du système climatique et qui pourront servir à valider les prédictions des modèles de circulation globale ainsi que les modèles d'évolution des calottes glaciaires. Tous les résultats présentés dans ce manuscrits sont originaux.

Le premier chapitre publié sous le titre « Selection of borehole temperature depth profiles for regional climate reconstructions » consiste en une étude de la nécessité de sélectionner des profils de températures non perturbés par des phénomènes non-climatiques lorsque l'on entreprend de faire une reconstitution régionale de l'HTSS. Afin d'évaluer si cette sélection est nécessaire, une comparaison des différentes méthodes de traitement de données et d'inversions a été effectuée afin de déterminer quelle méthode permet d'obtenir une HTSS combinant un résultat stable, fiable et ayant la meilleure résolution possible. Les multiples analyses sur les séries de données montrent que les différentes méthodes sont généralement cohérentes entres elles. Cependant, afin de minimiser les effets associés aux perturbations non-climatiques et de s'assurer que la reconstitution régionale de l'HTSS ne soit pas faussée par un signal perturbé, quelques étapes devraient être systématiquement mises en oeuvre : 1) sélectionner minutieusement les profils de température à utiliser afin d'éliminer tout profil susceptible d'être affecté par des perturbations non-climatiques ; 2) ajuster le paramètre de régularisation au niveau de bruit ainsi qu'au nombre de profils utilisé lors de l'inversion simultanée ; et 3) afin de confirmer que le résultat de l'HTSS est juste et de s'assurer qu'il n'y a pas d'instabilités dues à l'inversion, faire une moyenne des inversions individuelle de tous les profils utilisés lors

de l'inversion simultanée et la comparer à cette dernière. La résolution de l'HTSS obtenue d'une moyenne des inversions individuelles des profils sera généralement plus faible que celle de l'HTSS obtenue d'une inversion simultanée des mêmes profils, mais la solution sera invariablement plus stable. Une solution avec une résolution plus faible mais stable est toujours préférable à une solution instable. Les différentes analyses utilisées afin de tester la méthode de reconstitution régionale de l'HTSS ont également permis de confirmer les résultats obtenus lors d'études précédentes (Nielsen et Beck, 1989; Beltrami et Mareschal, 1991; Beltrami *et al.*, 1992; Beltrami et Mareschal, 1992; Wang *et al.*, 1994; Guillou-Frottier *et al.*, 1998; Majorowicz *et al.*, 1999; Gosselin et Mareschal, 2003; Beltrami et Bourlon, 2004). Entre autres, au cours des 500 dernières années, les régions étudiées ont subies un réchauffement de la température de surface d'une amplitude variant de 0.5 à plus de 1.0 K. Le signal de refroidissement attribué au petit âge glaciaire est corrélé et semble pratiquement synchrone entre la région Manitoba-Saskatchewan et la région de l'est du Canada. Cependant ce signal est totalement absent de la région du nord-ouest de l'Ontario qui s'étend sur quelques centaines de kilomètres au nord-ouest du Lac Supérieur (Gosselin et Mareschal, 2003).

L'étude formant le deuxième chapitre est publiée sous le titre « Recent climate variations in the subarctic inferred from three borehole temperature depth profiles in northern Quebec, Canada » et consiste en une reconstitution de l'HTSS au site minier Raglan, dans le grand nord québécois. Cette étude tente de clarifier certaines questions sur le réchauffement postérieur au petit âge glaciaire soulevées par des résultats contradictoires sur la période de refroidissement ayant eu lieu au milieu du 20^{e} siècle dans cette région de l'Arctique (Overpeck *et al.*, 1997; Hughen *et al.*, 2000; Przybylak, 2000; Kasper et Allard, 2001). Sur une période de deux ans, quatre mesures ont été effectuées dans trois forages d'exploration minière creusés à même le pergélisol. Les profils de températures sont inversés individuellement et simultanément afin de déterminer l'HTSS. De tous les profils mesurés, un seul est considéré comme n'étant pas affecté par des perturbations non-climatiques et est utilisé pour effectuer des HTSS détaillées des 400 et 800 dernières années. Trois méthodes de reconstitution sont utilisées indépendamment afin d'obtenir un résultat stable, fiable et ayant la meilleure résolution possible. Les résultats des trois méthodes sont corrélés et montrent le commencement du petit âge glaciaire (PAG) entre 1400 et 1500 ans AD. Les températures de surface ont chuté de plus de 0.3 K au minimum du PAG, il y a de ça 300 ans. Le réchauffement ultérieur au PAG fait ensuite grimper les températures de surface de plus de 1.3 K entre le milieu du 18^{e} siècle et le début du 20^{e} siècle. À partir des

années 1940, les températures de surface ont chuté de plus de 0.3 K sur une période de 40 ans, jusqu'au début des années 1990. Les résultats obtenus confirment le refroidissement constaté par l'étude des coins de pergélisol de Kasper et Allard (2001) et les études climatologiques de Jones et Kelly (1983) et Przybylak (2000), tout en apportant plus d'information sur l'amplitude et la chronologie de ce refroidissement. Depuis le début des années 1990, un réchauffement très sévère a lieu dans cette région, les températures de surface ayant grimpé de 1.7 K en 15 ans pour atteindre des valeurs de 2.3 K plus élevées qu'avant le PAG.

Le troisième chapitre porte le titre « 30000 years ground surface temperature history from deep boreholes across Canada : From last glacial maximum basal temperatures to Holocene climate optimum » et consiste en une reconstitution de l'HTSS sur une période allant du dernier maximum glaciaire (DMG), il y a 20000 ans, jusqu'à l'optimum climatique de l'Holocène, il y a environ 6000 ans. Cette étude tente de déterminer des valeurs de températures basales du glacier Laurentidien basées sur des données réelles afin de valider les valeurs prédites par les modèles. Des profils de température mesurés dans des forages très profonds (environ 2000 mètres) à six sites au Canada (trois dans le centre du pays, deux dans l'est et un sur la côte Atlantique) sont analysés en utilisant deux méthodes d'inversions indépendantes. De nouvelles mesures ont été combinées avec des données déjà publiées et ré-analysées afin de comparer objectivement les différentes températures basales ainsi que leur distribution spatiale. Les résultats montrent que les températures sous la portion sud du glacier Laurentidien ne sont probablement jamais descendues sous la barre des -2°C lors du DMG. Au DMG, les sites de Flin Flon (-1.9°C au centre de la portion sud du glacier) et de Sept-Îles (-1.6°C à la frontière est du glacier) montrent les températures les plus basses. Ces résultats confirment les prédictions des modèles isostatiques (Peltier, 2004) et d'observations géomorphologiques à la surface (Dyke *et al.*, 2002) qui suggèrent que les températures basales sous la portion sud du glacier devaient être près du point de fusion de la glace afin de permettre un écoulement rapide de la glace basale. Les reconstitutions des températures de surface de l'optimum climatique de l'Holocène ont été effectuées en utilisant les mêmes HTSS que pour les températures basales. Les résultats montrent des températures moyennes de surface de 6°C dans la région de Flin Flon entre 3000 et 4000 ans BP. La région de Sept-Îles a connu des températures de surface de 6°C entre 2000 et 3000 ans BP, tandis qu'à Sudbury des températures d'environ 8°C ont été enregistrées à la surface du sol entre 4000 et 6000 ans BP. Ces résultats sont corrélés chronologiquement avec les périodes chaudes identifiées par un grand nombre d'études utilisant différents proxies (Mott,

1973; Saarnisto, 1974; Ritchie, 1983; Björck, 1985; Ritchie, 1987; Woods et Davis, 1989; Liu, 1990; de Vernal *et al.*, 1993; Patterson *et al.*, 1997; Davis *et al.*, 2000; Boudreau *et al.*, 2005) et ont l'avantage de présenter des valeurs de températures absolues pour ces périodes.

Dans une perspective de travaux futurs, les résultats des chapitres portant sur le climat Arctique et sur les tempétratures basales pourraient être utilisés comme données d'entrées pour des modèles d'évolution du pergélisol afin de déterminer la réponse de celui-ci aux différents changements se produisant à la surface. Ainsi, il serait possible de voir à la fois où et quand le pergélisol aurait pu se former sous le glacier Laurentidien et combien de temps il aurait pu continuer à exister à la suite du retrait glaciaire. Aussi, dans le contexte des reconstitutions de l'HTSS de l'Arctique, de tels modèles permettraient de mieux comprendre comment les changements climatiques récents ont affecté les différentes régions de ce vaste territoire. Le pergélisol étant un phénomène uniquement régit par le climat, il serait intéressant de déterminer la vitesse à laquelle il répond aux changements de température à la surface.

Un projet de création d'un observatoire du pergélisol a été proposé par l'International Permafrost Association. Le projet consiste en une campagne de forage à plusieurs endroits dans l'Arctique afin d'installer des stations d'observation de l'évolution passée et présente du pergélisol. Cependant, les forages proposés ne sont que de quelques dizaines de mètres, des profondeurs insufisantes pour les reconstitutions de l'HTSS. Il serait souhaitable que quelques uns de ces forages soient creusés à des profondeurs de plus de 500 mètres afin de permettre l'évaluation des conditions de surface passées et ainsi déterminer l'évolution antérieure du pergélisol jusqu'aux conditions présentes. Ceci permettrait d'évaluer non seulement l'évolution naturelle du pergélisol, mais également la variabilité régionale du climat Arctique au cours du dernier millénaire.

La croissance des prix des métaux justifie l'exploration minière à des profondeurs qui étaient jusqu'à maintenant jugées inutiles dus à des coûts d'exploitation très élevés. Ainsi, le nombre de forages très profonds (plus de 2000 mètres) au Canada et ailleur dans le monde va invariablement augmenter. L'utilité de ces forages à été démontrée dans le troisième chapitre de cette thèse et il sera essentiel de mesurer ces nouveaux forages afin de permettre des reconstitutions de l'HTSS sur de longues échelles temporelles. Ces HTSS permettront sans doute d'améliorer la faible résolution spatiale des données existantes.

En somme, les reconstitutions de l'HTSS à partir de profils de température offrent un moyen unique d'obtenir de l'information sur les températures de surface là où de nombreuses autres méthodes sont limitées ou inexistantes. L'exploration minière au Canada, en particulier dans le nord du pays, est présentement en forte croissance et de nombreux sites jusqu'à ce jour inexplorés vont s'offrir à des analyses telles que celles présentées dans le présent manuscrit. Nous savons déjà qu'un réchauffement global a présentement lieu, mais en comprenant mieux la distribution spatiale des changements passés, nous serons en mesure de mieux déterminer les mécanismes qui causent cette distribution spatiale et ainsi de mieux prédire lévolution de ces changements dans le futur.

BIBLIOGRAPHIE

ALLARD, M., WANG, B. L. et PILON, J. A. (1995). Recent cooling along the southern shore of Hudson Strait, Quebec, Canada, documented from permafrost temperature measurements. *Arct. Alp. Res.*, 27(2):157–166.

ANDERSON, P. M., BARNOSKY, C. W., BARTLEIN, P. J., BEHLING, P. J., BRUBAKER, L., CUSHING, E. J., DODSON, J., DWORETSKY, B., GUETTER, P. J., HARRISON, S. P., HUNTLEY, B., KUTZBACH, J. E., MARKGRAF, V., MARVEL, R., MCGLONE, M. S., MIX, A., MOAR, N. T., MORLEY, J., PERROTT, R. A., PETERSON, G. M., PRELL, W. L., PRENTICE, I. C., RITCHIE, J. C., ROBERTS, N., RUDDIMAN, W. F., SALINGER, M. J., SPAULDING, W. G., STREET-PERROTT, F. A., THOMPSON, R. S., WANG, P. K., WEBB III, T., WINKLER, M. G. et WRIGHT JR., H. E. (1988). Climatic Changes of the Last 18,000 Years : Observations and Model Simulations. *Science*, 241:1043–1052.

BARTLETT, M. G., CHAPMAN, D. S. et HARRIS, R. N. (2004). Snow and the ground temperature record of climate change. *J. Geophys. Res.*, 109:4008.

BECK, A. E. (1982). Precision logging of temperature gradients and the extraction of past climate. *Tectonophysics*, 83:1–11.

BECK, A. E. et JUDGE, A. S. (1969). Analysis of heat flow data - 1.Detailed observations in a single borehole. *Geophys. J. R. Roy. Astr. S.*, 18:145–158.

BELTRAMI, H. (2001). Surface heat flux histories from inversion of geothermal data : Energy balance at the Earth's surface. *J. Geophys. Res.*, 106:21979–21994.

BELTRAMI, H. et BOURLON, E. (2004). Ground warming patterns in the Northern Hemisphere during the last five centuries. *Earth Planet. Sc. Lett.*, 227(3–4):169–177.

BELTRAMI, H., CHENG, L. et MARESCHAL, J.-C. (1997). Simultaneous inversion of borehole temperature data for determination of ground surface temperature history. *Geophys. J. Int.*, 129:311–318.

BELTRAMI, H., JESSOP, A. M. et MARESCHAL, J.-C. (1992). Ground temperature histories in eastern and central Canada from geothermal measurements : evidence of climatic change. *Global Planet. Change*, 19(2–4):167–184.

BELTRAMI, H. et MARESCHAL, J.-C. (1991). Recent warming in eastern Canada inferred from geothermal measurements. *Geophys. Res. Lett.*, 18(4):605–608.

BELTRAMI, H. et MARESCHAL, J.-C. (1992). Ground temperature histories for central and eastern Canada from geothermal measurements : Little ice age signature. *Geophys. Res. Lett.*, 19(7):689–692.

BELTRAMI, H. et MARESCHAL, J.-C. (1995). Resolution of ground temperature histories inverted from borehole temperature data. *Global Planet. Change*, 11(1–2):57–70.

BJÖRCK, S. (1985). Deglaciation chronology and revegetation in northwestern Ontario. *Can. J. Earth Sci.*, 22:850–871.

BLACKWELL, D. D., STEELE, J. L. et BROTT, C. A. (1980). The terrain effect on terrestrial heat flow. *J. Geophys. Res.*, 85:4757–4772.

BODRI, L. et CERMAK, V. (1997). Reconstruction of remote climate change from borehole temperatures. *Global Planet. Change*, 15(1–2):47–57.

BOUDREAU, R. E. A., GALLOWAY, J. M., PATTERSON, R. T., KUMAR, A. et MICHEL, F. A. (2005). A paleolimnological record of Holocene climate and environmental change in the Temagami region, northeastern Ontario. *J. Paleolimol.*, 33:445–461.

CARSLAW, H. S. et JAEGER, J. C. (1959). *Conduction of Heat in Solids.* Oxford University Press, New-York, second édition.

CERMAK, V. (1971). Underground temperature and inferred climatic temperature of the past millenium. *Palaeogeogr. Palaeocl.*, 10:1–9.

CHOUINARD, C., FORTIER, R. et MARESCHAL, J.-C. (2007). Recent climate variations in the subarctic inferred from three borehole temperature profiles in Northern Quebec. *Earth Planet. Sc. Lett.*, 263:355–369.

CHOUINARD, C. et MARESCHAL, J.-C. (2007). Selection of borehole temperature depth profiles for regional climate reconstructions. *Climate of the Past*, 3:297–313.

CLARK, P. U., ALLEY, R. B. et POLLARD, D. (1999). Northern Hemisphere Ice-Sheet Influences on Global Climate Change. *Science*, 286:1104–1111.

CLARK, P. U., LICCIARDI, J. M., MACAYEAL, D. R. et JENSON, J. W. (1996). Numerical reconstruction of a soft-bedded Laurentide Ice Sheet during the last glacial maximum. *Geology*, 24:679–682.

CLAUSER, C. et MARESCHAL, J.-C. (1995). Ground temperature history in central Europe from borehole temperature data. *Geophys. J. Int.*, 121(3):805–817.

DAVIS, M., DOUGLAS, C., CALCOTE, R., COLE, K. L., GREEN WINKLER, M. et FLAKNE, R. (2000). Holocene Climate in the Western Great Lakes National Parks and Lakeshores : Implications for Future Climate Change. *Conserv. Biol.*, 14(4):968–983.

DE VERNAL, A., GUIOT, J. et TURON, J.-L. (1993). Late and postglacial paleoenvironments of the Gulf of St.Lawrence : marine and palynological evidence. *Geog. Phys. Quat.*, 47(2):167–180.

DYKE, A. S., ANDREWS, J. T., CLARK, P. U., ENGLAND, J. H., MILLER, G. H., SHAW, J. et VEILLETTE, J. J. (2002). The Laurentide and Innuitian ice sheets during the Last Glacial Maximum. *Quaternary Sci. Rev.*, 21:9–31.

DYKE, A. S., MOORE, A. et ROBINSON, L. (2003). Deglaciation of North America. *Geological Survey of Canada Open File 1574.*

FAIRBANKS, R. G., MORTLOCK, R. A., CHIU, T.-C., CAO, L., KAPLAN, A., GUILDERSON, T. P., FAIRBANKS, T. W., BLOOM, A. L., GROOTES, P. M. et NADEAU, M.-J. (2005). Radiocarbon calibration curve spanning 0 to 50,000 years BP based on paired $^{230}Th^{234}U^{238}U$ and ^{14}C dates on pristine corals. *Quaternary Sci. Rev.*, 24:1781–1796.

FALLU, M. A., PIENITZ, R., WALKER, I. R. et LAVOIE, M. (2005). Paleolimnology of a shrub-tundra lake and response of aquatic and terrestrial indicators to climatic change in arctic Quebec, Canada. *Palaeogeogr. Palaeocl.*, 215:183–203.

FLATO, G. M., BOER, G. J., LEE, W. G., MCFARLANE, N. A., RAMSDEN, D., READER, M. C. et WEAVER, A. J. (2000). The Canadian Centre for Climate Modelling and Analysis global coupled model and its climate. *Climate Dynamics*, 16:451–467.

GOSSELIN, C. et MARESCHAL, J.-C. (2003). Recent warming in northwestern Ontario inferred from borehole temperature profiles. *J. Geophys. Res.*, 108(B9).

GOVAIRE, E. et GANGLOFF, P. (1989). Paléoenvironnement d'une plage tardiglaciaire de 10580 ans BP dans la région de Charlevoix, Qébec. *Geog. Phys. Quat.*, 43(2):147–160.

GUILLOU-FROTTIER, L., MARESCHAL, J.-C. et MUSSET, J. (1998). Ground surface temperature history in central Canada inferred from 10 selected borehole temperature profiles. *J. Geophys. Res.*, 103(B4):7385–7398.

HANSEN, J. et LEBEDEFF, S. (1987). Global trends of measured surface air temperature. *J. Geophys. Res.*, 92:13345–13372.

HARRIS, R. N. et CHAPMAN, D. S. (1995). Climate change on the Colorado Plateau of eastern Utah inferred from borehole temperatures. *J. Geophys. Res.*, 100:6367–6381.

HARRIS, R. N. et CHAPMAN, D. S. (1998). Geothermics and climate change 2. Joint analysis of borehole temperature and meteorological data. *J. Geophys. Res.*, 103(B4):7371–7384.

HARRIS, R. N. et CHAPMAN, D. S. (2001). Mid-Latitude (30°-60°N) climatic warming inferred by combining borehole temperatures with surface air temperatures. *Geophys. Res. Lett.*, 28:747–750.

HARTMAN, A. et RATH, V. (2005). Uncertainties and shortcomings of ground surface temperature histories derived from inversion of temperature logs. *J. Geophys. Eng.*, 4:299–311.

HICOCK, S. R. et DREIMANIS, A. (1992). Deformation till in the Great lakes region : Implications for rapid flow along the south-central margin of the Laurentide Ice Sheet. *Can. J. Earth. Sci.*, 29:1565–1579.

HILLAIRE-MARCEL, C. (1979). *Les mers post-glaciaires du Québec; quelques aspects.* Thèse de doctorat, Thèse de Doctorat d'État, Univ. Pierre et Marie Curie, Paris, France.

HOTCHKISS, W. O. et INGERSOLL, L. R. (1934). Post-glacial time calculations from recent measurements in the Calumet Copper Mine. *J. Geol.*, 42:113–142.

HOUGHTON, J. T., MEIRO FILHO, L. G., CALLANDER, B. A., HARRIS, N., KATTENBURG, A. et MASKELL, K. (1996). *Climate Change 1995 : The Science of Climate Change.* Climate Change 1995 : The Science of Climate Change, Edited by John T. Houghton and L. G. Meiro Filho and B. A. Callander and N. Harris and A. Kattenburg and K. Maskell, pp. 584. ISBN 0521564336. Cambridge, UK : Cambridge University Press, June 1996.

HUANG, S., POLLACK, H. N. et SHEN, P. Y. (2000). Temperature trends over the past five centuries reconstructed from borehole temperatures. *Nature*, 403:756–758.

HUGHEN, K. A., OVERPECK, J. T. et ANDERSON, R. (2000). Recent warming in a 500-year palaeotemperature record from varved sediments, Upper Soper Lake, Baffin Island, Canada. *Holocene*, 10(1):9–19.

IMBRIE, J., BOYLE, E. A., CLEMENS, S. C., DUFFY, A., HOWARD, W. R., KUKLA, G., KUTZBACH, J., MARTINSON, D. G., MCINTYRE, A., MIX, A. C., MOLFINO, B., MORLEY, J. J., PETERSON, L. C., PISIAS, N. G., PRELL, W. L., RAYMO, M. E., SHACKLETON, N. J. et TOGGWEILER, J. R. (1992). On the structure and origin of major glaciation cycles, 1, Linear responses to Milankovitch forcing. *Paleoceanography*, 7:701–738.

IPCC (2007). Climate Change 2007 : The Physical Science Basis. *Dans* SOLOMON, S., QIN, D., MANNING, M., CHEN, Z., MARQUIS, M., AVERYT, K. B., TIGNOR, M. et MILLER, H. L., éditeurs : *Contribution of Working Group I to the Fourth Assessment Report of the Intergovernmental Panel on Climate Change*. Cambridge University Press, Cambridge.

JACKSON, D. D. (1972). Interpretation of inaccurate, insufficient, and inconsistent data. *Geophys. J. R. Astron. Soc.*, 28:97–110.

JESSOP, A. M. (1971). The distribution of glacial perturbation of heat flow in Canada. *Can. J. Earth. Sci.*, 8:162–166.

JONES, P. D. et KELLY, P. M. (1983). The spatial and temporal characteristics of northern hemisphere surface air temperature variations. *J. Climatol.*, 3(3):243–252.

JONES, P. D., NEW, M., PARKER, D. E., MARTIN, S. et RIGOR, I. G. (1999). Surface air temperature and its changes over the past 150 years. *Rev. Geophys.*, 37(2):173–200.

JONES, P. D., WIGLEY, T. M. L. et WRIGHT, P. B. (1986). Global variations between 1861 and 1984. *Nature*, 322:430–434.

KASPER, J. N. et ALLARD, M. (2001). Late-Holocene climatic changes as detected by the growth and decay of ice wedges on the southern shore of Hudson Strait, northern Quebec, Canada. *Holocene*, 11(5):563–577.

KERWIN, M. W., OVERPECK, J. T., WEBB, R. S. et ANDERSON, K. H. (2004). Pollen-based summer temperature reconstructions for the eastern Canadian boreal forest, subarctic, and Arctic. *Quaternary Sci. Rev.*, 23:1901–1924.

KLEMAN, J. et HÄTTESTRAND, C. (1999). Frozen-bed Fennoscandian and Laurentide ice sheets during the Last Glacial Maximum. *Nature*, 402:63–66.

KUKKONEN, I. T. et JÕELEHT, A. (2003). Weichselian temperatures from geothermal heat flow data. *Journal of Geophysical Research (Solid Earth)*, 108:2163–+.

LABERGE, M. J. et PAYETTE, S. (1995). Long-term monitoring of permafrost change in a palsa peatland in northern Quebec, Canada : 1983-1993. *Arctic Alpine Res.*, 27(2):167–171.

LACHENBRUCH, A. H. et MARSHALL, B. V. (1986). Changing climate : Geothermal evidence from permafrost in the Alaskan Arctic. *Science*, 234:689–696.

LANCZOS, C. (1961). *Linear Differential Operators*. D. Van Nostrand, Princeton, N.J.

LANE, A. C. (1923). Geotherms from the Lake Superior copper country. *Bull. Geol. Soc. Am.*, 34:703–720.

LEWIS, T. J. (1992). Climatic Change inferred from underground temperatures. *Global Planet. Change*, 98(2–4).

LEWIS, T. J. (1998). The effect of deforestation on ground surface temperatures. *Global Planet. Change*, 18(1–2):535–538.

LICCIARDI, J. M., CLARK, P. U., JENSON, J. W. et MCCAYEAL, D. R. (1998). Deglaciation of a soft-bedded Laurentide ice sheet. *Quaternary Sci. Rev.*, 17:427–448.

LIU, K. (1990). Holocene paleoecology of the boreal forest and Great Lakes - St.Lawrence forest in Norhtern Ontario. *Ecol. Monogr.*, 60(2):179–212.

MAJOROWICZ, J. A., SAFANDA, J., HARRIS, R. N. et SKINNER, W. R. (1999). Large ground surface temperature changes of the last three centuries inferred from borehole temperatures in the Southern Canadian Prairies, Saskatchewan. *Global Planet. Change*, 20(4):227–241.

MAJOROWICZ, J. A., SKINNER, W. R. et ŠAFANDA, J. (2004). Large ground warming in the Canadian Arctic inferred from inversions of temperature logs. *Earth Planet. Sc. Lett.*, 221:15–25.

MAJOROWICZ, J. A., SKINNER, W. R. et SAFANDA, J. (2005). Ground Surface Warming History in Northern Canada Inferred from Inversions of Temperature Logs and Comparison with Other Proxy Climate Reconstructions. *Pure Appl. Geophys.*, 162:109–128.

MANABE, S. et BROCCOLI, A. J. (1985). The influence of continental ice sheets on the climate of an ice age. *J. Geophys. Res.*, 90:2167–2190.

MARESCHAL, J.-C. et BELTRAMI, H. (1992). Evidence for recent warming from perturbed geothermal gradients : Examples from eastern Canada. *Clim. Dynam.*, 6:135–143.

MARESCHAL, J.-C., JAUPART, C., GARIEPY, C., CHENG, L. Z., GUILLOU-FROTTIER, C., BIENFAIT, G. et LAPOINTE, R. (2000). Heat flow and deep thermal structurenear the southeastern edge of the Canadian Shield. *Can. J. Earth Sci.*, 37:399–414.

MARESCHAL, J.-C., JAUPART, C., ROLANDONE, F., GARIEPY, C., FOWLER, C. M. R., BIENFAIT, G. et CARBONNE, C. (2005). Heat flow, thermal regime, and rheology of the lithosphere in the Trans-Hudson Orogen. *Can. J. Earth Sci.*, 42:517–532.

MARESCHAL, J.-C., NYBLADE, A., PERRY, H. K. C., JAUPART, C. et BIENFAIT, G. (2004). Heat flow and deep lithospheric thermal structure at Lac de Gras, Slave Province, Canada. *Geophys. Res. Lett.*, 31:L12611.

MARESCHAL, J.-C., ROLANDONE, F. et BIENFAIT, G. (1999). Heat flow variations in a deep borehole near Sept-Iles, Québec, Canada : Paleoclimatic interpretation and implications for regional heat flow estimates. *Geophys. Res. Lett.*, 26(14):2049–2052.

MARSHALL, S. J. et CLARK, P. U. (2002). Basal temperature evolution of North American ice sheets and implications for the 100-kyr cycle. *Geophys. Res. Lett.*, 29:67–1.

MARSHALL, S. J., JAMES, T. S. et CLARKE, G. K. C. (2002). North American Ice Sheet reconstructions at the Last Glacial Maximum. *Quaternary Sci. Rev.*, 21(1).

MARSHALL, S. J., TARASOV, L., CLARKE, G. K. C. et PELTIER, W. R. (2000). Glaciological reconstruction of the Laurentide ice sheet : physical processes and modelling challenges. *Can. J. Earth Sci.*, 37:769–793.

MENKE, W. (1989). *Geophysical Data Analysis : Discrete Inverse Theory.* Numéro 45 de International Geophysical Series. Academic Press, San Diego.

MISENER, A. D. et BECK, A. E. (1960). *Methods and Techniques in Geophysics.* S. K. (Ed.), New York.

MIX, A. C., BARD, E. et SCHNEIDER, R. (2001). Environmental processes of the ice age : land, oceans, glaciers (EPILOG). *Quaternary Sc. Rev.*, 20:627–657.

MORITZ, R. E., BITZ, C. M. et STEIG, E. J. (2002). Dynamics of Recent Climate Change in the Arctic. *Science*, 297:1497–1502.

MOSEGAARD, K. et TARANTOLA, A. (1995). Monte Carlo sampling of solutions to inverse problems. *J. Geophys. Res.*, 100(B7):12431–12448.

MOTT, R. J. (1973). Palynological studies in Central Saskatchewan. *Geological Survey of Canada.*

NIELSEN, S. B. et BECK, A. E. (1989). Heat flow density values and paleoclimate determined from stochastic inversion of four temperature-depth profiles from the Superior Province of the Canadian Shield. *Tectonophysics*, 164(2–4):345–359.

OVERPECK, J., HUGHEN, K., HARDY, D., BRADLEY, R., CASE, R., DOUGLAS, M., FINNEY, B., GAJEWSKI, K., JACOBY, G., JENNINGS, A., LAMOUREUX, S., LASCA, A., MACDONALD, G., MOORE, J., RETELLE, M., SMITH, S., WOLFE, A. et ZIELINSKI, G. (1997). Arctic Environmental Change of the Last Four Centuries. *Science*, 278:1251–1256.

PARKER, R. L. (1994). *Geophysical Inverse Theory.* Princeton University Press, Princeton, New Jersey.

PATTERSON, R. T., MCKILLOP, W. B., KROKER, S., NIELSEN, E. et REINHARD, E. G. (1997). Evidence for rapid avian-mediated foraminiferal colonization of Lake Winnipegosis, Manitoba, during the Holocene Hypsithermal. *J. Paleolimol.*, 18:131–143.

PAYETTE, S., DELWAIDE, A., CACCIANIGA, M. et BEAUCHEMIN, M. (2004). Accelerated thawing of subarctic peatland permafrost over the last 50 years. *Geophys. Res. Lett.*, 31:18208.

PELTIER, W. R. (2004). Global Glacial Isostasy and the Surface of the Ice-Age Earth : The ICE-5G (VM2) Model and GRACE. *Annual Review of Earth and Planetary Sciences*, 32:111–149.

PERRY, H., JAUPART, C., MARESCHAL, J.-C. et BIENFAIT, G. (2006). Crustal heat production in the Superior province of the Canadian Shield and in North America, inferred from heat flow data. *J. Geophy. Res.*, 111:B04401.

PINET, C., JAUPART, C., MARESCHAL, J.-C., GARIEPY, C., BIENFAIT, G. et LAPOINTE, R. (1991). Heat flow and structure of the lithosphere in the eastern Canadian shield. *J. Geophy. Res.*, 96:19941–19963.

POLLACK, H. N., HUANG, S. et SHEN, P. Y. (1998). Climate change records in subsurface temperatures : A global perspective. *Science*, 282:279–281.

POLLACK, H. N., SHEN, P. Y. et HUANG, S. (1996). Inference of ground surface temperature history from subsurface temperature data : Interpreting ensembles of temperature logs. *Pure Appl. Geophys.*, 147(3):537–550.

PRESS, W. H., TEUKOLSKY, W. T., VETTERLING, W. T. et FLANNERY, B. P. (1992). *Numerical Recipes in Fortran. The Art of Scientific Computing.* Cambridge University Press, Cambridge, UK.

PRZYBYLAK, R. (2000). Temporal and spatial variation of surface air temperature over the period of instrumental observations in the Arctic. *Int. J. Climatol.*, 20:587–614.

PUTNAM, S. N. et CHAPMAN, D. S. (1996). A geothermal climate change observatory : First year results from Emigrant Pass in northwest Utah. *J. Geophys. Res.*, 101(B10):21877–21890.

RICHARD, P. et LABELLE, C. (1988). Histoire postglaciaire de la végétation au lac du Diable. *Geog. Phys. Quat.*, 43:337–354.

RIND, D. et OVERPECK, J. (1993). Hypothesized causes of decade-to-century-scale climate variability : climate model results. *Quaternary Sci. Rev.*, 12(6):357–374.

RITCHIE, J. C. (1983). The paleoecology of the central and norhtern parts of the glacial lake agassiz basin. *Dans* TELLER, J. T. et CLATON, L., éditeurs : *Glacial Lake Agassiz*, Geological Association of Canada Special Paper 26, pages 157–170.

RITCHIE, J. C. (1987). *Postglacial Vegetation of Canada.* Cambridge University Press, New-York, NY.

ROLANDONE, F., MARESCHAL, J.-C. et JAUPART, C. (2003). Temperatures at the base of the Laurentide Ice Sheet inferred from borehole temperature data. *Geophys. Res. Lett.*, 30(18): 1944.

ROMANOVSKY, V., BURGESS, M., SMITH, S., YOSHIKAWA, K. et BROWN, J. (2002). Permafrost temperature records : Indicators of climate change. *EOS Transactions*, 83:589–.

SAARNISTO, M. (1974). The deglaciation history of the Lake Superior region and its climatic implications. *Quaternary Res.*, 4:316–339.

SAMBRIDGE, M. et MOSEGAARD, K. (2002). Monte Carlo methods in geophysical inverse problems. *Rev. Geophys.*, 40:3–1.

SASS, J. H., LACHENBRUCH, A. H. et JESSOP, A. M. (1971). Uniform heat flow in a deep hole in the Canadian Shield and its paleoclimatic implications. *J. Geophys. Res.*, 76:8586–8596.

SERREZE, M. C. et FRANCIS, J. A. (2006). The arctic amplification debate. *Climatic Change*, 76:241–264.

SERREZE, M. C., WALSH, J. E., CHAPIN III, F. S., OSTERKAMP, T., DYURGEROV, M., ROMANOVSKY, V., OECHEL, W. C., MORRISON, J., ZHANG, T. et BARRY, R. G. (2000). Observational evidence of recent change in the northern high-altitude environment. *Climatic Change*, 46(1).

SHEN, P. Y. et BECK, A. E. (1991). Least squares inversion of borehole temperature measurements in functional space. *J. Geophys. Res.*, 96:19965–19979.

SHEN, P. Y. et BECK, A. E. (1992). Paleoclimate change and heat flow density from temperature data in the Superior Province of the Canadian Shield. *Global Planet. Change*, 98(2–4):143–165.

TARASOV, L. et PELTIER, W. R. (1999). Impact of thermomechanical ice sheet coupling on a model of the 100 kyr ice age cycle. *J. Geophys. Res.*, 104:9517–9546.

TARASOV, L. et PELTIER, W. R. (2004). A geophysically constrained large ensemble analysis of the deglacial history of the North American ice-sheet complex. *Quaternary Sci. Rev.*, 23:359–388.

TAYLOR, A. E., WANG, K., SMITH, S. L., BURGESS, M. M. et JUDGE, A. S. (2006). Canadian Arctic Permafrost Observatories : Detecting contemporary climate change through inversion of subsurface temperature time series. *J. Geophys. Res.*, 111:2411.

TIKHONOV, A. N. et ARSENIN, V. Y. (1977). *Solution of ill posed problems.* Wiley, New-York.

VASSEUR, G., BERNARD, P., VAN DE MEULEBROUCK, J., KAST, Y. et JOLIVET, J. (1983). Holocene paleotemperatures deduced from geothermal measurements. *Palaeogeogr. Palaeocl.*, 43:237–259.

WANG, B. et ALLARD, M. (1995). Recent climatic trend and thermal response of permafrost in Salluit, northern Quebec, Canada. *Permafrost Periglac.*, 6(3):221–233.

WANG, K. (1992). Estimation of ground surface temperatures from borehole temperature data. *J. Geophys. Res.*, 97(B2):2095–2106.

WANG, K., LEWIS, T. J., BELTON, D. S. et SHEN, P. Y. (1994). Differences in recent ground surface warming in eastern and western Canada : Evidence from borehole temperatures. *Geophys. Res. Lett.*, 21:2689–2692.

WANG, K., LEWIS, T. J. et JESSOP, A. M. (1992). Climatic changes in central and eastern Canada inferred from deep borehole temperature data. *Global Planet. Change*, 98(2–4):129–141.

WOODS, K. D. et DAVIS, M. B. (1989). Paleoecology of range limits : Beech in the upper peninsula of Michigan. *Ecology*, 70(3):681–696.